ROYAUME DU MAROC
Université Mohammed V - RABAT -
جامعة محمد الخامس – الرباط –
Faculté des sciences
كلية العلوم
CENTRE D'ETUDES DOCTORALES - SCIENCES ET TECHNOLOGIES

N° d'ordre 3272

THESE

En vue de l'obtention du : ***DOCTORAT***

Centre de Recherche : Centre de Recherche en Energie
Structure de Recherche : Centre de Recherche en Energie
Discipline : Physique
Spécialité : Mécanique et Sciences des Matériaux

Présentée et soutenue le 18/12/2019 par :

Wafa OUARHIM

Thermoset laminated composites in different configurations: From design to application

JURY

Saad CHARIF D'OUAZZANE	PES, ENSMR, Rabat	Président
Mohammed Ouadi BENSALAH	PES, FSR, Université Mohammed V, Rabat	Directeur de Thèse
Abou El Kacem QAISS	Expert, MAScIR, Rabat	Co-directeur de Thèse
Jamal ECHAABI	PES, ENSEM, Université Hassan II, Casablanca	Rapporteur/ Examinateur
Kamal GUERRAOUI	PES, FSR, Université Mohammed V, Rabat	Rapporteur/ Examinateur
Ahmed MZERD	PES, FSR, Université Mohammed V, Rabat	Rapporteur/ Examinateur
Rachid BOUHFID	Expert, MAScIR, Rabat	Examinateur
Noureddine DAMIL	PES, FSBM, Université Hassan II, Casablanca	Examinateur
Mohammed Jamal Eddine SEBBANI	PES, FSR, Université Mohammed V, Rabat	Examinateur

Année Universitaire: 2018/2019

"And of knowledge, you (mankind) have been given only a little" Surah Al-Isra [17:85]

Preface

The researches of this doctoral thesis was carried out at the Energy Research Center (Mechanics and Materials Laboratory) of the Faculty of Sciences of Mohammed-V University of Rabat, under the supervision of **Professor Mohammed-Ouadi BENSALAH,** in collaboration with Composites and Nanocomposites Center of MAScIR Foundation-Rabat, directed by **Professor Abou el kacem QAISS**.

I could not have achieved this work without a strong support group. First of all, I want to express sincere thanks to **Pr. Mohammed-Ouadi BENSALAH** (thesis supervisor), professor at Faculty of Sciences of Rabat, for allowing me to conduct this research under his auspices.

Saying thank you is not enough to express my gratitude to my co-supervisor **Pr. Abou El Kacem QAISS**, Director of Composite and Nanocomposite Center (CNC) in MAScIR Foundation, to have accepted my integration into his team and to supervise me during the entire process of developing this work, and whose availability, know-how and support have never failed me.

Also, I would like to acknowledge the assistance of **Pr. Rachid BOUHFID,** Researcher at CNC in MAScIR Foundation, who offered me valuable suggestions and advices.

I am deeply grateful to all members of the jury, for agreeing to read this manuscript, and to participate in the judgement of its scientific value:

Pr. Saad CHARIF D'OUAZZANE, Professor in ENSMR (Ecole Nationale Supérieure des mines de Rabat), President of the jury;

Pr. Jamal ECHAABI, Professor in ENSEM (Ecole Nationale Supérieure de L'Electricité et de la Mécanique) Casablanca (Hassan II University, Casablanca);

Pr. Nourddine DAMIL, Professor in Faculty of Sciences Ben M'sik (Hassan II University, Casablanca);

Pr. Kamal GUERRAOUI, Professor in Faculty of Sciences of Rabat (Mohammed-V University, Rabat);

Pr. Ahmed MZERD, Professor in Faculty of Sciences of Rabat (Mohammed-V university, Rabat);

Pr. Mohammed Jamal Eddine SEBBANI, Professor in Faculty of Sciences of Rabat (Mohammed-V University, Rabat).

I extend my sincere thanks to the general management of MAScIR Foundation for offering me the opportunity to prepare my doctoral thesis in a scientific research framework of international standards and for the financial support.

WAFA OUARHIM

Dedication

So many times I thought to offer you a few things as a sign of recognition for everything that you have consented to see me succeed, this time is the opportunity.

I dedicate this memory:

To all my teachers, especially Pr. Abou el kacem Qaiss and Pr. Rachid Bouhfid.

To my dear brother and my dear sisters and my family, who have always been there for me.

To my dear friends, Bouchra, Fatima-Zahra, Khadija, Hicham, and Abdellah. I wish you every success in your lives.

To you my dear mother; to show my deep gratitude, for all the sacrifices you make me happy with, the trust you receive in me and all the love you surround me with.

To you my dear father; you are the best father in this world, thanks to your encouragement, your trust and your moral and material support and for your infinite love, I express my gratitude, my deep love and my passion.

To my grandfather. To my grandmother, who would have liked to see that moment. May her soul rest in peace.

May Almighty Allah, preserve you and grant your health, long life and happiness.

Table of content

List of figures

Chapter I

Chapter II

Chapter III

Chapter IV

List of tables

Chapter I

Chapter II

Chapter III

Chapter IV

Terms and symbol glossary

C	Carbon atom
RTM	Resin Transfer Molding
1LG	Composite with one layer of glass fibers
1LJ	Composite with one layer of jute fibers
1YYJG	Composite with one layer of alternating jute and glass fibers (yarn-by-yarn)
5YYJG	Laminated composite with five layers of alternating jute and glass fibers (yarn-by-yarn)
7LLJG	Laminated composite with 7 layers of stacking jute and glass fibers (layer-by-layer)
CH_3COOH	Acetic acid
H_2O_2	Hydrogene peroxide
NaOH	Sodium Hydroxyde
$NaClO_2$	Sodium chlorite
FTIR	Fourier transform infrared
SEM	Scanning electron microscopy
V_f	Volume fraction of the fiber
V_m	Volume fraction of the matrix
ρ_f	Fiber density

ρ_m	Matrix density
CSMGPC	Chopped strand mats glass fibers reinforced with polyester resin composite
CSMGPGC	Chopped strand mats glass fibers reinforced with polyester resin coated with gelcoat composite
GFC	Glass fiber composite
WGPC	Woven glass fibers reinforced with polyester resin composite
TRFC	Treated Raffia fiber composite
RFC	Raw Raffia fiber composite
SCGTRG	Sandwich composite: Glass fiber/Treated Raffia fiber/Glass fiber
SCGRG	Sandwich composite: Glass fiber/Raw Raffia fiber/Glass fiber
RbWGF	Running blade reinforced with woven glass fibers
RbMGF	Runing blade reinforced with chopped strand mat glass fibers
RbMGFGC	Running blade reinforced with chopped strand mat glass fibers covered gelcoat

Abstract

This work focuses on the design and development of new thermoset composite materials. Indeed, composites reinforced with natural fibers, synthetic fibers, and both of them (hybrid composite) were selected for study in this thesis. For this purpose, two laminated configurations are used, including simple and hybrid laminated composites. This later, in turn, consists of three configurations: sandwich structure, inter-layer, and intra-layer configurations.

The fibers used in this study were Raffia and jute as natural fibers and glass as synthetic fiber reinforcing two thermoset matrices (epoxy and polyester) through hand lay-up technique. Different fiber forms are adopted including mat and woven.

The properties of the fibers/resin composites were defined by using tensile, flexural, torsion, shearing, droplet test, moisture absorption, thermal conductivity tests. Scanning electron microscopy (SEM) and Fourier transform infrared spectroscopy (FTIR) has been used to study the morphological and structural properties of the composites, respectively.

The experimental results for all laminated configurations are compared with theoretical models (mixing law, homogenization technique) and numerical simulation (ANSYS ACP). Therefore, a good agreement between results is found taking into account the considered assumptions.

Keywords: Laminated composites, thermoset matrices, hybridization, Sandwich structure, inter-layer & intra-layer configurations, Hand lay-up technique, tensile test, flexural test, shearing test, droplet test, moisture absorption, SEM, FTIR, Mixing law, Homogenization technique, numerical simulation.

Résumé

Ce travail a pour objectif la conception et le développement de nouveaux matériaux composites à matrices thermodurcissables. En effet, des composites renforcés par des fibres naturelles, des fibres synthétiques, et l'hybridation des deux sont objet d'étude dans cette thèse. Pour ce faire, les composites stratifiés simples et hybrides sont deux configurations utilisés dans ce travail. La configuration hybride, à son tour, se compose de trois structures : sandwich, inter-couche et intra-couche.

Les fibres naturelles (le raphia et le jute) et les fibres synthétiques (le verre) ont été choisies comme des renforts de deux matrices thermodurcissables (époxy et polyester). Différentes formes de fibres sont adoptées, notamment mat et tissé. La fabrication des composites stratifiés étudiés est assurée par la technique de stratification manuelle.

Les propriétés des composites fibres / résine ont été définies à l'aide d'essais de traction, de flexion, de torsion, de cisaillement, de test de gouttelettes, d'absorption d'humidité et de conductivité thermique. La microscopie électronique à balayage (MEB) et la spectroscopie infrarouge à transformée de Fourier (IRTF) ont été utilisées pour étudier, respectivement, les propriétés morphologiques et structurelles des composites.

Les résultats expérimentaux de différentes configurations de stratifiés sont comparés aux modèles théoriques (loi de mélange, technique d'homogénéisation) et à la simulation numérique (ANSYS ACP). Par conséquent, un bon accord entre les résultats a été observé en tenant compte des hypothèses retenues.

Mots clés : Composites stratifiés, Matrices thermodurcissables, Hybridation, Structure sandwich, inter-couche, intra-couche, Moulage manuelle, Essai de traction, Essai de flexion, Essai de torsion, Essai de cisaillement, Test de gouttelettes, Absorption d'humidité, MEB, IRTF, Loi de mélange, technique d'homogénéisation, simulation numérique.

GENERAL INTRODUCTION

Composite materials are becoming more and more an interesting choice for many industrial applications. They are found in important areas such as aeronautics, automotive, sports, naval or building, because of their good properties i.e. high mechanical strength and rigidity, high impact resistance, low weight, resistance to corrosion and low maintenance cost. Traditionally, composite materials are reinforced by synthetic fibers such as glass, carbon, aramid or ceramic fibers. These fibers are used because of their strength, rigidity, low moisture absorption, good compatibility with polymer resins. Glass fibers are those that are most commonly used because of their low cost, their ease of production and their specific mechanical characteristics. However, the main problem related to the use of these materials is their negative impact on human health and the environment, especially as today the standards relating to respect for the environment become more and more severe. Moreover, nowadays, there is no ecological and economical solution for recycling composite parts based on synthetic fibers at the end of their service life. In addition to being produced, these synthetic fibers require a significant amount of energy. Therefore, the growing environmental consciousness and legislation requirements is leading to the use of greener and environmentally friendlier materials. These regulatory restrictions have favored the emergence of biocomposite materials reinforced by natural fibers, mainly plant fibers. In recent years, the use of natural fibers in composites as an alternative to synthetic fibers has attracted more and more interest. This attention is due to a number of factors:

- Natural fibers are renewable resources;
- Lower cost;
- Lower density;
- They are biodegradable (however this can be a drawback during the lifetime of a product);
- Using biodegradable polymers as matrix, we can have totally biodegradable composite materials;
- Less abrasive to the processing equipment;
- Healthier in use due to their natural origins.

Lower density is the main feature why natural fibers used in composite materials are interesting in transport sector. Indeed, the use of natural fibers allows reducing the final mass of the composites parts leading to reduce transportation cost of products made of natural fiber composites as well as consumption of fuel and pollution is decreased. Thus, a weight saving in the field of transport involves saving of energy.

Nevertheless, the natural fibers also have negative points that compromise their use in demanding structural applications: hydrophilic behavior, porosity, low mechanical properties, low adhesion between the fibers and the matrix. The opposed nature of the two components of composite material (hydrophilic and hydrophobic behavior of natural fibers and matrix, respectively) renders them less adhesive which can affect the mechanical strength of the structure and subsequently reduce their service life. To minimize these problems, fibers and/or polymers are subjected to some modification treatments in their surface. These modification methods are of different efficiency for the adhesion between matrix and fiber.

Since natural fibers are inherently sensitive to water and have lower mechanical properties than synthetic fibers, fibers hybridization is a promising strategy to toughen composite materials. By combining at least two types of reinforcement, these hybrid composites offer a better balance in mechanical properties than non-hybrid composites.

The main aim of this work is to design and develop new thermoset composite materials. Indeed, composites reinforced with natural fibers, synthetic fibers, and both of them (hybrid composite) were selected for study in this thesis. Besides, different laminated configurations are used, including simple and hybrid laminated composites (Sandwich, inter-layer, and intra-layer configurations). In addition, the introduction of natural fiber in different forms (woven and random), while taking into consideration the limitations of the lignocellulosic reinforcement.

For this purpose, this work aims at the design, formulation, and modeling of thermosetting laminated composite materials whose reinforcement is a hybridization in terms of nature. The last chapter is devoted to an application of simple laminated composite material in the sporting field by producing running blade.

In order to achieve the objectives, the work done during this thesis is reported in this manuscript. Each of the four chapters ends with a conclusion and contains its own bibliographic references.

The first chapter is devoted to a bibliographical review going back to basics for the work envisaged. Therefore, it is oriented towards the restricted domain of composite materials (long fibers) with thermosetting organic polymer matrix.

The following chapters will describe the materials and methods used in this research, including description of the detailed preparation, the processing procedure, the test methods and the obtained results. The results of all tests will be presented and discussed, followed by a conclusion. In the final chapter, we summarize the whole results found through the presented works, before opening up new perspectives and future works.

The second chapter presents the effect of the alkaline treatment of laminated hybrid composite materials based on Raffia fibers and glass fibers in sandwich structure. The used matrix in this work is epoxy resin. A complete set of characterization is performed including structural, thermal, and mechanical (three-point bending test, shear test, droplet test). Results show that chemical treatment undergoes by Raffia fibers is at the origin of the improvement of the mechanical properties of sandwich composites compared with the composite reinforced with raw Raffia fibers. Finally, the mixing rule technique was used to predict the flexural modulus of the laminates using the mechanical parameters of each layer and the result was compared to the experimental data. It is assumed that Raffia fiber treatments will support the development of synthetic fiber reinforced sandwich polymer composites for industrial applications.

In chapter 3, a new use of jute fibers in the polyester matrix was used with glass fibers to compare between two different hybrid laminated configurations: inter-layer (layer by layer) and intra-layer (yarn by yarn). The composites are manufactured using the hand layup technique and the samples are characterized for moisture resistance and mechanical properties. The experimental bending modulus of both laminated configurations is compared with theoretical values as obtained by a combination of the mixing law and homogenization technique. The results show that the interlayer configuration of jute and glass fibers presents the least resistance to moisture compared to the other configurations studied. Finally, the theoretical mechanical predictions are found to be good (10% on average) despite the simplifications made in the calculations.

Chapter 4 is devoted to the study of different types of deformations (buckling, bending and relaxation) on the properties of simple laminated composites based on polyester as the matrix and glass fiber (GF) in two forms: woven (WGF) and chopped strand mat (CSM). Also, a

thin gelcoat based on clay particles was applied to the CSM samples to get a third series. The results showed that using the same thickness, the mechanical properties, especially in terms of bending and buckling, are influenced by the layers' number. Furthermore, a sports application is presented as an applied investigation for leg prosthesis. Three different running blades "Flex-foot Cheetah" were manufactured to be experimentally and numerically (ANSYS ACP software) characterized to simulate real conditions. The results showed good agreement between the experimental and numerical values in terms of total deformation.

Finally, a conclusion and perspectives complete this memory.

CHAPTER I
STATE OF THE ART*

1.1 Introduction

A composite material is a mixture of two or more materials of different natures and have complementary properties. The final material is then heterogeneous and has qualities superior to those of each of its constituents. Generally, a composite material consists of one or more discontinuous phases included in a continuous phase. The discontinuous phase, often more rigid and more resistant, is called reinforcement, while the continuous phase takes the name of matrix (Figure I. 1). The latter, usually less rigid, is mainly used to transmit the forces to the reinforcement, to protect against any impact or external damage and to give the desired shape to the composite. Sometimes, there is a need to add an additional phase: fillers and additives. Their role is to improve the physical and mechanical properties of the final composite or to make its implementation less difficult.

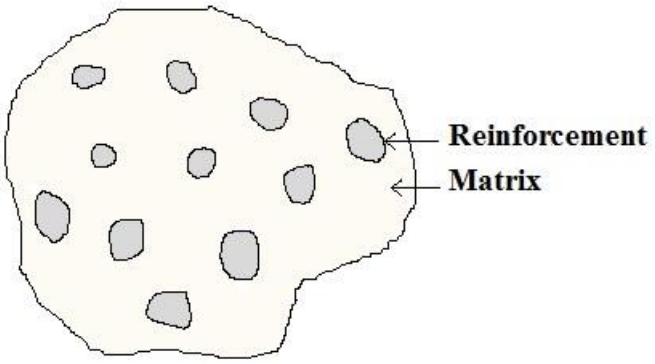

Figure I. 1: Representation of composite material.

Thermosetting composite - as opposed to thermoplastic composite - is termed a composite material - include a material consisting of at least two components with complementary

*

Some sections of this chapter are reprinted in part with permission from Ouarhim W, Zari N, Bouhfid R, Qaiss A el kacem. Mechanical performance of natural fibers–based thermosetting composites. **In: Mechanical and Physical Testing of Biocomposites, Fibre-Reinforced Composites and Hybrid Composites** 2019. p. 43–60.

properties - whose matrix is made of a thermosetting polymer. Generally, they exist three different nature of the matrix used in composites: organic, metallic and mineral matrices. Thermosetting composites fall into the category of organic matrix composite materials. These are the most widespread composite materials.

The polymer resins used as matrix for thermosetting composites are in liquid form. They consist of molecules arranged in a three-dimensional network maintained by strong chemical bonds, covalent bonds. These are irreversibly established during the polymerization.

In general, thermosetting resins are easy to shape. With a liquid, it is easy to impregnate the reinforcements that constitute the other main component of the composite. And the operating temperatures remain reasonable. On the other hand, the characteristic of thermosetting resins is that they cannot be remelted. Although it can be considered that all composite materials are recyclable, the recycling of thermosetting composites remains technically delicate and economically unattractive. As a matrix, the thermoset resin may also be used as a protective coating of the product. This is termed the gelcoat.

The composite materials that will be discussed in this thesis are based on thermosetting resins. Besides, this chapter is devoted to further highlighting composite materials based on natural and synthetic fibers, as well as their mixture called hybridization, in different configurations. The modelling section is also underlined at the end to predict the mechanical behavior of the laminated composites.

1.2 Components of thermoset composite material

As previously described, the composite materials addressed in this thesis are based on the thermoset resins. This section presents the components of thermoset composite material, namely the various thermoset matrices and the natural and synthetic reinforcements.

1.2.1 Matrices

Thermoset matrix plays a crucial role in the performance of thermoset composite [1]. These kinds of polymers ensure high stability, high rigidity, high dimensional stability, resistance to creep, and deformation under load lightweight as compared with metals and high electrical and thermal insulation properties. There are in the form of viscous liquid and powder resin, but, in general, they are usually liquid or malleable before polymerization. These types of matrices are made by mixing two components (a resin and a hardener) which are cured at room temperature. Nowadays, several kinds of thermosetting matrix exist, and more than 95% of thermoset composite parts are based on polyester and epoxy resins; of the two,

polyester systems predominate in volume by far. Other thermoset resins used in reinforced form are phenolics, vinylesters, polyimides, and silicones which are explicitly detailed in the following sections.

1.2.1.1 Polyesters

The polyester resin is a viscous liquid resin resulting from the condensation reaction between a glycol and an unsaturated dibasic acid. This polymer contains a double bond between its carbon atoms (C=C) and is characterized by its clear pale yellow color. It is classified as one of the most versatile synthetic copolymers. To polymerize this resin, it is mixed with its proper catalyst. There are two types of a polyester resin as standard laminating systems in the composite industry: Orthophthalic (ortho) and Iso-phthalic (iso) polyester resin. The orthophthalic resins are composed essentially of orthophthalic acid and constitute a good basic resin for various uses at low cost. This type of resin contains between 35% and 45% of styrene and are used in applications that do not require high temperature, high corrosion resistance, or high mechanical properties. On the other hand, the isophthalic polyester resins contain between 42% and 50% of styrene and are better suited for corrosion environments and elevated temperatures and have greater mechanical properties. Moreover, they are characterized by their performance, low cost, and extreme processing versatility.

1.2.1.2 Epoxy resins

Epoxy resin is a viscous liquid resin classified in the group of synthetic resin which contains an epoxide group in its chemical structure. It is characterized by its high adhesive properties (good adhesion with reinforcement), high chemical resistance, better moisture resistance, excellent mechanical properties, good fatigue resistance, low shrinkage, strong durability at low and high temperatures, and high electrical resistance, which justifies its numerous uses in modern industries. The epoxy resin having a transparent color is mixed with its suitable hardener (darker color) to polymerize and get an irreversible material.

1.2.1.3 Phenolic resins

Phenolic resins are a kind of thermoset matrices invented by Dr. Leo Baekeland in 1907. They are produced by the reaction of phenols with aldehydes. Also, this thermoset resin is characterized by its excellent properties such as high-temperature stability up to 300-350°C, high chemical stability [2,3], excellent fire retardancy, low smoke and toxicity emissions, and good friction properties. The phenolic resin is often dark-colored, from yellow to dark red, and has an excellent price/performance profile. Moreover, Bakelite or poly-oxybenzyl-

methylene-glycolanhydride is a kind of phenolic resin. This type of thermoset resin is used in mass transit and ducting.

1.2.1.4 Vinylester resins

Vinylester is a viscous liquid resin produced by the esterification of epoxy resin. It is a mixture of styrene and methacrylate epoxy compounds. Curing the vinylester resin can be carried out at ambient or elevated temperatures. This matrix is used in composite materials generally having reinforced glass fiber. Similar to polyester, it is characterized by its excellent mechanical and fatigue properties and chemical resistance.

1.2.1.5 Polyimides

Polyimides are synthetic colored polymers which include the imide group [4]. They are known for their flexural strength and flame and chemical resistance. This is why it is considered as a resistance polymer. Polyimides exist for thermoset and thermoplastic versions. Thermoset polyimides have no melt temperature but have a glass transition temperature, and the process to manufacture this thermoset polymer is irreversible. Thermoplastic polyimides offer continuous use of temperature to 240 °C and can be recycled.

1.2.1.6 Silicone resins

Silicone resins are a type of silicon material which resist to temperature up to 350 °C. Silicon resins are composed of silicon (Si), oxygen (O), and other organic groups. This non-aging resin has good resistance to tearing. But this resin also has drawbacks such as mass removal of the mold from 4 % to 12% after drying. In addition, the silicon resin is classified as a thermosetting resin because of its irreversible cycle, which means that the silicone resin is not recycled after curing Table I. 1.

Table I. 1: Mechanical characterization for thermoset matrices

Thermoset resins	Density (g/cm3)	Tensile strength (MPa)	Young's modulus (GPa)	Elongation (%)
Phenolic	1.2	40 - 50	3	1 - 2
Polyester	1.2	50 - 65	3	2 - 3
Epoxy	1.1 – 1.4	50 - 90	3	2 - 8
vinylester	1.15	70 - 80	3.5	4 - 6
Polyimide	1.42	70 - 150	2.5	8 - 70
Silicon	2.33	-	-	-

1.2.2 Reinforcements

Thermoset composite reinforced fibers can be used synthetic as well as natural. These two kinds of fibers ensure some properties to the final composite including stiffness, breaking strength, and hardness. Herein, the focus will be on synthetic reinforcements with different types as well as the natural reinforcement in terms of composition, types and chemical treatment used in these fibers in order to ensure their good adhesion with matrices.

1.2.2.1 Synthetic reinforcement

Synthetic reinforcements are manufactured through the polymerization process by linking monomers into polymers. The growth observed in this market was significant over the past seven years. The comprehensive application scope of the synthetic fibers covers clothing, home furnishing, automotive, filtration, and others. Clothing is the primary market for synthetic fibers which is the largest revenue-generating application area in this market. The mainly used synthetic reinforcements are glass fibers, aramid fibers, and carbon fibers. These fibers could be presented in various form, including chopped strand mat and woven.

1.2.2.1.1 Chopped strand mats

The mats are felt-like fabrics in which the short fibers are arranged in all directions (Figure I. 2). They are used to ensure better isotropy of the composite material and as a topcoat to hide the weft of a fabric. Generally, the mats are glass fiber. Some manufacturing processes require their uses.

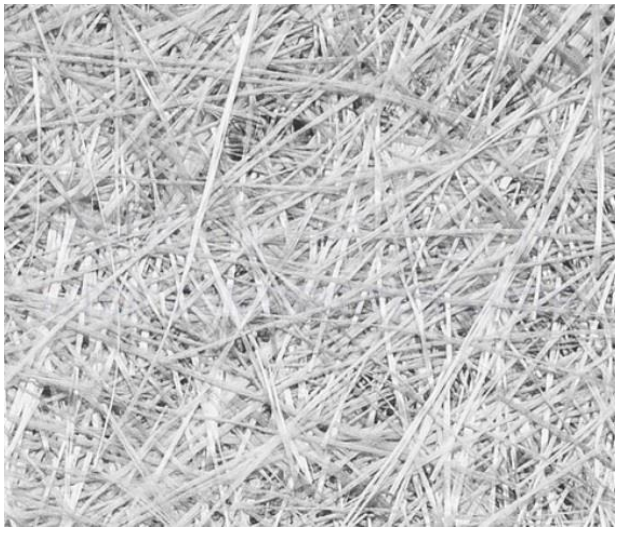

Figure I. 2: Chopped strand mat glass fibers.

1.2.2.1.2 Woven

The woven fabric, usually made from roving, is used for parts requiring high resistance to mechanical stresses when the method allows their use. They exist various types of weaving, including plain, and twill. The plain (usually called "taffeta" in this area) will be used for their flatness. Twill has more flexibility than plain and satins (even more flexible) will be used for their abilities to marry a given form. These last two types of fabrics also have the advantage over the plain to be less sensitive to the shrinkage (embuvage).

- Unidirectional weave

This type of the ply corresponds to a sheet of parallel strands, assembled and held together by light weft yarns and sewn perpendicularly (Figure I. 3(a)). Its purpose is to support a load in a given direction and gives an anisotropic composite.

- Twill weave

Twill weave is a fabric in which each strand passed above two weft strands and each weft strand passes above two warp strands (Figure I. 3(b) and I. 3(d)). This type of weaving offers great flexibility by providing a good density of threads.

- Plain weave

Plain weave corresponds to a fabric in which each warp strand passes successively below and above each weft strand (Figure I. 3(c)). During its implementation, it is characterized by good properties in terms of stability. However, this type of weaving has many successive interlacements creating then a large shrinkage. This corresponds to the undulation of the fibers which can reduce the overall mechanical properties.

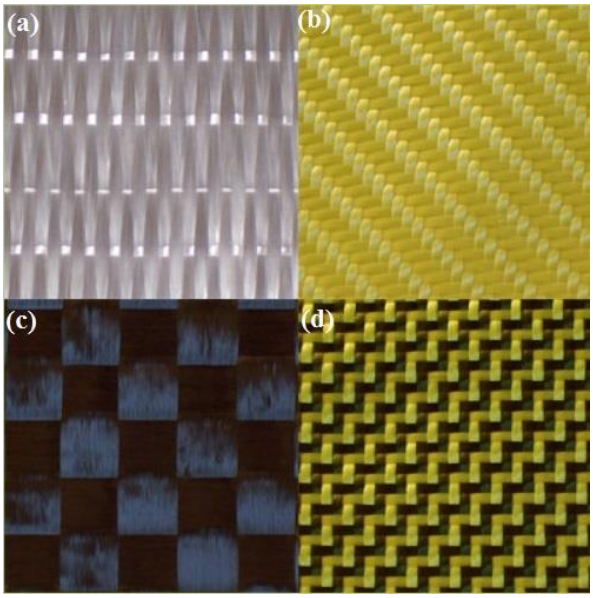

Figure I. 3: (a) Unidirectional woven glass fiber, (b) Twill of aramid fibers, (c) Carbon fiber plain, and (d) Twill of carbon fibers and aramid fibers.

1.2.2.2 Natural reinforcement

1.2.2.2.1 Composition and types

Contrary to synthetic fibers, natural fibers are renewable resources and are made of cellulose, hemicellulose, lignin, pectin, and wax. Generally, the quantity of pectin and wax are lower than other components. In addition, the percentage of all these constituents varies from one fiber to another because of their age and species. This percentage could also vary in different parts of the same plant [5]. Cellulose is the first abundant component in the vegetal world identified by Anselme Payen in 1938, suggesting that the cell walls of several plants consist of the same substance [6]. Cellulose is a linear polymer constituted by several glucose molecules ($C_6H_{10}O_6$) considered as a basic monomer and the repeat unit called cellobiose dimer as shown in Figure I. 4. Moreover, the cellulose chemical formula is $(C_6H_{10}O_6)_n$, where n is the number of the glucose molecule. This number differs from one plant to another depending on cellulose origin. As seen in Figure I. 4, the polymeric chain of the cellulose is oriented and possesses two ends, where one of them is reducing, meaning the hydroxyl group is free, and the other is non reducing, meaning that the hydroxyl group being engaged in an o-glycosidic bond [7].

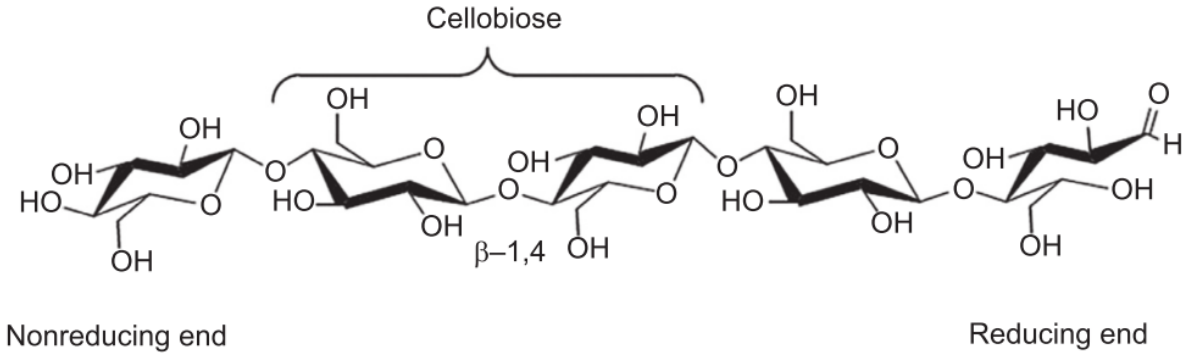

Figure I. 4: Cellulose Chain structure [8].

Hemicellulose is a polymer attached to several kinds of sugar units such as xylose ($C_5H_{10}O_5$), mannose ($C_6H_{12}O_6$), arabinose ($C_5H_{10}O_5$), glucose ($C_6H_{12}O_6$), glucuronic acid ($C_6H_{10}O_7$) as shown in Figure I. 5. Unlike cellulose, hemicellulose contains a large number of chain ramifications. It has a non-crystalline nature, and it is different from one plant to another [9]. It is very hydrophilic, soluble in alkali solution, and easily hydrolyzed in acids [10].

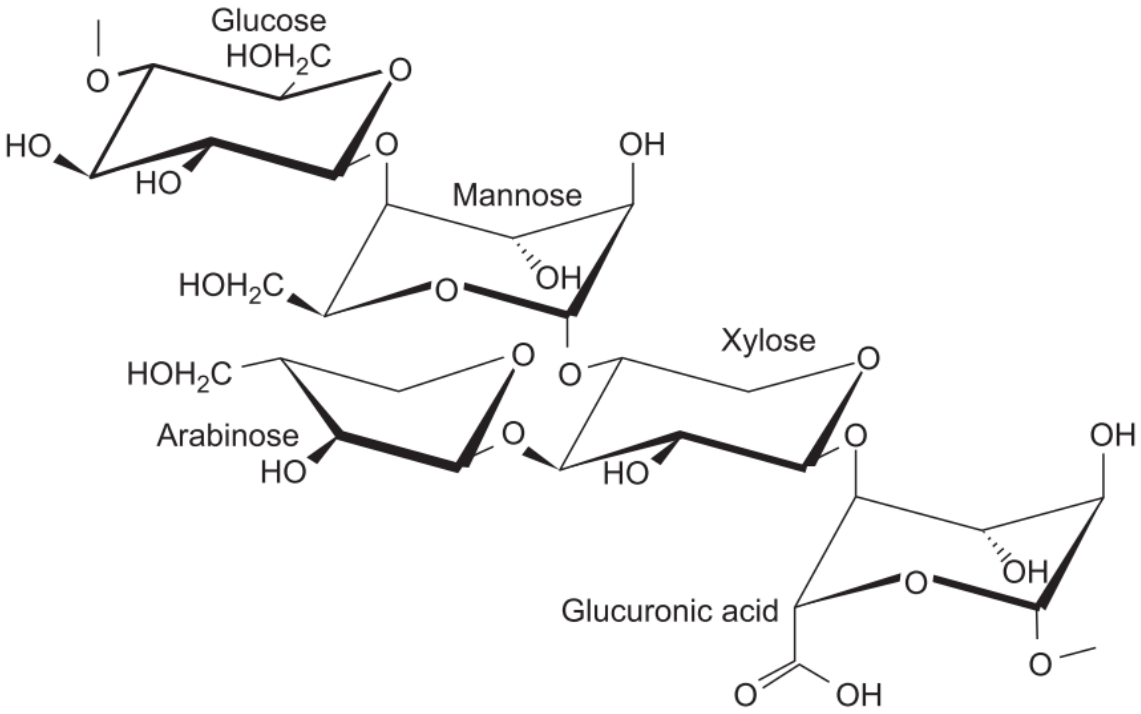

Figure I. 5: Hemicellulose structure [9].

Lignin, the second abundant biopolymer, is a three-dimensional polymer of phenolic nature (Figure I. 6). This component protects plants from attack by pathogenic organisms and contributes to the structural rigidity of cell walls. It has the hydrophobic character and is

totally amorphous. It gives coarse and stiff character to natural fibers [11,12], and its mechanical properties are less extent than those of cellulose [19]. The lignin is not hydrolyzed by acids, but it is soluble in alkali and easily condensable with phenol [13]. Consequently, different components of natural fibers have similar structures but vary widely as a function on their types [14]. In fact, the researchers have grouped the natural fibers into different types such as bast fibers, which are collected from the skin part of the plant or the bast surrounding the stem (such as flax, hemp, okra, jute); seed or fruit fibers, which are collected from seeds cases or from fruit of the plant (such as coir, cotton, milkweed, kapok); leaf fibers, which are derived from the leaves of the plant (such as abaca, cantala, pineapple, date palm, banana); grass fibers that are elongated sclerenchyma cells found mainly in the stems and leaves of plants (such as bagasse, Alfa, bamboo); and wood fibers, which are usually cellulosic elements mainly extracted from softwood trees such as timber and hardwood trees such as balsa.

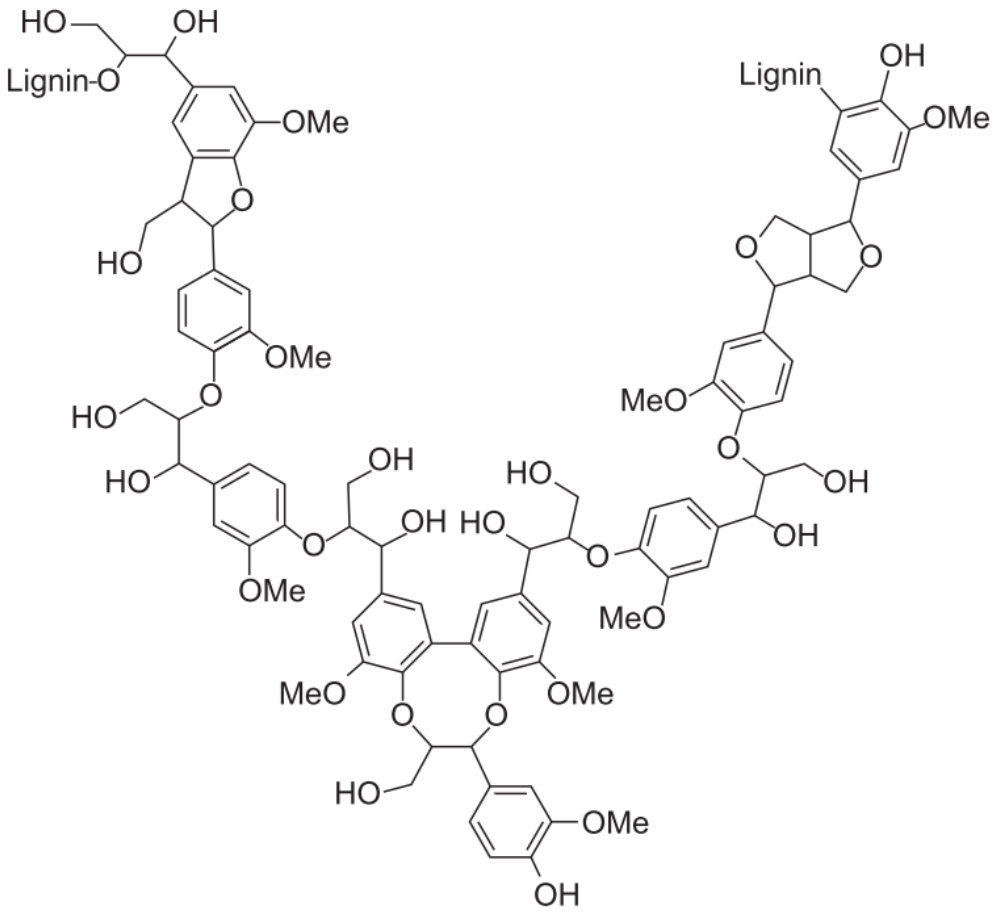

Figure I. 6: A lignin chain structure [15].

1.2.2.2.2 Chemical treatments of natural fibers

Natural fibers are characterized by a hydrophilic character, in contrast to thermoset matrices having a hydrophobic character. This incompatibility makes the adhesion between matrices and fibers imperfect. To overcome this problem, chemists consider that it is necessary to carry out the chemical modification of the surface. These chemical treatments include removal of impurities, addition of coupling agent, or grafting of compatibilizer groups to ensure the good adhesion between fiber and matrix and to improve the mechanical properties of material composites by increasing fiber strength and moisture resistance.

1.2.2.2.2.1 Alkaline treatment

The alkaline treatment or mercerization is a chemical treatment in which the natural fibers are immersed in a known concentration of aqueous sodium hydroxide (NaOH) for a given temperature and a period of time. The alkaline treatment modifies the surface of fibers by removing a certain rate of lignin, hemicellulose, wax, and oils covering the external surface of natural fibers [16]. For example, in the fibers of hemp, the alkaline treatment completely eliminates pectin without a residue, but the remaining lignin depends on the concentration of NaOH [17]. The partially removed lignin wax and hemicellulose enhance the matrix-fiber interface and ensure good adhesion between the matrix and natural fibers. If the treatment parameters are not optimized, the mercerization can cause fiber defibrillation, pore formation, and fiber embrittlement [18,19]. Alkaline treatment increases the density of fiber by removing non-cellulosic components (hemicellulose and lignin), which are less dense [20]. After mercerization, the fibers become more and more yellowish when the NaOH concentration increases [21].

1.2.2.2.2.2 Bleaching treatment

Bleaching or scouring treatment is used on the fibers after alkaline treatment. In this case, the neutralization is not necessary to make it on alkali-treated fibers. The bleaching treatment modifies the surface adhesion between matrix and fiber by removing residual lignin. Moreover, good bleaching results in an absence of lignin, which means that cellulose is the principal component of the fiber after this treatment. This component has a hydrophilic character such as thermosetting matrices, which are hydrophilic by nature. Consequently, this compatibility leads to a better adhesion between the matrix and the fiber.

The extracted cellulose is used typically to reinforce the composite [22], to extract the nanocrystaline cellulose [23], or to modify the surface of fiber to bring chemical characteristics, also named functionalization.

A mixture of hydrogen peroxide (H_2O_2) with sodium hydroxide (NaOH) and sodium chlorite ($NaClO_2$) with acetic acid (CH_3COOH) or chlorine dioxide gas (ClO_2) is used to extract the cellulose from alkali-treated natural fibers.

The process used to obtain bleached fibers is based on the dipping of natural alkali treated fibers in hydrogen peroxide mixed with sodium hydroxide (H_2O_2 + NaOH) or sodium chlorite mixed with alkali-acetic acid ($NaClO_2$ + CH_3COOH).

It is reported that the bleaching treatment by H_2O_2 requires repeating the process several times because the lignin does not readily withdraw from the first step as opposed to bleaching by the use of $NaClO_2$ where three times is sufficient [23]. After each bleaching, the washing is generally carried out [7]. The white fibers lead to the conclusion that the residual lignin is eliminated by the oxidation reactions which implies the increase of the surface ratio and therefore a better adhesion between the fiber and the matrix.

1.2.2.2.2.3 Silane treatment

As mentioned earlier, the hydrophilic nature of the natural fibers generated by the hydroxide groups as well as the hydrophobicity of the matrices makes the combination incompatible. In this case, the silane treatment improves the interface adhesion between natural fibers and matrix [24]. The silane molecules have bi-functional groups, where one of them reacts with the fibers and the other with the polymer.

The hydroxide groups in raw natural fiber surfaces are inactive. To activate them, the used fibers in functionalization treatments are already alkali-treated or bleached. Furthermore, the grafting rate of functionalization treatment is better in the case of bleached pretreated fibers than alkali pretreated fibers.

Functionalization of the fibers has been accomplished by the use of a silane coupling agent such as amino, methacryl, glycidoxy, mercapto, vinyl, trimethoxy, triethoxy, chlorine, azide, and alkylsilanes. Therefore, the silylation treatment reduces the number of hydroxyl groups of the natural fibers allowing the reduction of the absorption of the water and the improvement of the mechanical properties. In fact, the young modulus of fibers changes after silylation compared with the modulus of elasticity of raw natural fibers. On the other hand,

the tensile strength of the composite with silane-reinforced fibers is higher [24] as well as the flexural strength, which is also improved using this coupling agent [17]. Compared with alkali-treated fibers, the silane-treated fiber reinforced composite exhibits high mechanical properties [25].

1.2.2.2.2.4 Acetylation treatment

Acetylation treatment depicts a chemical reaction that introduces the acetyl function group into natural fibers. This treatment is carried out on fibers after its bleaching or its alkali treatment, which may destroy the hydrogen bonding in cellulosic hydroxyl groups to make them more reactive [26]. The hydroxyl groups are thereafter replaced by a hydrophobic acetyl group (CH3CO) inducing the change of the hydrophilic nature to the hydrophobic nature of the fiber [26,27].

The mainly used products for this treatment are the acetic anhydride, toluene, and a small amount of catalyst perchloric acid at 60 °C for 1-4 h [28]. Consequently, this treatment decreases the moisture rate of the fiber and increases the dimensional stability of the composites [29].

1.3 Comparison between natural and synthetic fibers

Despite their big differences in mechanical properties, natural fibers are useful as reinforcement in a composite material. It is true that natural fibers do not have the same mechanical properties as synthetic fibers. Nevertheless, in some specific applications, such as flexural or tensile, as can be the case for patios or composite beams used in park benches, they are interesting [30]. Tables I. 2 and I. 3 show some characteristics of these fibers [31–33]. Nevertheless, natural fibers defend themselves very well and can even compete with synthetic fibers. Table 4 summarizes quite well the advantages of each type of fiber.

Table I. 2: Comparison between natural fibers and Glass fibers.

	Natural fiber	**Glass fiber**
Density	Low	Double the natural fibers
Price	Low	Low but higher than natural fibers
Renewability	Yes	No
Recyclability	Yes	No
Energy expenditure	Low	High

Abrasion of machines	No	Yes
Health risk	No	Yes
Biodegradable	Yes	No

Table I. 3: Mechanical properties of different natural fibers and glass fibers.

Properties	**Fibers**					
	Glass	**jute**	**Coir**	**Hemp**	**Flax**	**Sisal**
Density (g/cm^3)	2.55	1.46	1.25	1.48	1.4	1.33
Young modulus (MPa)	2400	400 - 800	220	550 - 900	800 - 1500	600 - 700
Elongation modulus (MPa)	73	10 - 30	6	70	60 - 80	38
Elongation at yield (%)	3	1.8	15 - 25	1.6	1.2 – 1.6	2 - 3
Moisture rate (%)	-	12	10	8	7	11

In summary, natural fibers are less expensive and less damaging to the environment than synthetic fibers [34]. From a purely mechanical point of view, the synthetic fibers are interesting since their flexural, tensile, and impact properties are almost always superior to other fibers. However, in some applications, such as packaging, the goal is to have a fairly strong material but not necessarily the best; i.e. to have sufficient mechanical properties while reducing costs. It is in this area that natural fibers can be much more interesting than synthetic fibers, since they are less expensive. There are also all the environmental aspects that must be taken into account. Natural fibers usually have a lower net CO_2 balance than synthetic fibers [34]. They consume less energy, are biodegradable and usually cause less damage to shaping devices than fiberglass or carbon [35]. A last point of comparison is the density of natural fibers usually lower than that of synthetic fibers. This factor could be a key element in the field of transport, where weight reduction means a reduction in energy cost, thus saving money.

1.4 Type of thermoset composites

Different structures of the thermoset composite can exist including the laminated and simple composites. The simple thermoset composite is composed of one-layer, while the successive layers are in the laminated composite which termed plies. These plies can be made of fibers of the same nature or of different natures. In the latter case, the term “hybrid laminate” is used. The plies can have various configurations: thread, mat, fabric, etc. This section is devoted to further detailing the laminates.

1.4.1 Simple Laminated thermoset composites

Simple laminated composite consists of stacking successive layers of fibers of the same nature impregnated with resins. The orientation of the different plies is chosen according to the mechanical stresses that the structure must undergo. For example, the simple laminated composite of glass fibers is constituted only of layers of glass fibers which can be oriented at different angles.

1.4.2 Hybrid laminated thermoset composites

Faced with a strong need for lightening structures, composite materials are increasingly sought in the industrial sector, particularly in the transport sector. However, composite materials like any other material, in addition to being mechanically efficient, must perform other functions such as damping shock and vibration for good performance in service. To meet this double requirement, one of the solutions is to use the hybridization technique which consists in using within the same composite natural and synthetic fibers at the same time in order to exploit their respective advantages. In this context, this section is devoted to present the configurations used to gather both natural and synthetic fibers in the same structure.

1.4.2.1 Alternated layer configuration (inter-layer)

The inter-layer hybrids consisting of a series of layers, each of a different nature (Figure I. 7).

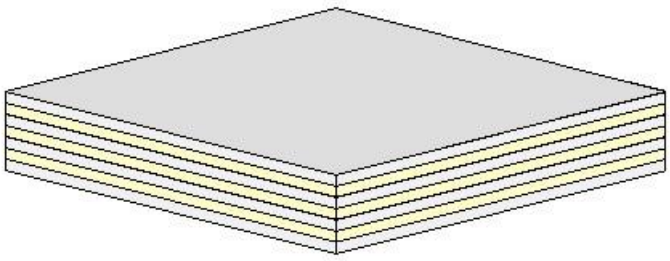

Figure I. 7: Alternated layer configurations (inter-layer).

1.4.2.2 Sandwich configuration

The principle of the sandwich technique is to applied on the core (lightweight material or structure characterized by the good properties in compression) two sheets or skin layers (characterized by the good tensile properties) (Figure I. 8). The main purpose of this process is to provide a structure that balances lightness and rigidity.

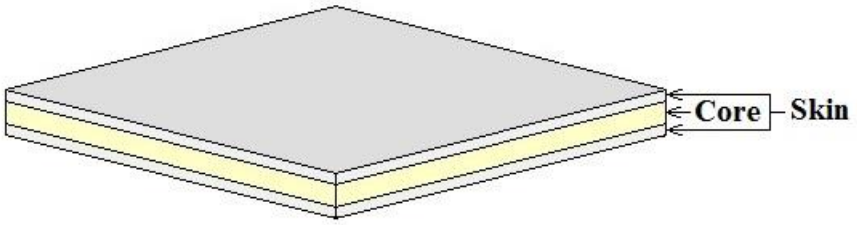

Figure I. 8: Sandwich configuration

In order to allow the sandwich structures to play their role efficiently, it is necessary to make sure of the perfect connection between core-skins, so as to distribute the forces between them. The assembly is carried out by bonding using compatible resins.

1.4.2.3 Intra-layer configuration

Intra-layer hybrid laminate consists of a sequence of identical layers which each one of them consisting of different reinforcement (Figure I. 9).

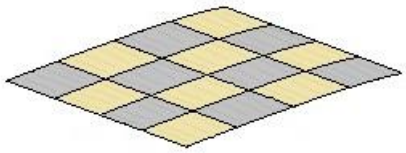

Figure I. 9: Intra-layer configuration (plain fabric).

1.5 Processing methods

After choosing the suitable thermoset matrix and natural fiber reinforcement, the processing phase is a key step because it influences the quality of the final product. There are various techniques to manufacture thermoset composite, including hand layup technique, resin

transfer molding process, and autoclave molding technique, which are emphasized and detailed in the following section.

1.5.1 Hand layup technique

Hand layup process is the most popular type of open molding. This technique is a slow and laborious manual method. This process involves the following steps: (1) coating the mold with a release anti-adhesive agent to avoid the sticking of the molded part to the mold surface, (2) forming the primer layer of the work piece by a gel coating, and (3) applying a layer of fine fiber reinforcing fabric (Figure I. 10). The used reinforcements in this kind of process are in the form of woven fabric and roving or chopped strands. The layer of the liquid matrix which is applied by a brush or a roller is placed in the fibers. This technique allows producing larger and more complex parts (such as swimming pools, storage tanks, boat hulls, bathtubs, duct and air handling equipment) with low-cost tools, but it consumes time and effort, and quality control is entirely dependent on the skill of laborers.

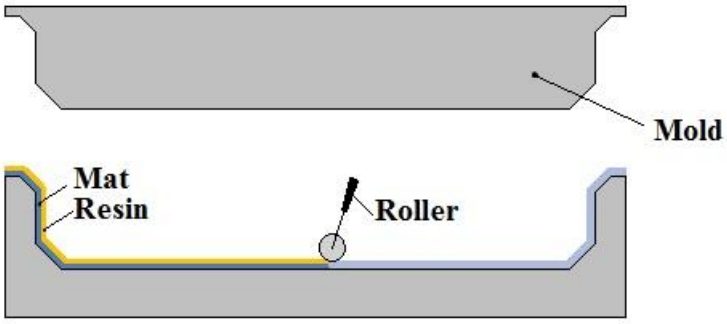

Figure I. 10: Hand layup process.

1.5.2 Resin transfer molding process

The resin transfer molding (RTM) process is a closed technique where the dry reinforcement is pre-shaped and oriented in the backbone of the real part known as the pre- form and which is inserted into a matched die mold (Figure I. 11). Then, the heated mold is closed and the liquid resin is injected. After curing, the mold is opened to retrieve the resultant composite. This technique has a number of advantages including the good surface finish of the components, minimal percentage of volatile emissions during processing, ability to mold complex structural shapes and bright shapes, low resultant voids, single use of low injection pressure. This technique also has disadvantages, such as the slowness of the curing time and the difficulty of using the complex parts in addition to the possibility of displacement of the

reinforcement during the transfer of the resin. This technique is investigated in various applications such as the manufacture of truck panels, boat hulls, wind turbine blades, aerospace and automotive parts, medical composites, bathroom accessories, etc.

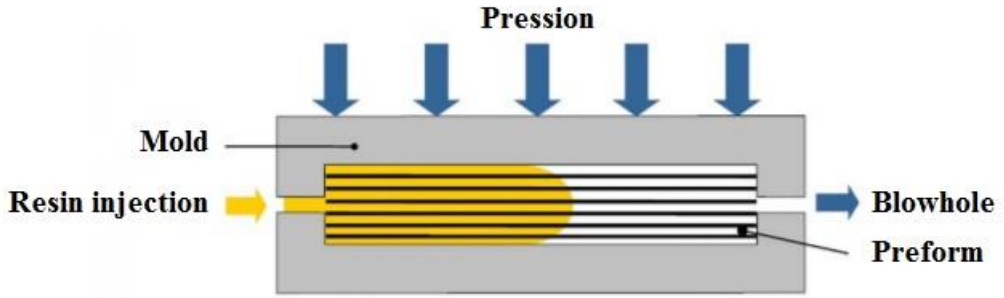

Figure I. 11: RTM process.

1.5.3 Autoclave molding technique

Autoclave molding is one of the open molding processes where the molded part is cured by application of the vacuum, heat, and pressure of the inert gases. The molded part (or piece) is placed in a plastic bag, where the air is exhausted by a vacuum pump. This removes air inclusions and volatile products from the molded part (Figure I. 12). Then, heat and inert gas pressure are applied in the autoclave causing curing and densification of the material. Finally, autoclave curing enables fabrication of consistent homogeneous materials. The method is relatively expensive and is used for manufacturing high-quality aerospace products. This process has some advantages such as the pressure that helps bond composite layers, the ability to manufacture pieces with high fiber loads, as well as high-quality products.

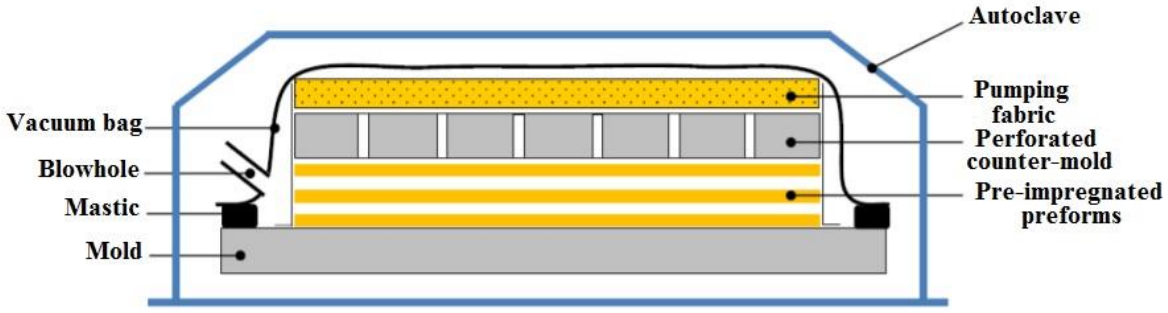

Figure I. 12: Autoclave molding technique

In this thesis, the technique used to elaborate different composites are hand layup process.

1.5.4 Effect of hybridization on the mechanical properties of the thermoset composite

Hybrid composites can be produced from natural fibers only (e.g. Raffia/jute), synthetic fibers (e.g. carbon/glass) or a combination of natural and synthetic fibers (e.g. jute/glass). In order to improve the properties of natural fibers, hybridization with synthetic fibers can be valuable. In this regard, several researchers have focused on the hybridization of natural fibers with synthetic fibers including glass fibers.

Davoodi et al. [36] studied a composite Kenaf/glass hybrid based an epoxy matrix. Their material is used for car bumpers. They aimed to find an alternative solution to a composite reinforced with strand chopped mat glass fibers in a thermoplastic matrix. Their results showed that the mechanical properties of the composite emanating from the combination of Kenaf with glass fibers were clearly superior to those of the glass composite alone. Therefore, hybridization of the glass with Kenaf provides mechanical strength to the original glass composite.

Studies have been conducted on the tensile and impact behavior of fiberglass and palm fiber based composite in an epoxy resin [37]. The hybridization of glass fibers with palm fibers has clearly improved the tensile and impact properties of the palm composite alone. Better impact resistance has been observed for hybrid composites when glass fibers are placed outside.

Hybridization of glass and jute folds in a polyester resin was analyzed in this reference [38]. Tensile, flexural and shear tests were carried out. It has been shown that the integration of the glass plies in the jute/epoxy composite has improved the mechanical properties of the starting jute/epoxy composite. They observed that the change in stacking sequence had a significant effect on the bending and shear stress of hybrid composites. In conclusion, it was pointed out that the hybrid laminate with two layers of glass on both sides of the jute layers was the best combination in terms of mechanical properties and cost.

Moreover, the hybridization effect of the flax/glass fibers based phenolic composite was studied [39], by varying the volume fraction of the glass fibers. The reinforcements used are unidirectional. The authors also investigated the influence of the stacking sequence between the flax and glass folds. In addition to experimental tests, they used the law of mixtures to predict the properties of hybrid tensile laminates. In view of the results, the glass composite obviously has high mechanical properties compared to the flax composite. Two types of breakage were considered in their work because of the difference between the elongation at break of flax fibers and that of glass fibers. If the volume fraction of the glass is important,

the flax fibers break first, but the hybrid composite should break for elongation at break equal to that of the glass composite. However, if the volume fraction of the flax fibers is important, the hybrid laminate should break at an elongation at break equal to the elongation at break of the flax composite. Moreover, it can be noted that the elongation at break increases with the volume fraction of the glass fibers. They have also demonstrated that the mechanical properties, particularly the Young's modulus of the hybrid composites have improved with the increase of the volume fraction of the glass fibers. In addition, the stacking sequence also has a significant impact on the mechanical properties of hybrid laminate composites. According to the authors of the study, the stacking sequence has a significant effect on the tensile strength in contrast to the Young's modulus.

In the same context, Amico et al. [40] investigated the hybrid composites of polyester resin reinforced with sisal and glass fibers. Various tests have been carried out on these materials. They showed that the stacking sequence influences the mechanical properties of hybrid materials. Their results also demonstrated that the sisal-glass hybrid composites had mechanical properties (flexural modulus and impact strength, particularly) close to those of a glass composite. According to these different studies, the best mechanical properties are obtained when the layers of which the fibers have high mechanical performances (stiffness, strength) are placed on either side of the composite.

1.6 Modelling of the mechanical behavior of laminated composites

As previously described, the laminated composites are obtained by superposition of several layers of the same or different nature. Each monolayer consisting of reinforcements pre-impregnated with resin. These reinforcements are most often unidirectional long fibers, short fiber or woven fibers. Moreover, the orientation of the reinforcement varies from one layer to the other of the laminated composite. The layer orientations are chosen to obtain specific mechanical properties. In addition, depending on the intended applications, the number of layers of laminate can vary from ten to several hundred.

The deformations of homogeneous and isotopic materials can be described quite simply with the elastic moduli and deformation stresses, which are the basic properties of raw materials. In the case of composites, each element has a different role and it is the combination of these properties that gives the final material its own characteristics. Although these final characteristics are the result of complex interactions between the reinforcement and the

matrix, it is possible to give a simple estimation using the "Mixtures law" applied to laminated composite as follows (Equation (1)):

$$W_c = \rho_c \times V_c = \rho_f . V_f + \rho_m . V_m \qquad with \qquad V_f + V_m = 1 \tag{1}$$

Which:

- V_f = Volume fraction of the fiber
- V_m = Volume fraction of the matrix
- W_c = Estimated weight of the composite
- ρ_f = Fiber density
- ρ_m = Matrice density

These are theoretical values; in fact, the presence of voids makes $V_f + V_m \leq 1$. For example, the elasticity modulus in tensile load can be estimated based on the respective modules of the fiber and the matrix (Equation (2)). This equation can be modelled by a system of associated springs in parallel.

$$E_{c,t} = E_{f,t} . V_f + E_{m,t} . V_m \tag{2}$$

Which,

- $E_{c,t}$ = Estimated Young modulus of the composite
- $E_{f,t}$ = Elasticity modulus in tensile of the fiber
- $E_{m,t}$ = Elasticity modulus in tensile of the matrix
- V_f = Volume fraction of fibers
- V_m = Volume fraction of matrix

In the case of the elasticity modulus in bending, the model corresponds to a series association of the springs. Thus, the corresponding equation would be (Equation (3)):

$$E_{c,f} = \frac{E_{f_f} . E_{m_f}}{E_{f_f} . V_m + E_{m_f} . V_f} \tag{3}$$

Which,

- $E_{c,f}$ = Estimated elasticity modulus of the composite in bending.
- $E_{f,f}$ = Elasticity modulus of the fiber in bending.

- $E_{m,f}$ = Elasticity modulus of the matrix in bending.
- V_f = Volume fraction of fibers
- V_m = Volume fraction of matrix

The two previous equations (equations (2) & (3)) allow to determine the upper ($E_{c,t}$) and lower ($E_{c,f}$) limits of the elasticity modulus of the composite, modelled by a linear curve and a hyperbola, respectively (Figure I. 13). Therefore, the real modulus of the composite is between these two curves.

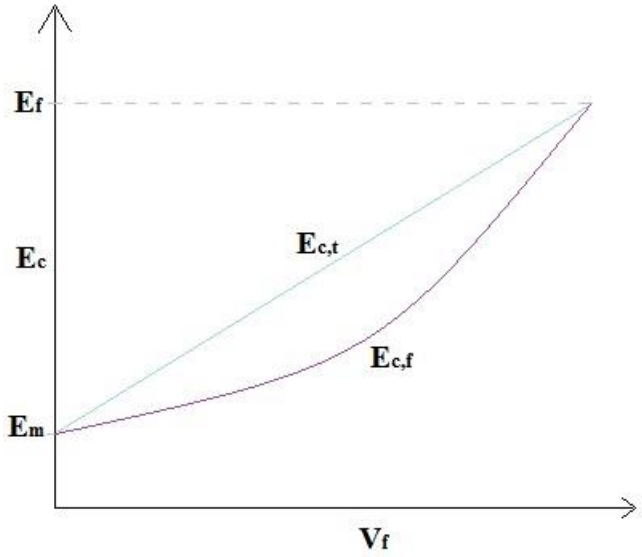

Figure I. 13: Modelling according the mixture law.

It should be reminder that some assumptions are considered to establish the modelling:

- The fibers are perfectly bonded to the matrix.
- The laminated materials are composed of several homogeneous and elastic layers stacked periodically and perfectly bonded to each other in the z-direction.
- The structure studied is in the form of a rectangular prism and its thickness is negligible (according to z) compared to the other two dimensions and thus remains constant.
- The normal to the midplane remains straight and normal to the median plane after deformation (assumption of small deformations).
-

In the same context, the homogenization technique was used by Nakhlaoui S. [41] have determine the behavior of the laminated composites using the properties of each layer and its corresponding thickness. This method is based on partially inverting the behavior law of each layer, then coupling the average stiffness tensor of all layers before partially re-reversing the behavior law (this technique is more detailed in Chapter IV). Using this model, she concluded that the laminated composite material whose layers exhibit an isotropic behavior gives a transverse isotropic material which isotropic axis is that of the stack. In addition, for a laminated composite material whose layers exhibit orthotropic behavior, the homogenized behavior is orthotropic.

References

[1] Saheb DN, Jog JP. Natural Fiber Polymer Composites : A Review 1999;18:351–63.

[2] Trindade WG, Hoareau W, Megiatto JD, Razera IAT, Castellan A, Frollini E, et al. Thermoset Phenolic Matrices Reinforced with Unmodified and Surface-Grafted Furfuryl Alcohol Sugar Cane Bagasse and Curaua Fibers : Properties of Fibers and Composites. Biomacromolecules 2005;6:2485–96.

[3] Achary PS, Ramaswamy R. Reactive Compatibilization of a Nitrile Rubber / Phenolic Resin Blend : Effect on Adhesive and Composite Properties. Appl Polym Sci 1998;69:1187–201.

[4] Orchin M, Macomber RS, Pinhas AR, Wilson RM. THE VOCABULARY AND CONCEPTS OF ORGANIC CHEMISTRY. Second. John Wiley & Sons, Inc., Hoboken, New Jersey; 2005.

[5] Ramamoorthy SK, Skrifvars M, Persson A. A Review of Natural Fibers Used in Biocomposites : Plant , Animal and Regenerated Cellulose Fibers. Polym Rev 2015;55:37–41. doi:10.1080/15583724.2014.971124.

[6] Amel BA, Paridah MT, Sudin R, Anwar UMK, Hussein AS. Effect of fiber extraction methods on some properties of kenaf bast fiber. Ind Crop Prod 2013;46:117–23. doi:10.1016/j.indcrop.2012.12.015.

[7] Savoye L. Reduction de l'impact environnemental du blanchiment au peroxyde d'hydrogène en milieu alcalin des pâtes mécaniques. 2011.

[8] Bledzki AK, Jaszkiewicz A. Mechanical performance of biocomposites based on PLA and PHBV reinforced with natural fibres - A comparative study to PP. Compos Sci Technol 2010;70:1687–96. doi:10.1016/j.compscitech.2010.06.005.

[9] Malha M. Mise en oeuvre, Caractérisation et modélisation de matériaux compoites: Polymère thermoplastique renforcé par des fibres de Doum. MOHAMMED V - Agdal, Faculté des Sciences Rabat, 2013.

[10] John MJ, Anandjiwala RD. Recent developments in chemical modification and characterization of natural fiber-reinforced composites. Polym Compos 2008:187–207. doi:10.1002/pc.20461.

[11] Ali M, Islam MN, Mian AJ, Sarwaruddin Chowdhury AM. Modification of Jute Fibre by Sulphonation for Diverse Textile Use. Text Inst 2014:37–41. doi:10.1080/00405000108659554.

[12] Reddy N, Yang Y. Structure and properties of high quality natural cellulose fibers from cornstalks. Polymer (Guildf) 2005;46:5494–500. doi:10.1016/j.polymer.2005.04.073.

[13] Ofomaja AE, Naidoo EB. Biosorption of copper from aqueous solution by chemically activated pine cone : A kinetic study. Chem Eng J 2011;175:260–70. doi:10.1016/j.cej.2011.09.103.

[14] Komuraiah A, Kumar NS, Prasad BD. Chemical Composition of Natural Fibers and its Influence on their Mechanical Properties. Mech Compos Mater 2014;50:359–76. doi:10.1007/s11029-014-9422-2.

[15] Arrakhiz FZ, Elachaby M, Bouhfid R, Vaudreuil S, Essassi M, Qaiss A. Mechanical and thermal properties of polypropylene reinforced with Alfa fiber under different chemical treatment. Mater Des 2012;35:318–22. doi:10.1016/j.matdes.2011.09.023.

[16] Faruk O, Bledzki AK, Fink HP, Sain M. Biocomposites reinforced with natural fibers: 2000-2010. Prog Polym Sci 2012;37:1552–96. doi:10.1016/j.progpolymsci.2012.04.003.

[17] Beckermann GW, Pickering KL. Engineering and evaluation of hemp fibre reinforced polypropylene composites: Fibre treatment and matrix modification. Compos Part A Appl Sci Manuf 2008;39:979–88. doi:10.1016/j.compositesa.2008.03.010.

[18] Al-Khanbashi A, Al-Kaabi K, Hammami A. Date palm fibers as polymeric matrix reinforcement: Fiber characterization. Polym Compos 2005;26:486–97. doi:10.1002/pc.20118.

[19] Ramamoorthy SK. Properties and Performance of Regenerated Cellulose Thermoset. Of Boras, 2015.

[20] Vardhini KJV, Murugan R, Selvi CT, Surjit R. Optimisation of alkali treatment of banana fibres on lignin removal. Indian J Fibre Text Res 2016;41:156–60.

[21] Fook LT, Yatim JM. An experimental study on the effect of alkali treatment on properties of kenaf fiber for reinforced concrete elements. Int J Res Eng Technol 2015;4:37–40.

[22] Verma D, Gope PC. The use of coir/coconut fibers as reinforcements in composites. biofiber, 2015, p. 285–319. doi:10.1533/9781782421276.3.285.

[23] Fardioui M, Stambouli A, Gueddira T, Dahrouch A, Qaiss AEK, Bouhfid R. Extraction and Characterization of Nanocrystalline Cellulose from Doum (Chamaerops humilis) Leaves: A Potential Reinforcing Biomaterial. J Polym Environ 2016. doi:10.1007/s10924-016-0784-5.

[24] Arrakhiz FZ, El Achaby M, Kakou AC, Vaudreuil S, Benmoussa K, Bouhfid R, et al. Mechanical properties of high density polyethylene reinforced with chemically modified coir fibers: Impact of chemical treatments. Mater Des 2012;37:379–83. doi:10.1016/j.matdes.2012.01.020.

[25] Suresh Kumar SM, Duraibabu D, Subramanian K. Studies on mechanical, thermal and dynamic mechanical properties of untreated (raw) and treated coconut sheath fiber reinforced epoxy composites. Mater Des 2014;59:63–9. doi:10.1016/j.matdes.2014.02.013.

[26] Paul A, Joseph K, Thorna S. EFFECT OF SURFACE TREATMENTS ON THE ELECTRICAL PROPERTIES OF LOW-DENSITY POLYETHYLENE COMPOSITES REINFORCED WITH SHORT SISAL FIBERS. Compos Sci Technol 1997;57:67–79.

[27] Bessadok A, Marais S, Gouanve F, Colasse L, Zimmerlin I, Roudesli S, et al. Effect of chemical treatments of Alfa (Stipa tenacissima) fibres on water-sorption properties. Compos Sci Technol 2007;67:685–97. doi:10.1016/j.compscitech.2006.04.013.

[28] Sampathkumar D, Punyamurth R, Venkateshappa SC. Effect of Chemical Treatment on Water Absorption of Areca Fiber. J Appl Sci Res 2012;8:5298–305.

[29] Venkatachalam N, Navaneethakrishnan P, Rajsekar R, Shankar S. Effect of Pretreatment Methods on Properties of Natural Fiber Composites : A Review. Polym Polym Compos 2016;24:555–66.

[30] Klyosov AA. Wood-Plastic Composites. vol. 53. New-Jersey: Wiley-Interscience; 2007. doi:10.1017/CBO9781107415324.004.

[31] Mwaikambo LY, Ansell MP. Mechanical properties of alkali treated plant fibres and their potential as reinforcement materials. Mater Sci 2016;41:2483–96. doi:10.1007/s10853-006-5075-4.

[32] Kalia S, Kaith BS, Kaur I. Pretreatments of Natural Fibers and their Application as Reinforcing Material in Polymer Composites - A Review. Polym Eng Sci 2009;49:1253–72. doi:10.1002/pen.

[33] Wambua P, Ivens J, Verpoest I. Natural fibres : Can they replace glass in fibre reinforced plastics ? Natural fibres : can they replace glass in fibre reinforced plastics ? Compos Sci Technol 2003;63:1259–64. doi:10.1016/S0266-3538(03)00096-4.

[34] Joshi S V., Drzal LT, Mohanty AK, Arora S. Are natural fiber composites environmentally superior to glass fiber reinforced composites? Compos Part A Appl Sci Manuf 2004;35:371–6. doi:10.1016/j.compositesa.2003.09.016.

[35] Franck RR. Bast and other plant fibers. Cambridge, Angleterre: Woodhead Publishing Limited in association with The Textile Institute.; 2005.

[36] Davoodi MM, Sapuan SM, Ahmad D, Ali A, Khalina A, Jonoobi M. Mechanical properties of hybrid kenaf/glass reinforced epoxy composite for passenger car bumper beam. Mater Des 2010;31:4927–32. doi:10.1016/j.matdes.2010.05.021.

[37] Hariharan ABA, Khalil HPSA. Lignocellulose-based hybrid bilayer laminate composite: Part I - Studies on tensile and impact behavior of oil palm fiber-glass fiber-reinforced epoxy resin. J Compos Mater 2005;39:663–84. doi:10.1177/0021998305047267.

[38] Ahmed KS, Vijayarangan S. Tensile, flexural and interlaminar shear properties of woven jute and jute-glass fabric reinforced polyester composites. J Mater Process Technol 2008;207:330–5. doi:10.1016/j.jmatprotec.2008.06.038.

[39] Zhang Y, Li Y, Ma H, Yu T. Tensile and interfacial properties of unidirectional flax / glass fiber reinforced hybrid composites. Compos Sci Technol 2013;88:172–7. doi:10.1016/j.compscitech.2013.08.037.

[40] Amico SC, Angrizani CC, Drummond ML. Influence of the stacking sequence on the mechanical properties of glass/sisal hybrid composites. J Reinf Plast Compos 2010;29:179–89. doi:10.1177/0731684408096430.

[41] Nekhlaoui S. COMPORTEMENT HYGROTHERMOELASTIQUE DES MATERIAUX COMPOSITES STRATIFIES. FACULTE DES SCIENCES RABAT, 2005.

CHAPTER II

STRUCTURAL LAMINATED HYBRID COMPOSITES BASED ON RAFFIA AND GLASS FIBERS: EFFECT OF ALKALI TREATMENT, MECHANICAL AND THERMAL PROPERTIES*

2.1 Abstract

This work deals with the effect of the alkaline treatment of laminated hybrid composite materials based on Raffia fibers and glass fibers in a sandwich structure. Structural analysis (Fourier Transform Infrared Spectroscopy) has shown that most of the changes caused by the alkaline treatment of Raffia fibers involve the removal of fiber surface from a certain amount of wax, hemicellulose, pectin, and lignin. These changes are at the origin of the improvement of the mechanical properties of the composites. Flexural modulus results show an increase of 3.4 GPa to 3.6 GPa for the untreated and treated Raffia fiber sandwich composites, respectively. The degree of interfacial adhesion quantified by a droplet test shows that the alkaline modification reveals a sharp increase in shear stress for processed Raffia fibers with a 38% gain compared to untreated fibers. In addition, the measurement of the thermal conductivity has proved that the alkaline treatment decreases the thermal conductivity of the fibers. Finally, the mixing rule technique was used to predict the flexural modulus of the laminates using the mechanical parameters of each layer and the result was compared to the experimental data. It is assumed that Raffia fiber treatments will support the development of synthetic fiber reinforced sandwich polymer composites for industrial applications.

---

*

Reprinted in part with permission from Ouarhim W., Essabir H., Bensalah M.O., Zari N., Bouhfid R., Qaiss A. (2018) “Structural laminated hybrid composites based on raffia and glass fibers: Effect of alkali treatment, mechanical and thermal properties”. **Composites Part B: Engineering**, 154, 128-137.

2.2 Résumé

Ce travail s'intéresse à l'effet du traitement alcalin des fibres de Raphia sur les matériaux composites hybrides (Fibre de verre/ fibres de Raphia/ fibres de verre) en structures sandwich. L'analyse structurelle (par spectroscopie infrarouge à transformée de Fourier) a montré que le traitement alcalin affecte essentiellement la surface de la fibre, et ce par l'enlèvement d'une quantité de la cire, hémicellulose, pectine et lignine. Ces changements sont à l'origine de l'amélioration des propriétés mécaniques des composites. Le module de flexion s'est accru de 3.4 GPa à 3.6 GPa, respectivement pour un composite sandwich à fibre de Raphia non-traité et traité. Le degré d'adhésion interfaciale, quantifié par le test des gouttelettes, montre une forte hausse de la contrainte de cisaillement pour les fibres de Raphia traitées, avec un gain de 38% par rapport à celles non-traitées. En outre, la mesure de la conductivité thermique a montré que le traitement alcalin diminue la conductivité thermique des fibres. Finalement, la loi de mélange est utilisée pour prédire le module de flexion des laminés moyennant les paramètres mécaniques de chaque couche, les résultats sont comparés aux données expérimentales. Il convient de conclure que les traitements chimiques de fibres de Raphia soutiendront le développement de composites polymères sandwich renforcés de fibres synthétiques pour des applications industrielles.

2.3 Introduction

The most used and best performing fibers are synthetic fibers because of their rigidity. However, growing environmental awareness and new legislation have stimulated the use of biofibre-reinforced polymer composites to meet industrial weight requirements [1,2]. Recently, the concept of green composite poses challenges to designers as a source of biodegradable reinforcing materials replacing synthetic fibers for new composites. Compared with synthetic fibers (glass, carbon or aramid fibers), natural fibers emerge because of their low cost, light weight, availability from renewable resources, thermal and acoustic insulation properties. [1-3]. However, they also have drawbacks, namely: low resistance to moisture and fire, incompatibility with the hydrophobic polymer matrix, a limited treatment temperature, a lower durability and a variation in quality and price [4-6]. Thus, the hybridization of natural and synthetic fibers seems promising.

There are two types of hybridization: interlaminated and intra-stratified. Interlamination or rolling consists of depositing different layers of fibers while in the case of laminates or intra-laminates, the two fibers are entangled in the same layer. By hybridizing, the disadvantages of one fiber can be offset by the virtues of the other [7,8]. The composite that combines synthetic fibers and natural fibers is characterized by high stiffness and low density. This hybrid composite retains good mechanical performance, but its cost is significantly reduced compared to the fully synthetic fiber reinforced composite [9,10]. Also, the factors influencing the final properties of the hybrid composites are: the nature of the matrix, the overall fiber content, the relative volume of the fibers, the molding process, the fiber-matrix interface [11]. Thus, the hybrid composite is in principle a laminated or sandwich structure. The most common structural composites are laminate composites and sandwich structure. A sandwich structure is a special form of laminated composite. It is composed of two thin face sheets and a thick lightweight core glued together [12-14]. Due to their extremely low weight, which enables the reduction of total weight, fuel consumption, transverse rigidity and corrosion resistance, they are widely used in the automotive industry, marine structures, infrastructure and defense. In structural sandwiches, the front sheets are for the most part identical in material and thickness, and are mainly resistant to plane and flexural loads. These structures are called symmetric sandwich structures [15]. However, in some particular cases, the face sheets may vary in thickness or material due to loading conditions or work environment. This configuration is called an asymmetrical sandwich structure [15]. In

addition, each layer is formed by immersing the fibers in the matrix resin material. The layers are usually orthotropic (i.e. with principal properties in the orthogonal direction of each layer) or transversely isotropic (with isotropic properties in the transverse plane) with the laminate then exhibiting anisotropy (with variable direction of main properties), orthotropy or near isotropy [16].

The glass fibers are used in the external faces of the structured sandwich composite, in addition, the core is filled with natural fibers. The natural fibers used are Raffia fibers which are characterized by their particular structure consisting of a superposition of layers. Since the fibers are derived from the epidermis of the leaves, the external structure of the layer in contact with the air is a juxtaposition of filaments parallel in the length direction and the underside of the fiber being in contact with the body of the sheet, has an alveolar structure in the form of a "honeycomb" [17]. In view of these advantages, the present study reports the mixture of Raffia and glass fibers in a structural sandwich in the thermosetting matrix. The method used to develop composites is based on the manual technique of liquid compression molding. A series of mechanical tests (morphological and structural characteristics, mechanical and thermal tests) are carried out for the laminate manufactured. The effect of laminated composite and superposed layers on mechanical properties is investigated. The flexural modulus prediction is calculated, and finally, the comparison between the experimental module and the predictive module is studied. The idea of using Raffia fibers in a thermoset matrix is not only to minimize the environmental impact of raffia fibers as residues, but also to maximize performance, functionality, sustainability, and profitability of these natural resources. The Raffia fibers could have a promising future as a new reinforcement in a thermoset sandwich composites, as a substitute for a large part of glass fibers, not only because of their low cost, low density, environmental friendliness and good mechanical properties but also in a context of valorizing abundant and unexploited Moroccan resources.

2.4 Materials and methods

2.4.1 Materials

The used raffia fibers are obtained from the raffia palm tree which grows in the wet soil in Madagascar. Moreover, the used glass fiber is chopped strand mat and it is issued by the SODEVIC (Morocco). The used resin in the current work is an epoxy SO 184 delivered by SORETP company from Casablanca Morocco. The chemical products used to treat the fiber

surface are NaOH (sodium hydroxide, Sigma Aldrich, 98%), and CH_3-COOH (Acetic acid, Riedel-de haën, 99–100%).

2.4.2 Raffia fiber preparation

The Raffia fibers are soaked in tap water to clean them. The resulting fibers are dried for 3 hours. Next, in order to reduce the size of the fiber, in particular the width, the hand carding is used, as shown in Figure II. 1.

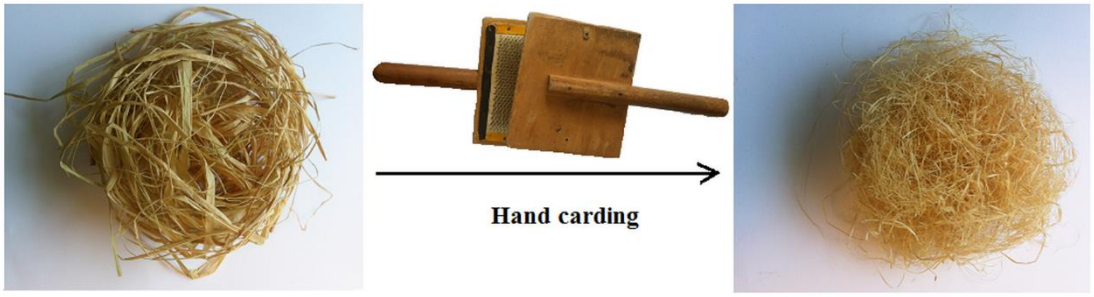

Figure II. 1: Reducing fiber width using hand carding.

Then, a few quantities of prepared fibers are treated by alkali treatment (NaOH) with 8 wt.% for 8 hours at ambient temperature. Before obtained the final reinforcement, they are neutralized using acetic acid.

2.4.3 Raffia fiber surface treatment

2.4.3.1 Alkali treatment

The raffia fibers were treated with a solution of NaOH at a concentration of 8% (1.6 mol/L sodium hydroxide aqueous solution) for 8 hours at room temperature then treated with acetic acid (100 mL) to neutralize the remaining hydroxide and finally washed with distilled water for several times. The fibers were air-dried for 12 hours before further use.

2.5 Experimental Procedure

2.5.1 The mold preparation

The used mold is composed of two plates of stainless steel with a screw-nut system to ensure the samples compression (Figure II. 2). The sample's dimension is (120 x 120) mm^2. The mold design authorizes the liberation of the excess resin after the compression of

impregnated fibers. To facilitate the demolding of the sample, a wax is used to cover the mold. Then, a transparent film is used to assure smooth samples surfaces.

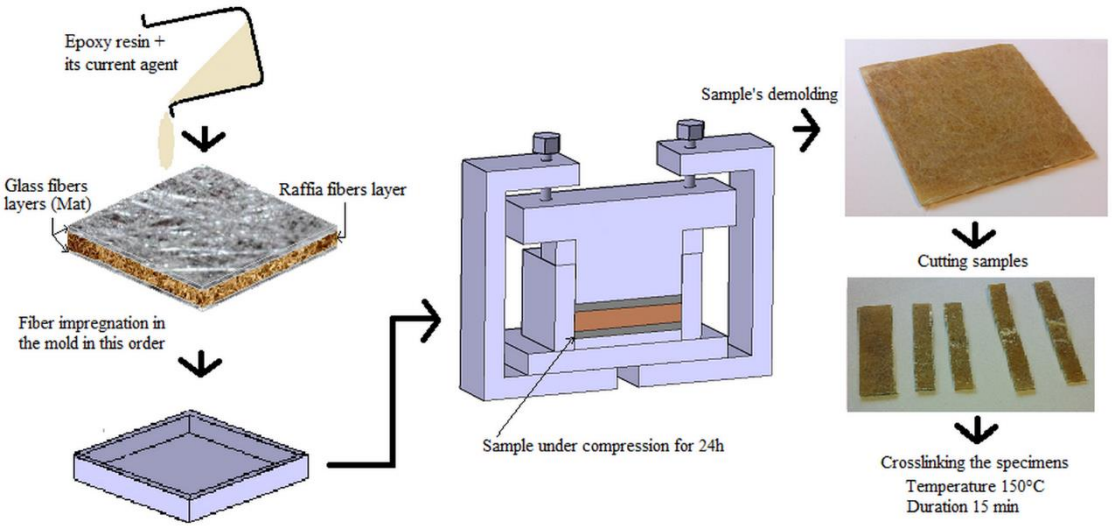

Figure II. 2: Different steps to elaborate the final sandwich composite.

2.5.2. ***Composite preparation***

The used method to elaborate all different composites is manual liquid composite molding. To manufacture the treated and untreated Raffia sample, a small quantity of resin is poured into the mold. The epoxy resin and its hardener were taken in the ratio of 2:1. The cleaned Raffia fibers are impregnated and distributed randomly in the resin, and subsequently the mold is closed.

Then shims were placed between the two plates to ensure the desired thickness (2 mm) and the four nuts are tightened at the same time until the shims stop moving. Finally, the sample is cured in the mold for 24 hours. It should be noted that the same method is applied in the case of glass fibers and sandwich samples. In this case, the thickness expected for the glass fiber samples is 1 mm. The sandwich samples consist of 3 layers as shown in Figure II. 2. The face sheets are made of 1 mm thick glass fibers, and the core consists of treated or untreated Raffia fibers of a thickness 2 mm. The percentage of Raffia fibers is greater than the percentage of glass fibers. However, 4 mm is the thickness required for sandwich samples (Table II. 1).

For the selected epoxy resin, the crosslinking temperature and crosslinking time are:

$$T_{Crosslinking} = 150°C \quad \text{and} \quad t_{Crosslinking} = 15\ min$$

Thus, the cutting samples are placed in the oven Venticell (MMM Med center Einrichtungen GmbH, USA) respecting the above data.

Table II. 1: Composite formulation

Designation		**Raw Raffia fiber layers (2mm)**	**Treated raffia fiber layers (2mm)**	**Glass fiber layers (1mm)**
RFC	Raw Raffia fiber composite	1	0	0
TRFC	treated raffia fiber composite		1	
GFC	Glass fiber composite	0	0	2
SCGRG	Sandwich composite: Glass fiber/ Raw Raffia fiber/ Glass fiber	1	0	2
SCGTRG	Sandwich composite: Glass fiber/ Treated Raffia fiber/ Glass fiber	0	1	2

2.6 Characterizations

2.6.1 Scanning electron microscopy (SEM)

Scanning electron microscopy (SEM) was used to evaluate the surface morphologies of untreated and treated Raffia fibers, the dispersion/distribution of fibers in the polymer matrix and to illustrate the interfacial adhesion between fibers and matrix. To obtain clean and accuracy fracture faces, all composites samples were cryo-fractured under liquid nitrogen.

2.6.2 Fourier transform infrared (FTIR)

Fourier transform infrared (FTIR) spectroscopy is used to determine the assignment of absorbance bands to specific molecular structures. The used FTIR is an ABB Bomem FTLA 2000-102 spectrometer (ATR: Specac 2 Golden Gate). Each spectrum was obtained with an accumulation of 16 scans with a resolution of $4cm^{-1}$.

2.6.3 Porosity

To determine the porosity of different elaborated composites, the density of each one of them is measured with the gas pycnometer (micromeritics AccuPyc II 1340, USA). This apparatus uses the gas displacement method to measure volume. The used gas is nitrogen. Contrariwise, the sample weight is measured manually with the analytical balance (Explorer Semi-Micro, EX125M Model, Switzerland) and then it is inputted manually to gas pycnometer. The equation (1) gives the theoretical density of composite. The difference between theoretical

density ρ_{theo} and the density measured with gas pycnometer ρ_{exp} allows estimating the volume fraction of porosity by the expression (2).

$$\boldsymbol{\rho_{theo} = \left(\rho_{fiber} \times V_{f_{fiber}}\right) + \left(\rho_{matrix} \times V_{f_{matrix}}\right)} \quad (1)$$

$$\boldsymbol{V_p = \frac{\rho_{theo} - \rho_{exp}}{\rho_{theo}}} \quad (2)$$

2.6.4 Mechanical testing

2.6.4.1 Flexural testing

The bending test used in this work is the three points. The specimen dimensions are 100 x 15 mm x mm and the sample support spanning 80 mm. The used machine is Tinius Olsen Horizon H10KT with the load cell of 5KN at a cross head of 5 mm/min in compression mode. The tests were performed for five specimens for each composite according to the ASTM D790 standard [18].

2.6.4.2 Shear testing

This test allows accessing to the shear in the three main planes. This test is performed with Tinius Olsen Horizon H10KT with the load cell of 5KN at a crosshead of 5 mm/min in a tensile mode as shown in Figure II. 3. The specimen used in this test is in the form of a rectangular flat strip with symmetrical centrally located v-notches, and the distance between v-notches is 12.74 mm. The tests were performed for five specimens for each composite according to according to the ASTM-D7078 standard [19].

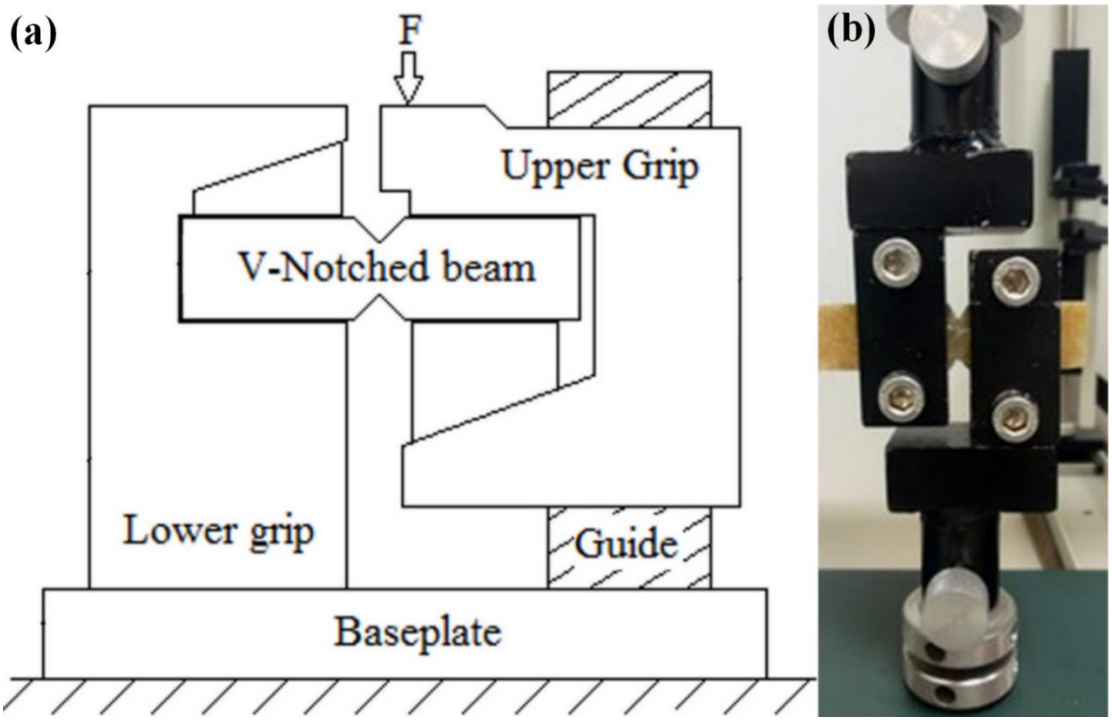

Figure II. 3: (a) principle of Iosipescu shear, (b) Homemade system.

2.6.4.3 Droplet test

To analyze the interfacial shear strength between fiber and matrix, micro-droplet bonding test was conducted. Single fiber was fixed with designed paper properly. Single drop of polymer was attached on the fiber. Figure II. 4 shows the procedure to make a specimen. As shown in this figure, the fibers are put it in Styrene-butadiene rubber (SBR) plate to have concentric resin droplet on the fiber.

Using a 1 kN Tinius Olsen Horizon H10KT, tests were conducted with a fixed cross-head displacement speed rate at 3 mm/min. Fives replicates for each sample of both treated and untreated fibers were tested. Moreover, the diameter of the fiber was measured from the nearest point of the droplet to the fiber contacts on both sides.

The analysis was conducted using the following equation (3):

$$\tau = \frac{F}{\pi DL} \tag{3}$$

Where τ is the interfacial shear strength (MPa), D is the single fiber diameter (m), and L is the embedded length (m).

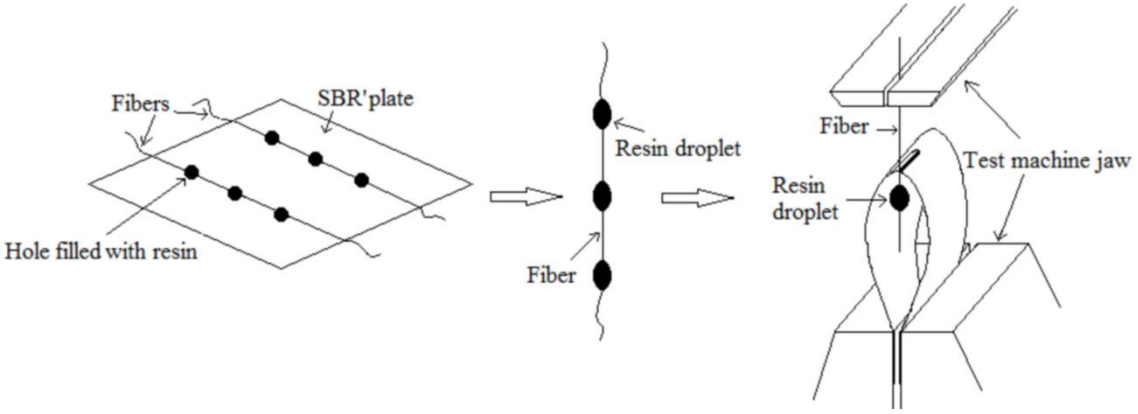

Figure II. 4*:* Droplet test method.

2.6.5 Thermal conductivity testing

This test is performed by the "MCR 500" Rheometer to reach a temperature of 60 ° C (desired temperature) on one side of the composite and the temperature values on the other side are recorded via " Testo 176 T4 " recorder connected to a probe that is attached to an aluminum disc characterized by its good thermal conductivity (Look Figure II. 5). The software "Testo comfort Software basic 5" is used to analyze the obtained results.

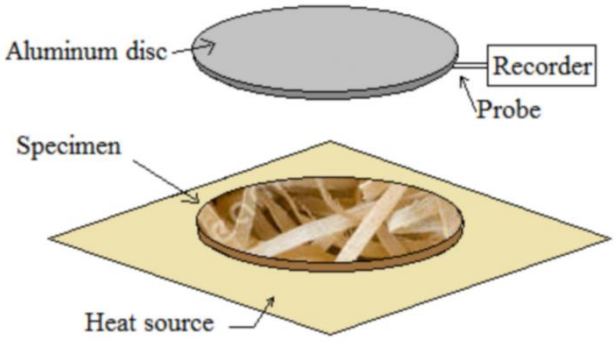

Figure II. 5: Thermal conductivity principle.

2.7 Results and discussion

2.7.1 Morphological properties

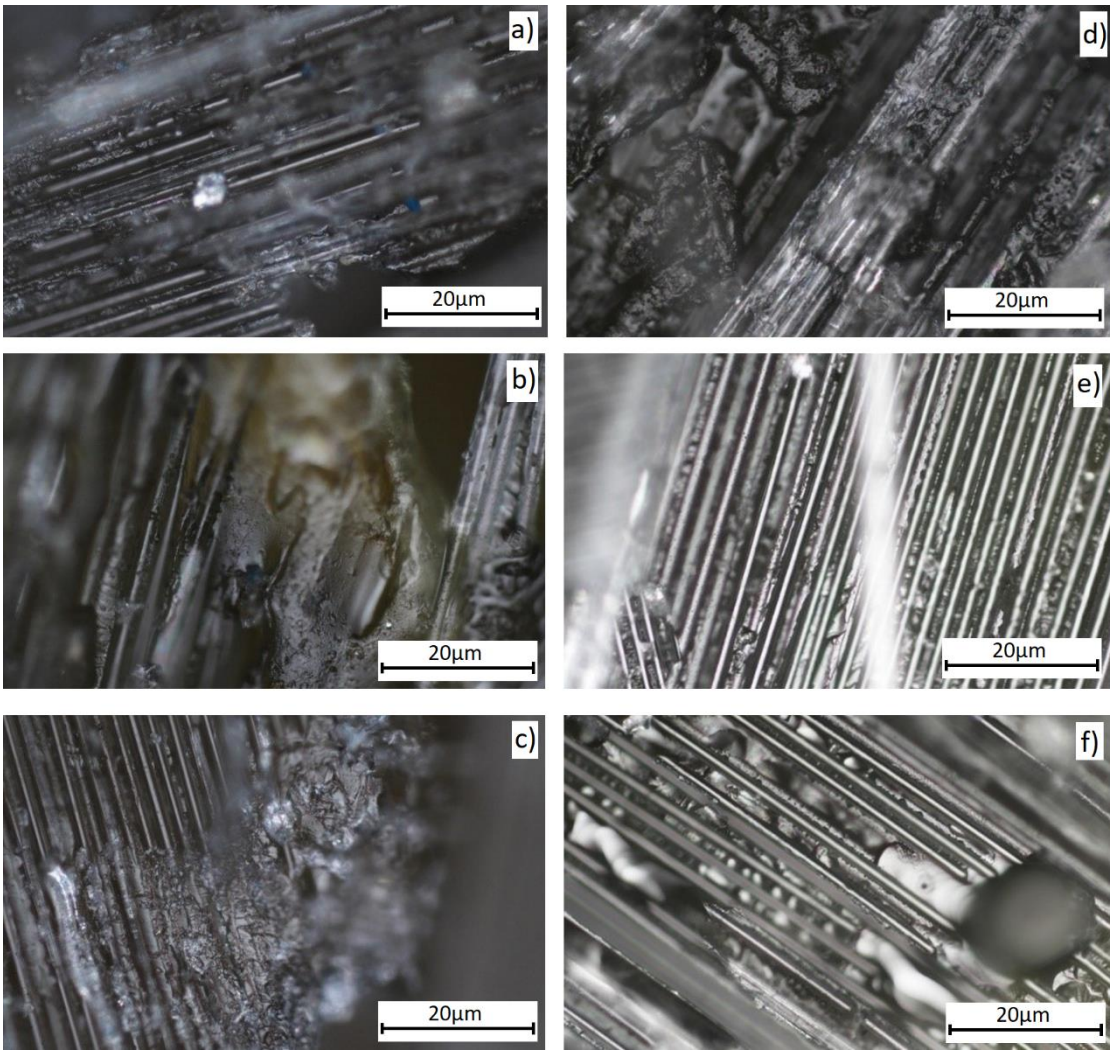

Figure II. 6: SEM images of composites of Raffia fiber surface: (a, b, c) Untreated fibers; (d, e, f) Alkali treated fibers

The microscopic analysis of the fibers allows characterization of the structural changes occurring during the treatment, which facilitates the cleaning and the smoothing of the fibers. The morphological properties of Raffia fibers are observed by optical microscopy. Figure II. 6 shows untreated and processed surfaces of Raffia fibers. The Figure II. 6 (a) show the large view of the composite structure and it is clear the good distribution and distribution of the raffia fibers on the matrix with the existence of some fibers pull outs which is due the weak of the adhesion between matrix and untreated raffia fibers. As illustrated in Figure II. 6 (b), it is deduced that it is difficult to visualize a clear morphology of the untreated fibers surface and this is due to the existence of impure and amorphous materials on the surface of the

fibers, which makes it rougher [3, 20]. The surface of untreated Raffia fibers is covered with fats, waxes or polysaccharides (hemicellulose, pectin, lignin). Also, it has been observed that the structure of Raffia fibers consists of several fibrillary strands of which consists of an arrangement of cellulose microfibrils covered with hemicellulose and lignin. Untreated fibers show a very slight improvement in morphology, which leads to poor bonding between the fibers and the matrix, that is clear by visualizing the Figure II. 6 (c) which is clear a decohesion area between fibers and the polymer indicating a poor interfacial adhesion.

Figure II. 6 (d, c) shows a change in the surface appearance of Raffia fibers after alkali treatment. They have a clean, rough and smooth morphology with pores, allowing a good physical interaction/mechanical anchoring with the polymeric matrix chains. This demonstrates that the untreated fibers were larger than the treated fibers and that the surface roughness of the fiber is reduced due to the partial dissolution of the amorphous parts (waxes, hemicelluloses, pectins, lignin) [3, 20]. After alkaline treatment the surface of Raffia fibers becomes depleted of non-cellulosic material leading to a clearer visualization of cellulosic fiber surface (cellulose microfibrils) allowing the determination of the diameter of the cellulose microfibrils (around 3.5 μm and 5 μm) (Figure II. 6 (b)). In the other hand, Figure II. 6 (c) shows that the alkali treated fibers are loosely embedded in the matrix and that the voids between fibers and matrix are almost inexistent giving better fibers /matrix interfacial area. Also, this treatment allowed the removal of lignin and hemicellulose from the surface of the fibers [3, 20] thus contributing to the improvement of the fiber-matrix interfacial bond of the Raffia fiber.

2.7.2 Structural results (FT-IR)

Several research studies have explored the possibility of improving the performance of composites. Among the key factors for obtaining good performance is the affinity of the matrix-fiber interface. Based on previous studies, the alkaline treatment removes non-cellulosic components, waxes, oil, etc. from the surfaces of the fibers leading to a good interfacial adhesion between these fibers and the matrix [21-23]. In our case, in order to increase the ability of the Raffia fibers and the epoxy matrix to have good affinity and compatibility, the fibers have been subjected to an alkaline treatment. Figure II. 7 shows the effect of alkaline treatment of Raffia fibers on the extraction of non-cellulosic components.

The appearance of the main spectral bands (1734, 1640, 1250 and 897 cm^{-1}) corresponding to the lignocellulosic components (cellulose, hemicellulose, pectin and lignin) constituting the

Raffia fibers [21-23] is clearly visible. After alkalization, the removal of hemicellulose, lignin and pectin was performed and confirmed by the disappearance of the band at 1734 cm^{-1} [23], indicating complete cleavage of these ester bonds. Peak intensity at 1640 cm^{-1} was reduced, reflecting a partial removal of lignin since this peak is attributed to C = C of aromatic skeletal vibrations in lignin. In addition, the reduction in peak intensity around 1267 cm^{-1} after alkalization reflects the preferential removal of hemicellulose materials instead of lignin [21-24].

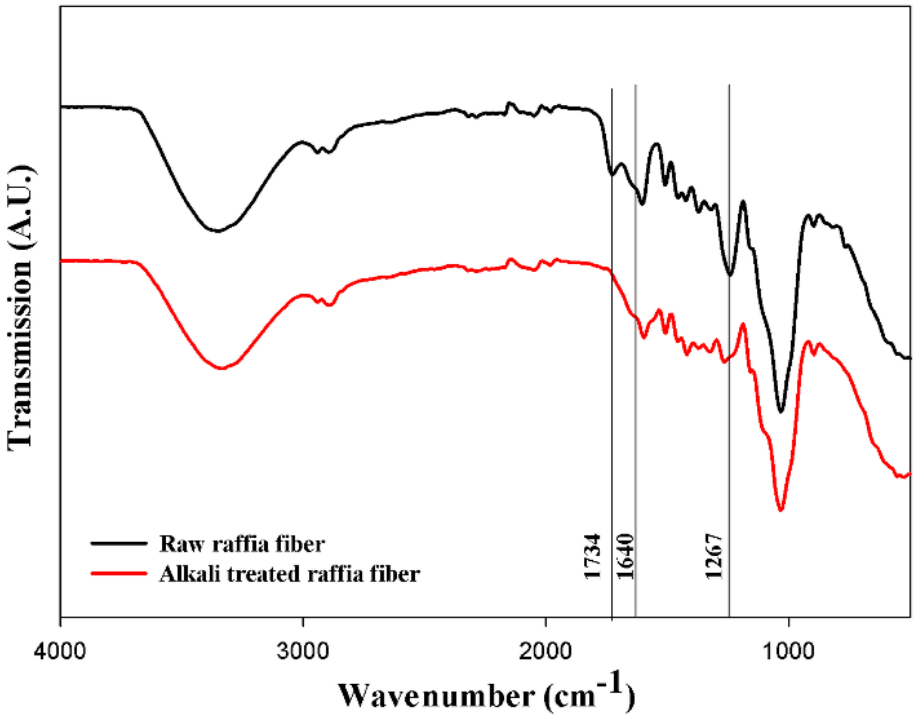

Figure II. 7: FTIR spectra (ATR module) of Raw and alkali treated Raffia fiber.

2.7.3 Composite porosity

Table II. 2 shows the density of the various components of the composite materials: epoxy resin, raw Raffia fibers, alkali-treated Raffia fibers and glass fibers. In order to measure the effective density of the glass fibers, a cutting is carried out and not grinding because it causes the dissociation of the coating of the fibers. The density of the glass fibers is about 2.5 g/cm^3 and that of the epoxy resin is about 1.16 g/cm^3.

Table II. 2 shows that the alkaline treatment of Raffia fibers has a significant effect on density. It has been confirmed by the FTIR analysis (Figure II. 7) that the alkalization of the fibers eliminates a certain amount of hemicellulose, lignin, wax, oils and other impurities

[23,24]. The density of Raffia fibers treated by mercerization is higher than that of raw Raffia fibers. This result is in agreement with the literature because this treatment eliminates the non-cellulosic components (hemicellulose and lignin) which are denser than the cellulosic components.

Table II. 2: Density of different composite components

	ρ (g/cm^3)	**Standard deviation (g/cm^3)**
Epoxy resin	1.1601	0.0001
Raw Raffia fibers	1.0671	0.0041
Alkali Treated Raffia fibers	1.5577	0.0058
Glass fibers	2.5163	0.0069

The theoretical density is calculated using the expression (4):

$$\boldsymbol{\rho_{theo} = \rho_{fiber} \times V_{f_{fiber}} + \rho_{matrix} \times V_{f_{matrix}}} \quad (4)$$

The theoretical density is calculated and compared to the experimental values (Table II. 2).

If the experimental and theoretical value does not coincide, the difference may be attributed to the porosity existence which is calculated by equation (5).

$$\boldsymbol{V_p = \frac{\rho_{theo} - \rho_{exp}}{\rho_{theo}}}$$

(5)

A high percentage of porosity in the composite material implies a significant decrease in mechanical characteristics. Therefore, determining the percentage of porosity makes it possible to evaluate the quality of the composite. Table II. 3 summarizes the theoretical and experimental density of different manufactured composites and their porosity. From Table II. 3, the glass fiber layer has the lowest porosity percentage (1.85 %) because of the high affinity between the epoxy resin and the glass fibers. However, it has been observed that the porosity of the composites is strongly related to the surface structure of the Raffia fibers. Indeed, the alkaline treatment causes a decrease in the percentage of porosity of Raffia fibers which goes from 4.18 % to 2.34 %. The same applies to sandwich composites where the

percentage of porosity goes from 3.6 % to 2.8 %. This is because the alkali treatment allows the removal of non-cellulosic compounds from the surface of Raffia fibers, which improves interfacial adhesion and increases resin penetration by reducing the void percentage on the structure of the composites.

Table II. 3: Theoretical and experimental density of different elaborated composites and their porosity.

	$V_{f\ fibers}$	ρ theoretical	ρ experimental		Porosity (%)
			P (g/cm3)	Std. Dev.	
Raw Raffia fibers layer	0.1323	1.1578	1,1094	0.0002	4.1802
Alkali treated Raffia fibers layer	0.1690	1.2273	1,1985	0.0003	2.3451
Glass fibers layer	0.3108	1.5816	1,5523	0.0002	1.8544
Sandwich with Raw Raffia Fibers	0.1791	1.3061	1,2589	0.0004	3.6101
Sandwich with alkali treated Raffia fibers	0.1633	1.3360	1.2981	0.0004	2.8368

2.7.4 Mechanical testing

2.7.4.1 Flexural properties

Figure II. 8 shows the results of a set of experiments conducted on the various developed composites (RFC, TRFC, GFC, SCGRG, SCGTRG). The flexural modulus of raw Raffia fiber composites (2.4GPa) is lower than that of processed Raffia fiber composites (2.7 GPa). This increase (12.5%) is due essentially to the treatment which improves the interfacial adhesion of the fiber with the matrix and allows the resin to penetrate the fiber bundle during the manufacturing process. Oil, hemicellulose, pectin and other unknown materials should be removed from the surface of Raffia fiber for better adhesion [25-27]. The removal of waxes and non-cellulosic compounds during the chemical modification and treatment exposes hydroxyl groups on the surface and promotes interfacial bonding between the fiber surface and the epoxy resin matrix. This interaction has a positive effect on the bending properties of composites by increasing the stress transfer capacity of the matrix to the fiber via interfacial adhesion [28]. Glass fiber composites have a higher flexural modulus (4 GPa) compared to sandwich composites which is due to the intrinsic properties of glass fibers. However, the flexural bending modulus of sandwich composites made from raw fiber is 3.4 GPa and that of the sandwich composites with treated fiber is 3.6 GPa. This result implies that the

mercerization treatment improves the bending properties of sandwich composites [25] which can be explained by the transfer of a high load of fibers into the matrix during the loading conditions (flexural test). The second reason for this improvement is the high penetration of the resin into the treated fibers, which decreases the possibility of detachment of the fibers from the matrix during the charging process.

In the case of untreated fibers, the epoxy resin could not penetrate the fiber and this is due to two phenomena: the high porosity of the composite (empty fibers) and the weak interaction of the fibers core with the surrounding matrix. This is in agreement with the results obtained (Table II. 3) and which confirms that the sandwich composite produced by untreated fibers has a greater porosity (3.6 %) compared to those made by treated fibers (2.8 %) and this is one of the reasons for the low bending properties.

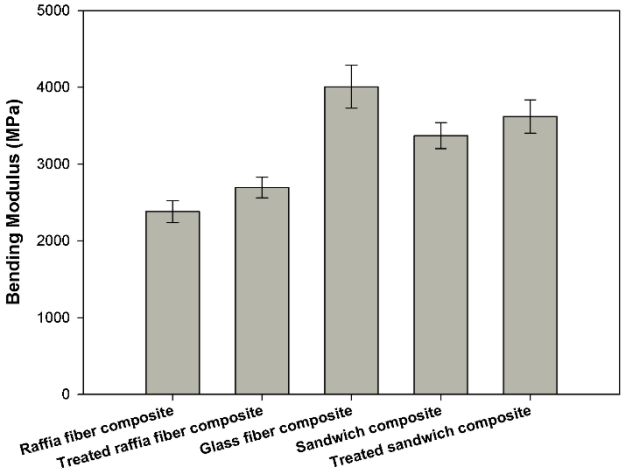

Figure II. 8: Curve of bending modulus versus all different elaborated composites.

2.7.4.2 Shear properties

The Iosipescu shear test is a versatile and useful method for measuring the shear properties of a wide variety of materials. It can be applied to both isotropic and anisotropic solids, including metals, polymers, as well as randomly oriented fiber reinforced composites. Also, it can be used to measure both shear properties across the thickness and plane of materials.

Figure II. 9 elucidates the shear stress of composites: RFC, TRFC, SCGRG and SCGTRG. In this study, Shear strength is high in the case of glass fiber sandwich composites (407.7 and 600.6 MPa), whereas in the absence of glass fibers, the shear strength of the composites is low (109, 4 and 205.9 MPa). By analyzing the effect of the alkaline treatment on the

properties of the Iosipescu shear, it is deduced that the alkaline fibers have the highest values compared to the untreated fibers. The results show a gain of 88 % and 47.3% respectively for composites without and with glass fibers. We deduce the effect of the addition of glass fibers on shear strength which increases due to the intrinsic properties of these fibers [29]. The second key factor concerns the chemical treatment of Raffia fibers which have a direct effect on the surface structures of the fibers as well as the degree of interfacial adhesion between the fibers and the matrix.

Generally, during the Iosipescu shear test, several regions have high stress concentrations. Maximum stress concentrations are reached near the root of the notch and along the edges of the samples on the internal loading surfaces. The load-induced compression stresses emanating from the internal load zones deform the stress field in the test section and therefore the stress distributions are not symmetrical with respect to the notch axis. Cracks tend to break into the root of the cut and propagate parallel to the fibers on opposite sides of the internal load points [29]. The concentration of the shear stress at the end of the notch is mainly responsible for crack initiation whose growth in the main stress plane is prevented by the aligned fibers. These cracks relieved localized stress concentrations at the ends of the notches. The damaged areas consist of numerous small interracial cracks, extensive fiber flexion, and fiber shrinkage. However, the interfacial adhesion between the fibers and the matrix is considered to be one of the main factors determining the shear properties of Iosipescu materials. The combination of randomly processed glass fibers and Raffia fibers improves the shear strength of the composite. As a result, glass fibers with their superior intrinsic mechanical properties confer higher strength, while the alkaline treatment of Raffia fibers reduces tension and promotes interfacial adhesion between a natural fiber and a polymer matrix by eliminating the high amount of lignin that supports and promotes the transfer of shear stress between fibers and matrix [28].

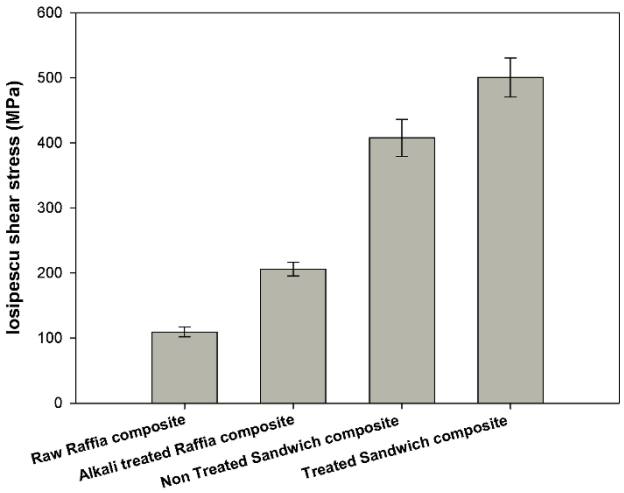

Figure II. 9: Curve of Iosipescu shear stress (MPa) versus all different elaborated composites.

2.7.4.3 Droplet test

The interfacial shear strength between Raffia fiber and epoxy resin has been measured by using a microdroplet test, using microdroplet frequently reported test and which is a variation of fiber pull-out technique allowing to directly evaluate the interfacial resistance to the shear between the fiber and the resin [29-31]. Since only a single fiber is used in the microdroplet test, it provides a simple means to isolate and to characterize the interface adhesion between fiber and matrix [29-31]. The obtained microdroplets are exploitable for pull-out testing. Figure II. 10 illustrates the interfacial shear strength values obtained from the microdroplet tests associated with raw and treated Raffia fiber. It is concluded that the value of the shear stress of treated Raffia fiber is 38% higher than that of raw Raffia fiber, which mean that the alkali treatment improves the state of interfacial shear strength between matrix droplet and fiber. The variation in interfacial shear strength between untreated and treated Raffia fibers can be explained by the removal of lignin and hemicellulose which leads to voids in the fibers, and causes anchoring between the fibers and the matrix that enters them into the interfibrillary regions. On the other hand, after removal of the non-cellulosic elements by the alkaline treatment, the free hydroxyl groups can react as curing agent with the epoxide group present in the epoxy resin contributing to its cross linking and consequently the increase of the interfacial adhesion between the treated fiber and the epoxy resin [28].

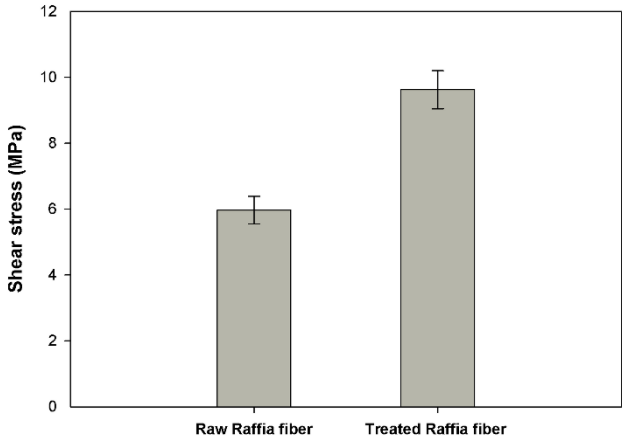

Figure II. 10: Curve of shearing stress during a drop test of raw and treated one Raffia fiber.

2.7.4.4 Thermal conductivity

Thermal conductivity is one of the key parameters in the field of thermal insulation materials. The thermal conductivity property of composite materials depends on several parameters such as matrix density, morphology and density of the fillers as well as the homogeneity and the interface loads of the matrix [33-35].

In our case, the thermal conductivity properties are given with the temperature values after a stabilization measurement time. Figure II. 11 shows that the thermal conductivity of composites decreases with the addition of Raffia fibers. The values of temperature decrease of 58 °C, 57 °C and 53 °C in 1200 s in the case of composites based on glass fibers, composites based sandwich untreated and treated fibers respectively. This behavior of the composite may be due to the low thermal conductivity of the Raffia fibers.

On the other hand, by studying the effect of fibers alkali treatment on the composites thermal conductivity, it appears (Figure II. 11) that this treatment reduces the thermal conductivity of the sandwich composite. During the treatment, the impurity and wax on the surface of Raffia fibers are removed, which increases the number of pores on the fibers surface [33]. These pores are zones of attachment of the polymeric chains and hence reduce the percentage of areas of voids between the fibers and the matrix (good interfacial adhesion) on the composite structure. The reduction of voids on the structure of the composites leads to a decrease in their thermal conductivity. These results indicate that sandwich composites reinforced with alkali-treated Raffia fibers have a good thermal insulation property [33]. In view of the result

obtained; these sandwich composites can be used in the building sector to reduce energy consumption.

These pores constitute zones of fixation of the polymer chains and consequently reduce the zones of percentage of voids between the fibers and the matrix (good interfacial adhesion) on the composites structure which leads to a decrease in their thermal conductivity. These results indicate that sandwich composites reinforced with alkali-treated Raffia fibers have a good thermal insulation property [33]. On the basis of these results, these sandwich composites can be used in the building sector to reduce energy consumption.

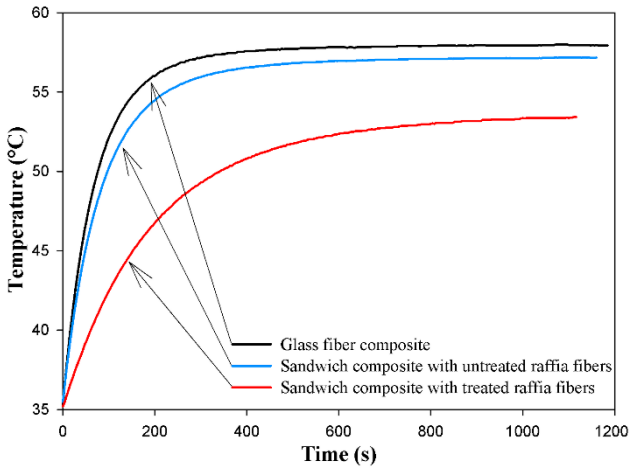

Figure II. 11: Evolution of temperature versus time of raw and alkali treated Raffia fiber sandwich composites.

2.8 Flexion modeling

To predict the composite mechanical properties, several models have been proposed based in different assumptions. The Voigt (parallel) and Reuss (serial) models do not consider the fiber-matrix interaction and consider a single fiber principal direction [3,36,37]. On the other hand, the Tsai-Pagano and Hirsch models account for a relative contribution of the parallel and serial models. The first, considers a random orientation and uniform fibers dispersion and distribution, and the second, introduces the fibers orientation and stress concentration effects on the empirical parameter [3,36,37].

In this study, the Voigt model was selected to predict flexural properties, especially flexion bending modulus which can be expressed by the following equation (6):

$$\mathbf{E_v = V_{f_1} \cdot E_1 + V_{f_2} \cdot E_2 + V_{f_3} \cdot E_3 + \cdots + V_{f_n} \cdot E_n} \quad (6)$$

Which E_v is the Voigt elastic modulus of laminated composed with n layers, V_f and E_f are, respectively, the volume fraction of a fiber layer and elastic moduli of a fiber layer. Before using the Voigt model, it is important to notice their hypotheses: good dispersion and distribution, good interfacial adhesion and a parallel fiber orientation.

Also,

$$\mathbf{V_{f_i}} = \frac{\mathbf{V_i}}{\mathbf{V_T}} \tag{7}$$

Which V_i and V_T are the volume of the fiber layer (number i) and the volume of the laminated composite, respectively. Thus, the equation (6) becomes:

$$\boldsymbol{E_v} = \frac{\boldsymbol{L.l.h_1}}{\boldsymbol{L.l.h_t}}.\mathbf{E_1} + \frac{\boldsymbol{L.l.h_2}}{\boldsymbol{L.l.h_t}}.\mathbf{E_2} + \frac{\boldsymbol{L.l.h_3}}{\boldsymbol{L.l.h_t}}.\mathbf{E_3} + \cdots \ldots . + \frac{\boldsymbol{L.l.h_n}}{\boldsymbol{L.l.h_t}}.\mathbf{E_n} \tag{8}$$

Which L, l, h_i and h_t are, respectively, the composite length, the width of the laminated, the thickness of the fiber layer number I, and the total thickness of the laminated composite.

Finally, after simplification, the resulted equation (9) is presented as follow.

$$\mathbf{E_v} = \mathbf{E_{sandw}} = \frac{\mathbf{1}}{\mathbf{h_t}}.\sum_{\mathbf{i=1}}^{\mathbf{n}} \mathbf{h_i}.\mathbf{E_i} \tag{9}$$

To conclude that the obtained equation (6) corresponds to the "mixing law". Appling the above resulted equation to our case, the flexural bending modulus of the two sandwich structured composites is obtained using the flexural bending modulus of each layers and the following equations (10) and (11) allow to find them.

$$\mathbf{E_{f_{TRT\ sandw}}} = \mathbf{2}.\frac{\mathbf{1}}{\mathbf{4}}.\mathbf{E_{f_{GF}}} + \frac{\mathbf{2}}{\mathbf{4}}.\mathbf{E_{f_{TRT\ Raffia}}} \tag{10}$$

$$\mathbf{E_{f_{unTRT\ sandw}}} = \mathbf{2}.\frac{\mathbf{1}}{\mathbf{4}}.\mathbf{E_{f_{GF}}} + \frac{\mathbf{2}}{\mathbf{4}}.\mathbf{E_{f_{unTRT\ Raffia}}} \tag{11}$$

Which $E_{f\ TRT\ sandw}$ and $E_{f\ unTRT\ sandw}$ are the bending modulus of sandwich composite reinforced with alkali treated Raffia fibers and the bending modulus of sandwich composite reinforced with untreated Raffia fibers, respectively. $E_{f\ GF}$, $E_{f\ TRT\ Raffia}$ and $E_{funTRT\ Raffia}$ are, respectively, the flexural modulus of glass fibers, the flexural modulus of alkali treated Raffia fibers and

flexural modulus of raw Raffia fibers. It is worth noticed that the 1/4 and 2/4 represent the contribution of glass fibers and Raffia fibers in structured sandwich composites.

Table II. 4 summarized the comparison between empiric and experimental results. It was observed a good fitting between the empiric and the experimental data, with a deviation of 8% and 4.5 % in case of untreated and treated Raffia fiber sandwich respectively. These values are assumed to be reasonable since in case of the alkali treated fibers sandwich all hypothesis are verified, especially the good interfacial adhesion between fibers and matrix. However, in the case of untreated fiber sandwich the previous analysis shows a poor interfacial adhesion. Thus o the difference between the fitting percentage is due to the higher interfacial adhesion in the case of treated fibers.

Table II. 4: Comparison between theoretical and empiric results of flexural bending modulus of sandwich composite reinforced with raw Raffia fibers and treated Raffia fibers.

	Experimental bending modulus (GPa)	**Theoretical bending modulus (GPa)**	**Difference between experimental and theoretical bending modulus (%)**
Sandwich composite with raw Raffia fibers	3.469	3.194	7.927
Sandwich composite with alkali treated Raffia fibers	3.617	3.452	4.56

2.9 Conclusion

In this work the hybrid sandwich composite based on Raffia fibers (core) and glass fibers (surface) was manufactured and the effect of alkaline treatment of Raffia fibers on the structural, thermal and mechanical properties were investigated. It was identified from microscope graphs that non-cellulosic materials were removed from alkali treated fibers. FTIR spectra show that alkali treated Raffia fibers eliminate the non-cellulosic materials leading to higher interfacial adhesion. After analysis: bending test, shearing test, droplet test, and thermal conductivity measurement, it was deduced that the alkali treated Raffia fiber based sandwich composite has the highest properties compared to untreated Raffia fiber based sandwich composite. To predict the flexural bending modulus of the sandwich-structured composite, the law used for this purpose is the mixing rule applied using the flexural bending modulus of each layer. The imminent prospective will be the development and reinforcement of Treated raffia fibers to improve the mechanical, dynamic mechanical

properties of sandwich composite structure based on thermosets matrix that will receive higher consideration in the research fields for further investigations.

Acknowledgements

This work was supported by MAScIR; Moroccan Foundation for Advanced Science, Innovation and Research, MESRSFC and CNRST, Morocco grant no. 1970/15. Authors would like to greatly thank Mehdi Ait Dahi for his fruitful technical support and assistance.

References

[1] Sarasini, F., Fiore, V. A systematic literature review on less common natural fibres and their biocomposites. *Journal of Cleaner Production* 2018; 195: 240-267.

[2] Fiore, V., Botta, L., Scaffaro, R., Valenza, A. Pirrotta, A. PLA based biocomposites reinforced with Arundo donax fillers. *Composites Science and Technology* 2014; 105, 110-117.

[3] Malha, M., Nekhlaoui, S., Essabir, H., Benmoussa, K., Bensalah, M.-O., Arrakhiz, F.-E., … Qaiss, A. Mechanical and thermal properties of compatibilized polypropylene reinforced by woven doum. *J Appl Polym Sc* 2013;130:4347-4356.

[4] Kakou, C.A., Essabir, H., Bensalah, M.O., Bouhfid, R., Rodrigue, D., Qaiss, A. Hybrid composites based on polyethylene and coir/oil palm fibers . J. Reinfor. Plast. Compos. 2015; 34 : 1684-1697.

[5] El Mechtali, F. Z., Essabir, H., Nekhlaoui, S., Bensalah, M. O., Jawaid, M., Bouhfid, R., & Qaiss, A. Mechanical and Thermal Properties of Polypropylene Reinforced with Almond Shells Particles: Impact of Chemical Treatments. *J. Bion. Eng.* 2015; *12* :.

[6] Scaffaro, R., Lopresti, F., Botta, L. PLA based biocomposites reinforced with Posidonia oceanica leaves. Compos. Part B 2018; 139 : 1-11.

[7] Swolfs, Y., McMeeking, R. M., Rajan, V. P., Zok, F. W., Verpoest, I., & Gorbatikh, L. Global load-sharing model for unidirectional hybrid fibre-reinforced composites. *J. Mech. Phys. Solid 2015;84*;380–394.

[8] Jawaid, M., Abdul Khalil, H. P. S., Noorunnisa Khanam, P., & Abu Bakar, A. Hybrid Composites Made from Oil Palm Empty Fruit Bunches/Jute Fibres: Water Absorption, Thickness Swelling and Density Behaviours. *J. Polym. Env.*2011; *19*: 106–109.

[9] Aslan, M., Tufan, M., Küçükömeroğlu, T. Tribological and mechanical performance of sisal-filled waste carbon and glass fibre hybrid composites. Compos. Part B 2018; 140 :241-249.

[10] Safri, S.N.A, Sultan, M.T.H., Jawaid, M., Jayakrishna, K. Impact behaviour of hybrid composites for structural applications: A review. Compos. Part B 2018; 133: 112-121.

[11] Almeida Jr, J. H. S., Amico, S. C., Botelho, E. C., & Amado, F. D. R. Hybridization effect on the mechanical properties of curaua/glass fiber composites. *Compos. Part B:* 2013; *55*:492–497.

[12] Taiqu, L., Hou, S., Nguyen X., Han, X. Energy absorption characteristics of sandwich structures with composite sheets and bio coconut core. Compos. Part B 2017; 114: 328-338.

[13] Botta L., Fiore,V., Scalici, T., Valenza, A., Scaffaro, R. New Polylactic Acid Composites Reinforced with Artichoke Fibers. *Materials* 2015; 8: 7770-7779 .

[14]. Frazão, C., Barros, J., Filho, R.T., Ferreira, S., Gonçalves, D. Development of sandwich panels combining Sisal Fiber-Cement Composites and Fiber-Reinforced Lightweight Concrete. Cemen Conc Compos 2018; 86 :206-223.

[15] Tan, Z.H., Zuo, L., Li, W.H., Liu, L.S., Zhai, P.C. Dynamic response of symmetrical and

asymmetrical sandwich plates with shear thickening fluid core subjected to penetration loading Mater 2016; 94: 105-110.

[16] Nekhlaoui, S., Qaiss, A., Bensalah, M. O., Lekhder,A. A New Technique of Laminated Composites Homogenization, Adv. Theor. Appl. Mech. 2010; *3*:253–261.

[17] Sarikanat, M., Seki, Y., Sever, K. Cenk Durmuşkahya. Determination of properties of Althaea officinalis L. (Marshmallow) fibres as a potential plant fibre in polymeric composite materials. Comp Part B 2014; 57: 180-186.

[18] ASTM D790. (2015). Standard Test Method for Flexural Properties of Unreinforced and Reinforced Plastics and Electrical Insulation Materials. *ASTM Standards*, 1–11.

[19] ASTM-D7078. (2010). Standard Test Method for Shear Properties of Composite Materials by the V-Notched, 1–13.

[20] Essabir, H., Jawaid, M., Qaiss, A., Bouhfid, R.Mechanical and Thermal Properties of Polypropylene Reinforced with Doum Fiber: Impact of Fibrillization. In: Jawaid M., Sapuan S., Alothman O. (eds) Green Biocomposites. Green Energy and Technology. Springer, Cham ; (2017)pp 255-270.

[21] Ait Laaziz, S., Raji, M., Hilali, E., Essabir, H., Rodrigue, D., Bouhfid, R., Qaiss, A.Bio-composites based on polylactic acid and argan nut shell:Production and properties.I. J. Bio. Macromol. 2017; 104:30–42.

[22] Boujmal, R., Kakou, C.A., Nekhlaoui, S., Essabir, H., Bensalah, M-O., Rodrigue, D., Bouhfid, R. Qaiss A. Alfa fibers/clay hybrid composites based on polypropylene: Mechanical, thermal, and structural properties. J. Thermoplast. Comp. Mater. 2017 : 1–18.

[23] Essabir, H., Bouhfid, R., Qaiss A. Alfa and doum fiber-based composite materials for different applications. In : Lignocellulosic Fibre and Biomass-Based Composite Materials : Processing, Properties and Applications, by : M jawaid, P Md Tahir, M Saba (Eds).Woodhead Publishing Series in Composites Science and Engineering. Elsevier. 2017, Pages 147–164.

[24] Essabir, H., Boujmal,R., Bensalah, M-O., Rodrigue, D., Bouhfid,R., Qaiss, A. Mechanical and thermal properties of hybrid composites: Oil-palm fiber/clay reinforced high density polyethylene.Mech. Mater. 2016; 98:36–43.

[25] Yousif,B.F., Shalwan,A., Chin,C.W., Ming, K.C. Flexural properties of treated and untreated kenaf/epoxy composites.Materi. Design 2012; 40 :378–385.

[26] Mylsamy, K., Rajendran, I. The mechanical properties, deformation and thermomechanical properties of alkali treated and untreated Agave continuous fibre reinforced epoxy composites. Mater. Des. 2011;32:3076–84.

[27] Towo, A.N., Ansell, M.P. Fatigue evaluation and dynamic mechanical thermal analysis of sisal fibre–thermosetting resin composites. Compos. Sci. Technol. 2008;68:925–32.

[28] Qaiss, A., Bouhfid, R., Essabir, H. Effect of processing conditions on the mechanical and morphological properties of composites reinforced by natural fibres.Manufacturing of natural fibre reinforced polymer composites, 2015,pp: 177-197.

[29] Zhang, W., Cotton, C., Sun, J., Heider, D., Gu, B., Sun, B., Chou, T-W. Interfacial

bonding strength of short carbon fiber/acrylonitrile-butadiene styrene composites fabricated by fused deposition modeling.Compos.Part B2018; 137: 51-59.

[30] Lee, M-W., Wang, T-Y., Tsai, J-L. Characterizing the interfacial shear strength of graphite/epoxy composites containing functionalized graphene. Compos. Part B 2016; 98 :308-313.

[31] Zu, M., Li, Q., Zhu, Y., Dey, M., Wang, G., Lu, W., Deitzel,J.M., Gillespie, J.W., Byun,J-H., Chou, Tsu-Wei. The effective interfacial shear strength of carbon nanotube fibers in an epoxy matrix characterized by a microdroplet test. Carbon 2012, 50; 1271-1279.

[32] Kang,S-K., Lee,D-B., Choi, N-S. Fiber/epoxy interfacial shear strength measured by the microdroplet test. Compos. Sci. Technol. 2009; 69:245–251.

[33] Sair, S., Oushabi, A., Kammouni, A., Tanane, O., Abboud, Y., Oudrhiri, H.F., Laachachi, A., El Bouari, A. Effect of surface modification on morphological, mechanical and thermal conductivity of hemp fiber: Characterization of the interface of hemp –Polyurethane composite. Case. Stud. Therm. Eng. 2017; 10 : 550-559.

[34] Huang, X., Alva, G., Jia, Y., and Fang, G. Morphological characterization and applications of phase change materials in thermal energy storage: A review. Renew. Sustain. Energy Rev.2017; 72: 128-145.

[35] Boukhattem, L., Boumhaout, M., Hamdi, H., Benhamou, B., and Nouh, F. A.Moisture content influence on the thermal conductivity of insulating building materials made from date palm fibers mesh. Constr. Build. Mater. 2017;148: 811-823.

[36] Essabir, H.,Bensalah, M.O.,Rodrigue, D.,Bouhfid, R.,Qaiss, A..Structural,mechanical and thermal properties of bio based hybrid composites from waste coir residues : Fibers and shell particles. Mech. Mater. 2016; 93 :134–144.

[37] Essabir, H., Hilali, E., El Minor, H., Bensalah, M. O., Bouhfid, R., Qaiss, A.. Mechanical and Thermal Properties of Polymer Composite Based on Natural Fibers: Moroccan Luffa Sponge/High Density Polyethylene. J. Biobas. Mater. Bioenergy 2015; 9: 1–8.

CHAPTER III

HYBRID COMPOSITES AND INTRA-PLY HYBRID COMPOSITES BASED ON JUTE AND GLASS FIBERS: A COMPARATIVE STUDY ON MOISTURE ABSORPTION AND MECHANICAL PROPERTIES*

3.1 Abstract

Natural fibers are used as reinforcement in composites due to advantages such as high stiffness, lower density, lower cost, environmentally friendly nature and high availability. Nevertheless, these fibers have some drawbacks such as low moisture resistance and incompatibility with most polymers. This work compares two different hybrid configurations: inter-layer (layer by layer) and intra-layer (yarn by yarn). The fibers used are jute (*Corchorus capsularis*) and glass, while the matrix selected is polyester. The composites are manufactured using the hand layup technique and the samples are characterized for moisture resistance and mechanical properties. The experimental bending modulus of both laminated configurations is compared with theoretical values as obtained by a combination of the mixing law and homogenization technique. The results show that the interlayer configuration of jute and glass fibers presents the least resistance to moisture compared to the other configurations studied. Finally, the theoretical mechanical predictions are found to be good (10% on average) despite the simplifications made in the calculations.

*

Reprinted in part with permission from Ouarhim W, Essabir H, Bensalah M-O, Zari N, Rodrigue D, Bouhfid R, Qaiss A. Hybrid composites and intra-ply hybrid composites based on jute and glass fibers: a comparative study on moisture absorption and mechanical properties. **Composites Part B: Engineering** (Under review).

3.2 Résumé

L’utilisation des fibres naturelles comme renforcement des matériaux composites présente plusieurs avantages telles qu'une rigidité élevée, une faible densité, un faible coût, une nature écologique et une la disponibilité. Néanmoins, ces fibres présentent aussi des inconvénients tels qu'une faible résistance à l'humidité et une incompatibilité avec la plupart des polymères. Ce travail compare deux configurations hybrides différentes : inter-couche (couche par couche) et intra-couche (fil par fil), à travers l’utilisation des fibres de jute (Corchorus capsularis) et de verre comme renfort de la matrice polyester. La mise en œuvre des composites s’est faite par la technique de stratification manuelle, tandis que la caractérisation des échantillons s’est faite en termes de résistance à l'humidité et de propriétés mécaniques. Ainsi, le module de flexion expérimental des deux configurations stratifiées a été comparé aux valeurs théoriques obtenues par la combinaison de la loi de mélange et de la technique d'homogénéisation. Les résultats ont montré que la configuration inter-couche des fibres de jute et de verre présente la moindre résistance à l'humidité par rapport aux autres configurations étudiées. Enfin, les prédictions mécaniques théoriques corrèlent très bien avec les résultats expérimentaux (10% en moyenne) malgré les simplifications apportées aux calculs.

3.3 Introduction

Composite structures offer industrials and designers new possibilities to combine shapes and materials to increase performance. Besides their lightweight, durability and flexibility, they have high potential for future development. These materials are characterized by higher specific strength than metals, non-metals and even alloys, combined with lower specific gravity, better creep and fatigue resistance, as well as good resistance to corrosion and oxidation. They are used in large areas such as automotive and marine applications (shafts, hulls, spars), aeronautical applications (rocket components), aircraft and safety equipment (ballistic protection and airbags).

The performance of these materials is derived from the matrix and reinforcement performance. With respect to matrices, thermoset resins, such as polyester, are the most widely used in composites and are able to replace very expensive steels and alloys. They are characterized by their high specific strength and stiffness, good fatigue behaviour, limited corrosion and good resistance to chemicals and ambient conditions. They are also easy to repair and insensitive to magnetic radiation. On the other hand, the introduction of natural fibers like jute [1], sabra [2], raffia [3], and coir [4] in polymer composites can lead to eco-friendlier materials. This solution has various advantages such as biodegradability, non-toxicity, low density, renewability, availability and continuous supply of raw materials leading to low cost, high toughness and limited health hazard. However, the incorporation of synthetic fibers such as glass and carbon in polymer matrices still remains the main solution to improve the mechanical properties over the incorporation of natural fibers. But using synthetic fibers alone creates environmental problems during disposal [5]. Thus, the use of both types of fibers in a polymer matrix allows to obtain a more environmentally friendly composite with good mechanical properties. Moreover, the combination of natural fibers and synthetic fibers decreases the weight of the resulting composite compared to a composite made form synthetic fibers alone.

A blend of natural and synthetic fibers in the same composite material can be made via three configurations: (1) interlayer or layer-by-layer consists in placing layers made of different fibers, (2) intralayer or yarn-by-yarn means that both fibers are entangled within a single layer, (3) intra-yarn or fiber-by-fiber consists in intertwisting both fibers within a single yarn [6], and this technique is called hybridization.

Via hybridization, the advantages of one type of fiber is improving the limitations of the others [7]. So hybrid composites contain two or more type of fillers with similar or different natures. They can also offer multi-functionalities that cannot be obtained with a single reinforcement. For example, a mixture of natural and synthetic fibers allows the production of composite materials with high mechanical properties [8,9]. Furthermore, the hybrid effect is associated to a synergic effect between the materials.

One way to produce a composite structure is using a weaving technique to obtain an intra-ply configuration. Different weaving patterns can be created such as plain, basket, twill and satin. These weaving patterns enhance the mechanical properties of the final woven fabric composites [10]. For example, Venkateshwaran et al. [11] studied the effect of three weaving patterns (plain, twill and basket) on the mechanical properties of banana-epoxy composites. It was found that the plain type weaving pattern was better at improving the overall mechanical properties.

In this work, a comparison between two different hybridization configurations is made: inter-layer (layer-by-layer) and intra-layer (yarn-by-yarn). The reinforcements selected are jute and glass fibers to use the same fiber weight fraction for both architectural designs (layer-by-layer and yarn-by-yarn) of laminated composites to compare their water absorption and mechanical properties. The plain weave is chosen due to better fiber interlacing in the warp and weft direction [11]. Three types of composites are manufactured: one layer of jute fibers, one layer of glass fibers, and one intra-layer of jute and glass fibers. Finally, a simple modelling of the laminated composites is performed taking into account the experimental results of the single-layer composites and a comparison between the experimental and theoretical flexion moduli is presented.

3.4 Material and methods

3.4.1 Material properties

The jute fibers were supplied by SONAJUTE (Casablanca, Morocco) with a grammage of 0.02 g/cm^2. This fiber is classified as highly lignified whose chemical and mechanical properties are reported in Table III. 1. Visually, jute is a dull fiber characterized by a rough and hairy texture in touch, as well as a warm but rough feeling. On the other hand, the glass fibers were in the form of roving and woven provided by Detail chimie (Morocco). The grammage of the woven fiber is 0.04 g/cm^2. Finally, the polymer matrix was a dicarboxylic acid with an alcohol (hardener) generating a polyester resin after the reaction. This resin

tends to have a yellowish tint and is used in several applications. To initiate the curing reaction, the catalyst (methyl ethyl ketone peroxide) was mixed with the resin which decomposes to generate free radicals. It should be noted that the hardener (10 wt.%) and catalyst (2.5 wt.%) content was selected as recommended by the supplier.

Table III. 1: Chemical and mechanical properties of jute fibers [12,13], glass fibers [14] and polyester resin [15].

Properties	Jute fibers	Glass fibers	Polyester resin
Cellulose (%)	61-71	-	-
Hemicellulose (%)	13.6-20.4	-	-
Lignin (%)	12-13	-	-
SiO_2 (%)	-	55-68	-
CaO (%)	-	6-25	-
Al_2O_3 (%)	-	12-18	-
Density (g/cm^3)	1.30-1.46	2.46-2.60	1.2
Elongation (%)	1.5-1.8	4.8-5.7	2-3
Tensile strength (MPa)	398-800	3400-4900	50-65
Young's modulus (GPa)	10-30	68-87	3

3.4.2 Weaving step

Unlike other fabric architectures, woven fabrics do not stretch and are easy to handle. Thus, weaving is the most commonly used fabric making process giving a firm fabric. The weave used in this work is a plain weave.

The process of weaving roving glass fibers into jute fabrics was performed manually. The alternate jute fibers are taken off in both directions where they are replaced by the roving glass fibers by passing the weft yarn over a warp as shown in Figure III. 1. Thus, the glass and jute fibers alternate within the same layer; i.e. the yarns are co-woven in both directions in a fabric (Figure III. 2) to obtain a hybrid yarn fabric. Finally, this operation was repeated until 6 pieces of 200 × 200 mm^2 of co-woven fabrics were obtained. It should be noticed that each layer of this co-woven fabric contains horizontally 35 fiber strands of glass fibers and 34 fiber strands of jute fibers, while vertically a total of 36 and 35 fibers strand of glass and jute fibers, respectively are present. The initial length of both fibre strands before plain weaving was around 218 mm and the weight of the glass and jute fibers strand was 0.2336 g and 0.0432 g, respectively.

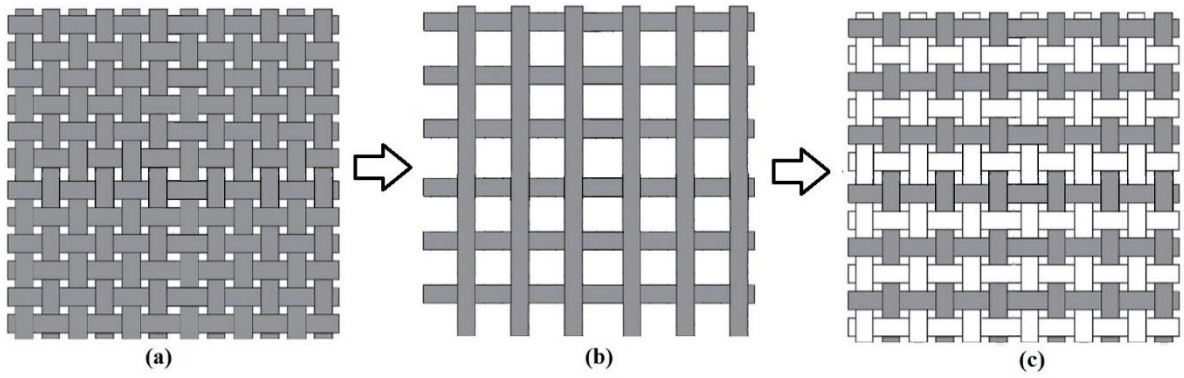

Figure III. 1: The used weaving method: (a) jute fabric, (b) jute fabric after removing alternated fibers in both directions, (c) resulting fabric: substituting alternated jute fibers for glass fibers (plain weaving).

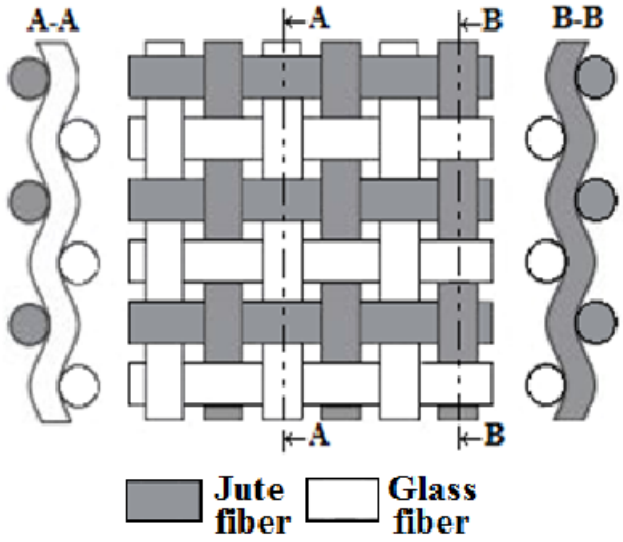

Figure III. 2: The intra-ply glass and jute co-woven fibers in two directions.

3.4.3 Composite preparation

Wooden molds of 20 × 20 cm^2 were used with different thicknesses. Then, a thin layer of wax was applied on all sides of the molds to make improve demolding. A total of 5 different composites were manufactured: a laminated composite with layers of alternating jute and glass fibers (hybrid yarns composite), a composite with one layer of alternating jute and glass fibers, a laminated composite with layers of both fibers stacked into each other (hybrid layer composite), a composite with one layer of jute fibers and one layer of glass fibers. Here, a total of 5 layers for the alternated jute and glass fibers was selected arbitrarily to produce the hybrid yarns composites.

To compare two laminated composites, the weight fraction of the reinforcements was selected. In fact, the weight fraction of the jute fiber and the glass fiber in the alternated fiber composite and in the composite with stacking layers of the two different fibers must be equivalent. Thus, the equivalent layers of jute fibers and glass fibers corresponding are 2 layers of jute fibers and 5 layers of glass fibers which represent 15.24 wt.% of jute fibers and 84.76 wt.% of glass fibers. However, to have the correct stacking of the layers, the configuration of the composite with 3 layers of jute and 4 glass fibers layers can be adopted. This new configuration increases the weight fraction of jute fibers to 26.5 wt.% while decreasing the glass fiber content to 73.5 wt.%. Table III. 2 presents the weights as well as the weight and volume fractions of reinforcements in each composite. The density of the jute fibers, woven glass fibers, roving glass fibers and resin are 1.38, 2.64, 2.55 and 1.23 g/cm^3, respectively.

Table III. 2: Weight, weight fraction and volume fraction of reinforcement in the different composites.

Sample	Reinforcements weight (g)		Weight fraction of jute	Weight fraction of glass	Volume fraction of jute	Volume fraction of glass
	Jute	Glass				
Laminated composite with five layers of alternating jute and glass fibers	14.9040	82.9280	0.1524	0.8476	0.2467	0.7533
Laminated composite with 7 layers of stacking jute and glass fibers	23.5001	65.1762	0.2650	0.7350	0.3965	0.6035
Composite with one layer of alternating jute and glass fibers	2.9808	16.5856	0.1524	0.8476	0.2467	0.7533
Composite with one layer of jute fibers	7.8335	-	-	-	-	-
Composite with one layer of glass fibers	-	16.2940	-	-	-	-

The technique used to produce the composites listed above is hand layup. The matrix used is a mixture of the dicarboxylic acid with its hardener and catalyst with a suitable weight ratio as provided by their supplier. This mixture was stirred by hand to increase the bond between the three products. During processing, the air gaps formed between the layers are gently squeezed out using a spiked roller. Figure III. 3 shows the method of layer stacking for

specimens of alternating layers and alternating yarns of jute and glass fibers. After composite manufacturing, the samples are cured at room temperature for 2 h. Table III. 3 reports on the characteristics of the five different composites obtained in terms of their code, thickness and ply orientation.

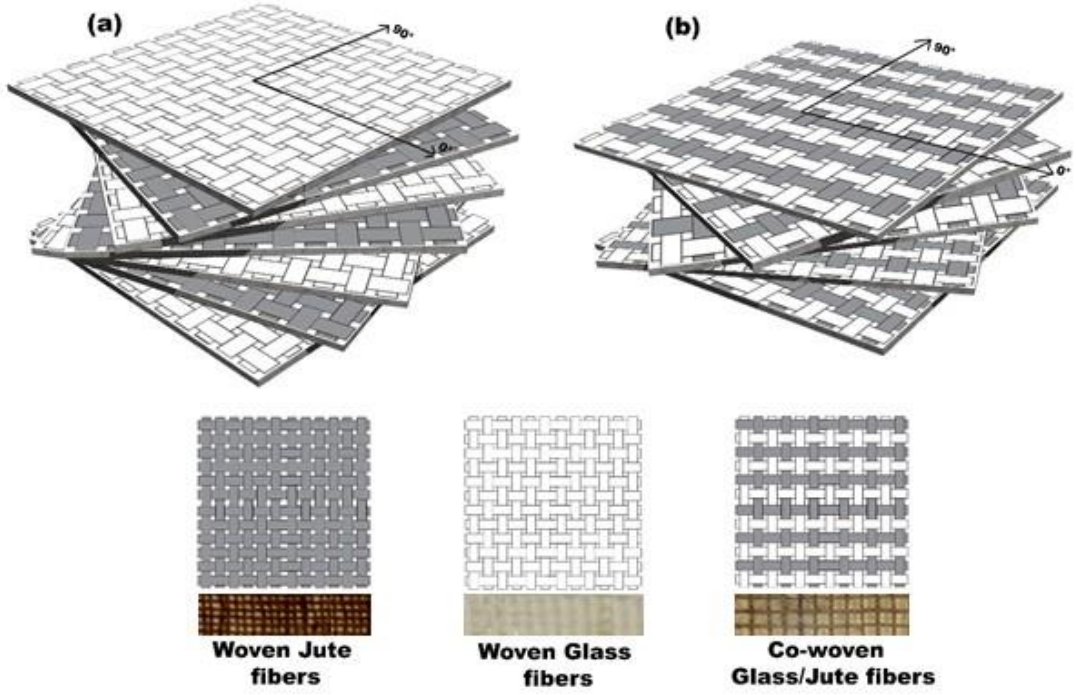

Figure III. 3: Layer stacking: (a) for composite of alternating layers and (b) for composite of alternating yarns.

Table III. 3: Sample code, thickness and ply orientation of the five types of composite studied.

Sample code	Composite description	Thickness (mm)	Ply orientation (^{o})
5YYJG	Laminated composite with five layers of alternating jute and glass fibers (yarn-by-yarn)	7.4	0/22.5/45/67.5/0
7LLJG	Laminated composite with 7 layers of stacking jute and glass fibers (layer-by-layer)	6.0	0/15/30/45/60/75/0
1YYJG	Composite with one layer of alternating jute and glass fibers (yarn-by-yarn)	2.0	UD
1LJ	Composite with one layer of jute fibers	2.6	UD
1LG	Composite with one layer of glass fibers	1.3	UD

3.4.4 Moisture absorption

To measure the moisture absorption of selected composites (5YYJG and 7LLJG), four samples were immersed in saline water at room temperature after being placed overnight in an oven at 80°C. Then, their moisture absorption (*M*) was followed for 30 days and determined as:

$$M = \frac{(W - W_0)}{W_0}\ 100(\%) \quad (1)$$

where W_0 is the weight of the sample before immersion and W is the weight of the sample after immersion.

3.4.5 Composite porosity

Fiber and composite density was measured using a gas pycnometer (Micromeritics AccuPyc II 1340). This apparatus uses the gas displacement method to measure the volume. Five purges were performed for each volume measurement and the sample mass was measured by a precision balance EXPLORER OHAUS. The density of the composites and the fibers is reported as the average of three measurements. During this test, the temperature was 20-22°C. Then, the porosity (*P*) was calculated as:

$$P(\%) = \left(1 - \frac{\rho_{exp}}{\rho_{pyc}}\right) \times 100 \quad (2)$$

where ρ_{exp} and ρ_{pyc} are the experimental density and measured density with pycnometer, respectively.

3.4.6 Mechanical characterization

The mechanical properties of the composites, especially their tensile, flexural and torsion properties, were characterized to compare between them and used in the modelling section. Tensile testing was carried out on a Tinius Olsen Horizon H10KT machine (USA) equipped with an extensometer (100R, Tinius Olsen) at room temperature according to ISO 527-01 (2012) [16]. The load was measured using a 5 kN load cell at a crosshead speed of 5 mm/min. The gauge length was 100 mm. This test was carried out on the composites with one layer (1LJ, 1LG and 1YYJG) for which the dimensions were 20×150 mm^2. The final results are reported as the average of three samples of each composite type. Tensile modulus was calculated from the slope of the initial straight line of the stress-strain curve. It should be noticed that the laminated composites (7LLJG and 5YYJG) were not subjected to tensile tests

because of the limited capacity of our tensile machine. For this reason, the laminated composites were only tested in three-point bending and the bending modulus is reported.

Three-point bending test was also carried out on a Tinius Olsen Horizon H10KT machine in the compression mode with the load applied to the middle of the composite beam. This test was performed according to ASTM D790-03 [17] on the laminated composites (7LLJG and 5YYJG). Three samples of each laminated composites were tested. The flexural modulus and flexural strength were calculated from Equation (3) and (4) [17], respectively.

$$E_f = \frac{L^3 m}{4bd^3} \tag{3}$$

$$\sigma_f = \frac{3PL}{2bd^2} \tag{4}$$

where L is the support span (mm), b is the width of the sample (mm), d is the thickness of the sample (mm), m is the slope of the tangent to the initial straight-line portion of the load-deflection curve (N/mm) and P is the load at a given point on the load-deflection curve (N). For 7LLJG, the dimensions were 18.6×6×150 mm^3, while the dimensions for 5YYJG were 19.4×7.4×150 mm^3. A 5 kN load cell was used with a crosshead speed of 5 mm/min and a span length of 125 mm.

For torsion testing, an ARES-LS Rheometer (TA instruments, England) in the torsion rectangular mode was used. The sample dimensions were 10 x 70 mm^2, while the thickness depends on the thickness of the composite produced (1LJ, 1LG and 1YYJG). The tests were carried out at room temperature under a strain of 0.05 using a frequency sweep from 0.1 to 40 Hz. The final results are reported as the average of three measurements and the shear modulus reported was the value for a frequency of 0.1 Hz to approximate a quasi-static condition.

3.4.7 Modelling section

Prediction of the elastic behavior of the laminated composites was performed by using the mechanical properties of each layer and the 1YYJG composite. The laminated composites reinforced with woven fibers (7LLJG and 5YYJG) were modelled using the classic theories of homogenization, while 1YYJG was modelling using the simple mixture law.

The homogenization technique was used to determine the behavior of the laminated composites using the properties of each layer and its corresponding thickness. This method is

based on partially inverting the behavior law of each layer, then coupling the average stiffness tensor of all layers before partially re-reversing the behavior law.

Some assumptions are considered to establish this modelling:

- The fibers are perfectly bonded to the matrix.
- The laminated materials are composed of several homogeneous and elastic layers stacked periodically and perfectly bonded to each other in the z-direction as shown in Figure III. 4.
- The structure studied is in the form of a rectangular prism and its thickness is negligible compared to the other two dimensions (i.e. $\vec{x}$ and $\vec{y}$) and thus remains constant.
- The normal to the midplane remains straight and normal to the median plane after deformation (assumption of small deformations).

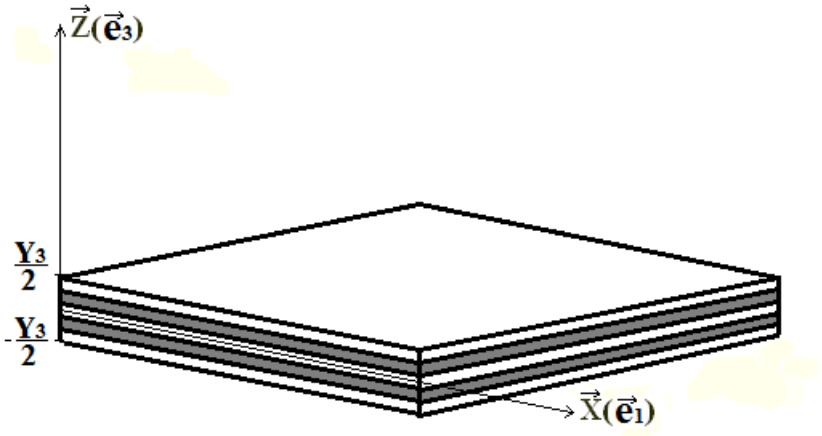

Figure III. 4: Periodic stacked layers of the composite.

The origin of the axes is on the center of the basic cell characterized by the coordinates Y=]-1/2, 1/2[×]-1/2,1/2[× y with y=]-Y_3/2,Y_3/2[with the coordinates of (0, y_1, y_2, y_3) [18].

The elasticity coefficients at a microscopic scale A(y) are only function of Y_3. They are periodic in y and constant in each section. The local coefficient of the heterogeneous volume in a macroscopic scale, Aε(x), is given by Aε(x) = A(x_3/ε) and is εy-periodic [18]. The brackets <.> indicate the average of size of the one-dimensional basic cell y to give:

$$< f(y_3) >_Y = \frac{1}{Y_3} \int_{-\frac{Y_3}{2}}^{\frac{Y_3}{2}} f(y_3) dy_3 \qquad (3)$$

The displacement vector u and the stress tensor σ are periodic functions with an unspecified period in y_1 and y_2. They are only function of the scalar variable y_3 considered as the solution for the following equilibrium problem written for a one (y)-dimensional system [18]:

$$\begin{cases} \frac{d}{dy_3}\left(\sigma_{i3}(y_3)\right) = 0 \quad in\ Y, \quad i \in \{1,2,3\} & (4-1) \\ \sigma(y_3) = A(y_3)e(y_3) \quad in\ Y & (4-2) \\ e(y_3) = E + \frac{1}{2}\left[\nabla_y(u(y_3) + \left(\nabla_y\left(u(y_3)\right)\right)^T\right] \quad in\ Y & (4-3) \\ y_3 \to \sigma(y_3), \quad y_3 \to u(y_3) \quad Y - Periodical & (4-4) \end{cases} \tag{4}$$

where *E* is the second-order symmetric tensor independent of y. The fourth-order tensor *M*(y_3) is introduced to relate the stress and elasticity tensors as:

$$\sigma(y_3) = M(y_3)E \tag{5}$$

The homogenous behavior law is a relationship obtained by taking the average over Eq. (5) as [18]:

$$< \sigma(y_3) >_Y = < M(y_3) >_Y < e(y_3) >_Y \tag{6}$$

The homogeneous coefficients *Q* are obtained by:

$$Q = < M(y_3) >_Y \tag{7}$$

As reported earlier, the 5YYJG composite contains 5 layers. Each layer of 20 cm contains horizontally 35 fiber strands of glass fibers and 34 fiber strands of jute fibers, while vertically having 36 and 35 fiber strands of glass and jute fibers, respectively. The Young's modulus of the 1YYJG composite is calculated using the simple mixing law as [10]:

$$E = V_{f_{GF}} E_{GF} + V_{f_{JF}} E_{JF} + V_{f_M} E_M \tag{8}$$

Where Vf_{GF}, Vf_{JF} and Vf_M are the volume fraction of the glass fiber, jute fiber and polyester matrix, respectively. E_{GF}, E_{JF} and E_M are the Young's modulus of the glass fiber, jute fiber and polyester matrix, respectively. Then, the same method as described above was used for the 7LLJG composite.

3.5 Results and discussion

3.5.1 Density and porosity

The density of the different fibers used and the five composites produced is reported in Table III. 4. It can be seen that the density of a mixture of natural fibers with glass fibers in a composite is lower compared to a composite based on glass fibers alone. Table III. 4 also shows that the porosity of 5YYJG is 4.6% compared to 4.3% for 7LLJG which is similar. In

this case, even if present, voids in the composite have a similar negative effect on the mechanical properties as described later [19].

Table III. 4: Density of the fibers, resin and composites with the porosity of the two laminated composites.

Sample	Density (g/cm^3)	Standard deviation (g/cm^3)	Porosity (%)
Jute fibers	1.389	0.024	-
Woven glass fibers	2.643	0.001	-
Roving glass fibers	2.560	0.032	-
Polyester resin	1.235	0.001	-
1YYJG	1.367	0.033	-
1LJ	1.260	0.023	-
1LG	1.488	0.027	-
5YYJG	1.380	0.015	4.6
7YYJG	1.411	0.021	4.3

3.5.2 Moisture absorption

The use of composites in the marine industry requires the understanding of moisture absorption under different conditions as the environment has a direct effect on the moisture absorption rate [20]. This is why the effect of water immersion on the durability of composites must be experimentally studied and Figure III. 5 presents the moisture absorption as a function of immersion time for 7LLJG and 5YYJG.

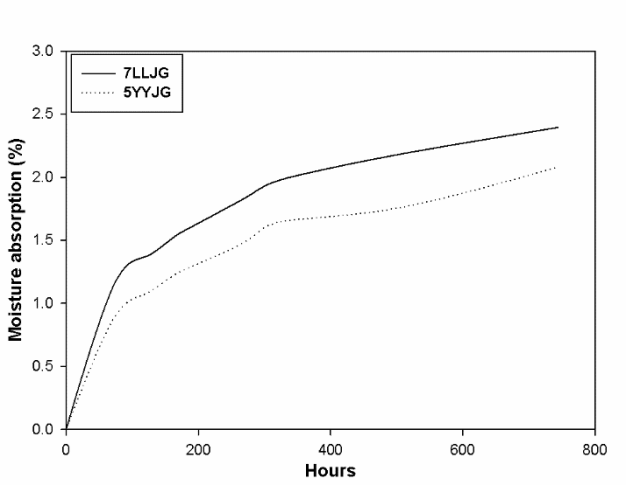

Figure III. 5: Moisture absorption as a function of time for samples 7LLJG and 5YYJG.

Figure III. 5 shows that 5YYJG presents a lower moisture absorption than 7LLJG. In our case, the weight of 7LLJG increased by 2.39% comparing to 2.08% for the hybrid yarns composite after 31 days. This represents a 13% difference. Liao et al. [21] showed that the saturation of glass fiber composites is usually reached within 2 or 3 months with an equilibrium moisture absorption of 1.5%. Here, the polyester moisture absorption can be neglected [22]. So, the main weight increase can be associated to the presence of jute fibers with a value of 26.5% for 7LLJG and 15.2% for 5YYJG. Generally, the hydrophilic character of natural fibers leads to higher moisture absorption causing weak bonding between the fibers and the polymer breaking the hydrogen bonds present at the cell wall [23–25]. In particular, the presence of hemicellulose in natural fiber accounts for most of the moisture absorption of these bio-fillers [26,27].

So 5YYJG has better moisture resistance compared with the other composite having the same overall fiber volume fraction. But it is worth to note that 5YYJG has a thickness of 7.4 mm compared to 6.0 mm for the hybrid 7LLJG composite. This result can be explained by the fact that the diffusivity behaviour of one layer of the hybrid alternating yarns of jute/glass fibers containing one half of the fibers content is less than in the case of the one layer of the hybrid alternating layers of jute/glass fibers which contains 3 layers of 100% natural fibers. The presence of the tow undulation inside the weaves provides an easier diffusion path [28]. Thus, the configuration of the woven composites is also a parameter influencing the weight gain (moisture absorption).

3.5.3 Mechanical properties

The three samples 1LJ, 1LG and 1YYJG were tested in tension up to breakup. A typical stress-strain curve is shown in Figure III. 6(a) to extract the Young's modulus and tensile strength. These results are presented in Figure III. 6(b) (Young's modulus and tensile strength for the three one-layer samples). The Young's modulus and tensile strength of the layer of glass fiber are higher than for the two other composites. However, the results indicate that the tensile strength and Young's modulus of 1YYJG are higher than for 1LJ but lower than 1LG. This indicates that hybridization produced a material with intermediate tensile properties between glass or jute fibers used alone [29]. Moreover, the tensile properties of the natural fiber-reinforced composites are low because of the different nature of the matrix (hydrophobic) and the fibers (hydrophilic) limiting compatibility and adhesion. Finally, to

improve the mechanical properties and durability of natural fiber composites, hybridization with synthetic fibers like glass is a promising technique.

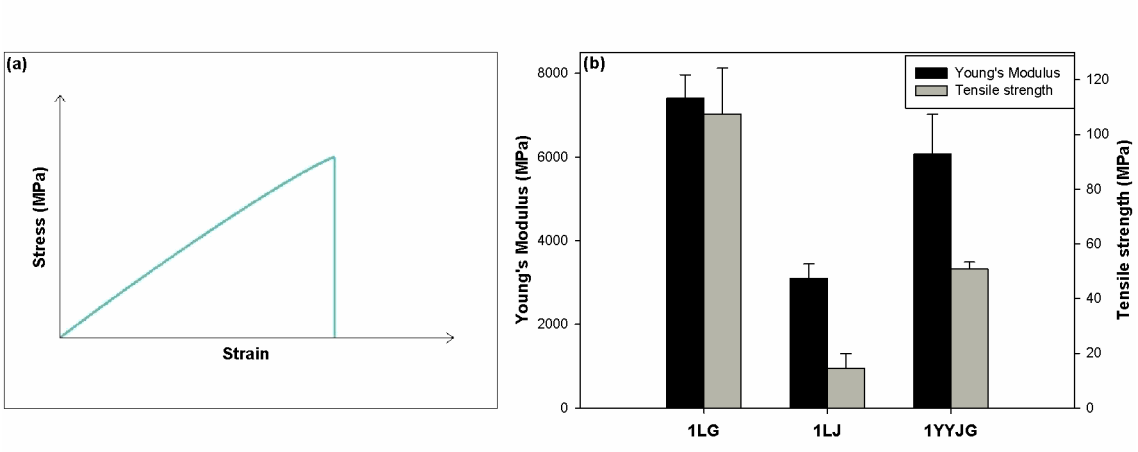

Figure III. 6: (a) Typical tensile stress-strain curve, (b) Young's modulus and tensile strength of 1LG, 1LJ, and 1YYJG composites.

To complete the mechanical characterization, three-point bending tests were performed up to break-up. A typical flexural stress-deflexion curve and the flexural properties of both composites (5YYJG and 7LLJG) are presented in Figure III. 7(a) and 7(b), respectively. The results show that 7LLJG has higher flexural modulus and flexural strength (8.8 GPa and 143 MPa, respectively) compared to 5YYJG (5.2 GPa and 88 MPa, respectively). These results indicate that the flexural modulus of 7LLJG is 40% higher than that of 5YYJG and the flexural strength of 5YYJG is 38% lower than that of 7LLJG. It is interesting to note that the 7LLJG composite contains glass fabric layers in both the compressive and tension sides allowing to explain the difference between both composites. When both intra-ply jute/glass layers were placed at the compressive and tension sides as is the case of 5YYJG, lower flexural strength but higher ductility is obtained [30]. Additionally, 5YYJG with around 85 wt.% of glass fiber (5 layers) has lower flexural properties compared to 7LLJG with only 73.5 wt.% (7 layers). This observation can be justified by the fact that the flexural properties are also related to the stacking sequence and are controlled by the external layers of reinforcement [31]. Thus, the stacking sequence and number of layer directly affect the flexural properties of the composites. Finally, by visual observation (naked eye), the fractured surfaces of the samples show fiber "pull-out" from the matrix. This also affect the mechanical response of the composites by limiting the possibility of the matrix to transfer the stresses to the reinforcements (fibers).

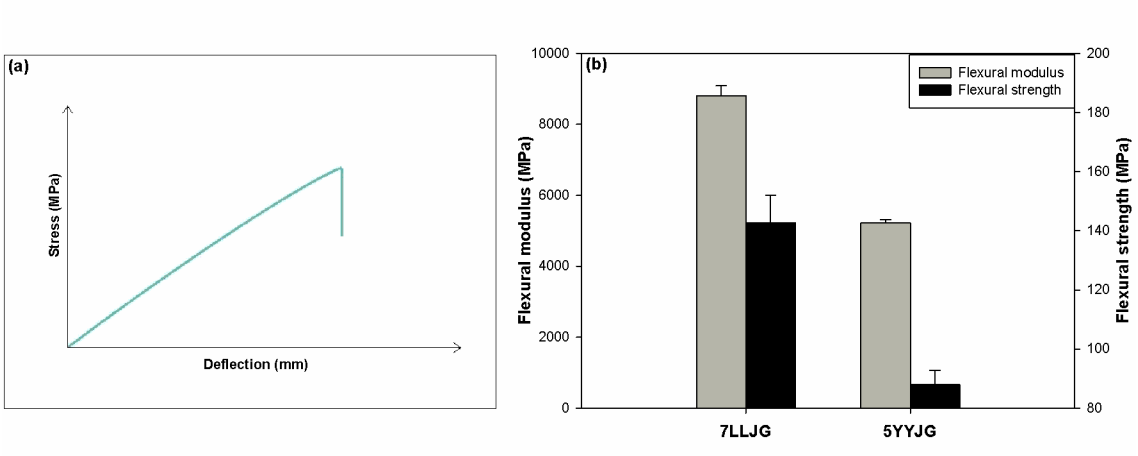

Figure III. 7: (a) Typical flexural stress-deflection curve and (b) flexural properties of the 7LLJG and 5YYJG composites.

Figure III. 8 presents the torsion properties of 1LG, 1LJ and 1YYJG. The loss factor (tan(δ)) gives a measure of the balance between the elastic and viscous behavior of materials and is defined as the ratio between the loss modulus (*G'*) and storage modulus (*G''*) as:

$$tan(\delta) = \frac{G''}{G'} \tag{9}$$

Figure III. 8(a) shows that the damping factor of the one layer composites decreases with increasing frequency which is due to the incorporation of the fibers in the matrix allowing to reduce the viscoelastic lag between the stress and the strain [32]. It is also evident from Figure III. 8(a) that firstly, the damping factor of 1LJ is higher than for the 1LG composite. Secondly, the damping factor of 1YYJG has the same behavior (curve shape) than the other composites and closely follows the loss factor of glass fibers. These results indicate that the interfacial bonding in jute fiber composite is lower than for the hybrid composite and glass fiber, in this order [33]. Thus, 1YYJG has higher damping factor compared to single jute and glass composites, meaning that, by intra-ply hybridization, the interfacial bonding could be better.

On the other hand, the complex torsion modulus (*G**) is calculated as [34]:

$$G^* = \sqrt{G'^2 + G''^2} \tag{10}$$

Figure III. 8(b) shows that the torsion modulus increases with increasing frequency meaning that they behave like an elastic solid under shear [35]. Also, the variation of the torsion modulus of 1LG is higher than that of 1LJ. Furthermore, 1YYJG exhibits a torsion modulus between the curve of both 1LG and 1LJ, but closely follows the 1LG curve. This observation

can be explained by the fact that the hybridization has a direct effect on torsion properties and represents an intermediate behaviour between both situations where each fiber is used alone [8,9,36].

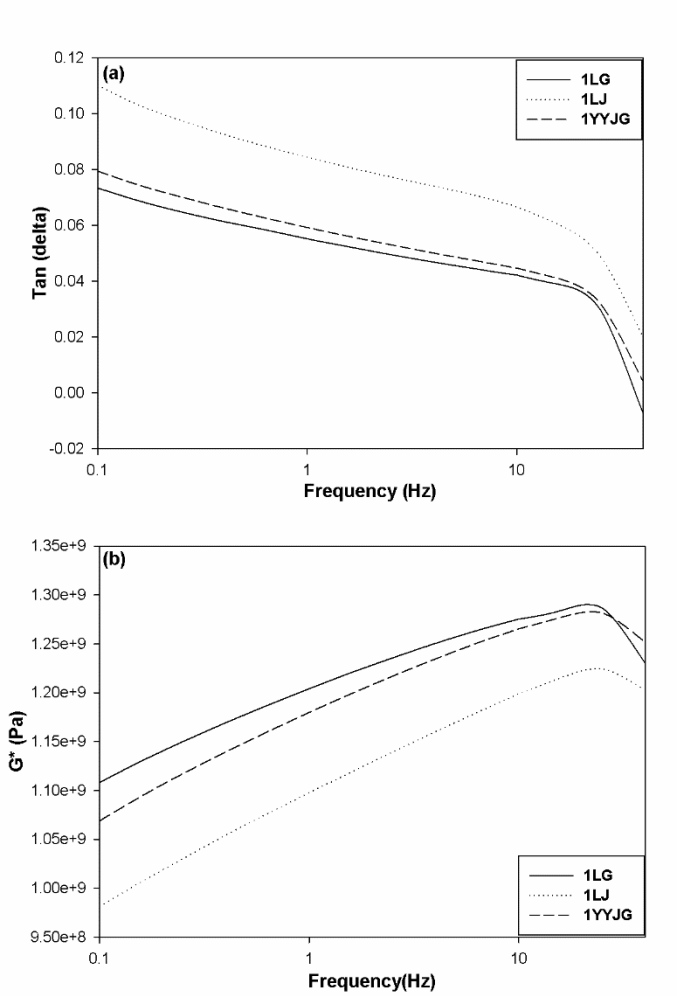

Figure III. 8: (a) Loss factor and (b) torsion modulus of 1LG, 1LJ and 1YYJG as a function of frequency.

3.5.4 Model application

In this section, the elastic behavior of the laminated composites is theoretically investigated. The homogenisation method and mixture law are the two techniques used to determine the behaviour of the resulting composites of 7 and 5 layers expressed in the system of reference axis (L, T, T') and (x, y, T'). The idea is to define each layer behavior in its principal base (L, T, T') and then defining the behaviour of each layer at an angle θ relative to the longitudinal direction 'L'.

It should be noted that the material is considered to be orthotropic although the properties are not the same in the three directions and the thickness is small compared with the other dimensions. This means that we can neglect the e_3 dimension; i.e. it is assumed that the fiber is a solid whose transversal shrinkage is negligible, so the Poisson's ratio of the material is associated to that of the matrix [37].

The stiffness tensor (S) of materials composed of one layer of woven fibers characterized by E_L, E_T, G_{LT}, ν_{LT}, E_x, E_y, G_{xy}, ν_{xy} is expressed in the 0° direction as:

$$S = \begin{pmatrix} \frac{1}{E_L} & -\frac{\nu_{LT}}{E_L} & -\frac{\nu_{LT}}{E_L} & 0 & 0 & 0 \\ -\frac{\nu_{LT}}{E_L} & \frac{1}{E_T} & -\frac{\nu_{TT'}}{E_T} & 0 & 0 & 0 \\ -\frac{\nu_{LT}}{E_L} & -\frac{\nu_{TT'}}{E_T} & \frac{1}{E_T} & 0 & 0 & 0 \\ 0 & 0 & 0 & \frac{1+\nu_{TT'}}{E_T} & 0 & 0 \\ 0 & 0 & 0 & 0 & \frac{1}{2.G_{LT}} & 0 \\ 0 & 0 & 0 & 0 & 0 & \frac{1}{2.G_{LT}} \end{pmatrix} \quad (11)$$

As mentioned earlier, the shear modulus is obtained using the torsion results. In order to determine the stiffness tensor of the other layers which differ from the first layer with an angle θ, it is necessary to go through the coordinate transformation matrix (r) defined as:

$$r = \begin{pmatrix} cos\theta^2 & sin\theta^2 & 0 & 0 & 0 & 2.cos\theta.sin\theta \\ sin\theta^2 & cos\theta^2 & 0 & 0 & 0 & -2.cos\theta.sin\theta \\ 0 & 0 & 1 & 0 & 0 & 0 \\ 0 & 0 & 0 & cos\theta & sin\theta & 0 \\ 0 & 0 & 0 & -sin\theta & cos\theta & 0 \\ -cos\theta.sin\theta & cos\theta.sin\theta & 0 & 0 & 0 & cos\theta^2 - sin\theta^2 \end{pmatrix} \quad (12)$$

Equations (13-21) are then used to determine the component of the stiffness tensor in the (x, y, T') base of the orthotropic material:

$$S'_{11} = S_{11}.cos^4\theta + S_{22}.sin^4\theta + (2.S_{12} + S_{66}).sin^2\theta.cos^2\theta \quad (13)$$

$$S'_{12} = (S_{11} + S_{22} - S_{66}).sin^2\theta.cos^2\theta + S_{12}.(sin^4\theta + cos^4\theta) \quad (14)$$

$$S'_{13} = S_{13}.cos^2\theta + S_{23}.sin^2\theta \quad (15)$$

$$S'_{16} = [2.(S_{11} - S_{12}) - S_{66}].sin\theta.cos^3\theta + [2.(S_{12} - S_{22}) + S_{66}].sin^3\theta.cos\theta \quad (16)$$

$$S'_{22} = S_{11}.sin^4\theta + S_{22}.cos^4\theta + (2.S_{12} + S_{66}).sin^2\theta.cos^2\theta \quad (17)$$

$$S'_{33} = S_{33} \quad (18)$$

$$S'_{44} = S_{44}.cos^2\theta + S_{55}.sin^2\theta \quad (19)$$

$$S'_{55} = S_{44}.sin^2\theta + S_{55}.cos^2\theta \quad (20)$$

$$S'_{66} = 2.[2.(S_{11} + S_{22} - 2.S_{12}) - S_{66}].sin^2\theta.cos^2\theta + S_{66}.(sin^4\theta + cos^4\theta) \quad (21)$$

Then, the components of the rigidity tensor (Q) in the case of a plane stress field are obtained via:

$$Q_{11} = \frac{S_{22}}{S_{11}.S_{22} - S_{12}^2} \quad (22)$$

$$Q_{12} = \frac{S_{12}}{S_{11}.S_{22} - S_{12}^2} \quad (23)$$

$$Q_{22} = \frac{S_{11}}{S_{11}.S_{22} - S_{12}^2} \quad (24)$$

$$Q_{66} = \frac{1}{S_{66}} \quad (25)$$

After calculation, the elastic modulus can be obtained as:

$$E_{theo} = \frac{Q_{11}^2.Q_{33} + 2.Q_{13}^2.Q_{12} - 2.Q_{11}.Q_{13}^2 - Q_{33}.Q_{12}^2}{Q_{11}.Q_{33} - Q_{13}^2} \quad (26)$$

For the 1YYJG composite, the predicted Young's modulus is calculated using the mixture law and the results are shown in Table III. 5.

By taking:

$$E_{GF} = 69 \text{ GPa}; E_{JF} = 30 \text{ GPa}; E_M = 3 \text{ GPa}$$

the theoretical result leads to the 1YYJG composite having a Young's modulus of 9.13 GPa, compared with the experimental value of 6.07 GPa which represents a 33% difference. This difference can be explained by the fact that the woven fibers are in reality curled while the calculations are made for straight fibers [38]. Thus, to improve on the prediction and account for the wavy shape of the woven fibers, corrections must be applied. In this work, the correction factor obtained from our previous work on Doum fiber is used (γ = 0.75) [39]. For example, the Young's modulus of 1YYJG becomes 6.85 GPa via:

$$E_{corr} = \gamma\, E_{lin} \quad (27)$$

where E_{corr}, γ, E_{lin} are the corrected Young's modulus, the correction factor and the Young's modulus of the straight fibers. Thus, the corrected Young's modulus is closer to the experimental value indicating that the fiber structure has an important effect of the overall behaviour of the composites.

Table III. 5: Predicted and experimental elastic modulus of the manufactured composites.

	E_{pred} (GPa)	E_{exp} (GPa)	Standard deviation (GPa)
1YYJG	6.85	6.07	0.55
7LLJG	6.70	8.80	1.40
5YYJG	6.04	5.21	0.59

Table III. 5 presents a comparison between the predicted and experimental elastic modulus of the three manufactured composites. It can be seen that good agreement is obtained between the calculated and experimental values. Also, the elastic modulus of 7LLJG is higher than for 5YYJG. The small differences between the results are mainly due to imperfect adhesion between the fibers and the matrix and other variations related to fiber orientation and distribution in sizes and space.

3.6 Conclusion

Composite samples made from jute and glass fibers were made using a polyester matrix. For similar fiber weight ratio, two different hybrid configurations were compared to determine its effect using a laminated architecture (intra-layer and inter-layer configurations). The composites were subjected to morphological characterization and moisture absorption, as well as tensile, bending and torsion deformation. The main conclusions of this study are:

- Whatever the laminated architecture, hybridization has a positive effect on the mechanical properties, moisture resistance and morphology of the composites.
- The laminated configuration has a direct effect on the properties of the composites.
- The tensile and torsion properties of sample 1YYJG have intermediate properties between the samples produced using glass (1LG) or jute (1LJ) fibers alone.
- The flexural properties have a direct relationship with the stacking sequence and are controlled by the external layers of reinforcement [31]. Thus, sample 5YYJG containing a layer of glass fiber in the skins has higher flexural properties compared to the inter-layer composite of jute and glass fibers.

- The homogenization technique combined with the mixing rule was successfully used to predict the elastic properties of the samples produced. The deviations between the calculated and measured values can be related to imperfect adhesion between the fibers and matrix as well as other assumptions related to the fibers themselves (orientation, sizes, distribution, etc.).

References

[1] Abdellaoui H, Bensalah H, Echaabi J, Bouhfid R, Qaiss A. Fabrication, characterization and modelling of laminated composites based on woven jute fibres reinforced epoxy resin. Mater Des 2015;68:104–13.

[2] Ouarhim W, Essabir H, Bensalah M, Rodrigue D, Bouhfid R. A Comparison between Sabra and Alfa Fibers in Rubber Biocomposites. J Bionic Eng 2019;16:754–67.

[3] Ouarhim W, Essabir H, Bensalah M-O, Zari N, Bouhfid R, Qaiss A el kacem. Structural laminated hybrid composites based on raffia and glass fibers: Effect of alkali treatment, mechanical and thermal properties. Compos Part B Eng 2018;154:128–37.

[4] Romli FI, Nizam A, Shakrine A, Rafie M, Laila D, Abdul A. Factorial Study on the Tensile Strength of a Coir Fiber- Reinforced Epoxy Composite. Procedia - Soc Behav Sci 2012;3:242–7.

[5] Rajesh M, Pitchaimani J. Mechanical Properties of Natural Fiber Braided Yarn Woven Composite: Comparison with Conventional Yarn Woven Composite. J Bionic Eng 2017;14:141–50.

[6] Swolfs Y, Gorbatikh L, Verpoest I. Fibre hybridisation in polymer composites: A review. Compos Part A Appl Sci Manuf 2014;67:181–200.

[7] Jawaid M, Abdul Khalil HPS. Cellulosic/synthetic fibre reinforced polymer hybrid composites: A review. Carbohydr Polym 2011;86:1–18.

[8] Dalbehera S, Acharya SK. Study on mechanical properties of natural fiber reinforced woven jute-glass hybrid epoxy composites. Adv Polym Sci Technol 2014;4:1–6.

[9] Velmurugan R, Manikandan V. Mechanical properties of palmyra/glass fiber hybrid composites. Compos Part A Appl Sci Manuf 2007;38:2216–26..

[10] Jacob M, Thomas S. Biofibers and biocomposites. Carbohydr Polym 2008;71:343–64.

[11] Venkateshwaran N, ElayaPerumal A, Arwin Raj RH. Mechanical and Dynamic Mechanical Analysis of Woven Banana/Epoxy Composite. J Polym Environ 2012;20:565–72.

[12] Khan JA, Khan MA. The use of jute fibers as reinforcements in composites. Biofiber Reinf. Compos. Mater., 2015, p. 3–34.

[13] Li H, Yang W. Electrospinning Technology in Non-Woven Fabric Manufacturing. In: Jeon H-Y, editor. Non-woven Fabr., InTech; 2016, p. 33–54.

[14] Wallenberger FT, Bingham PA. Fiberglass and Glass Technology. Springer; 2010.

[15] Ouarhim W, Zari N, Bouhfid R, Qaiss A el kacem. Mechanical performance of natural fibers–based thermosetting composites. Mech. Phys. Test. Biocomposites, Fibre-Reinforced Compos. Hybrid Compos., 2019, p. 43–60.

[16] Standard B, Iso B. ISO 527-5:2009Plastics — Determination of tensile properties. Part 2009;1:527–1.

[17] D790 ASTM. Standard Test Method for Flexural Properties of Unreinforced and Reinforced Plastics and Electrical Insulation Materials. ASTM Stand 2015:1–11.

[18] Nekhlaoui S, Qaiss A, Bensalah MO, Lekhder A. A New Technique of Laminated Composites Homogenization. Adv Theor Appl Mech 2010;3:253–61.

[19] Mishra V, Biswas S. Physical and mechanical properties of bi-directional jute fiber epoxy composites. Procedia Eng 2013;51:561–6.

[20] Ashik KP, Sharma RS, Guptha VLJ. Investigation of moisture absorption and mechanical properties of natural /glass fiber reinforced polymer hybrid composites. Mater Today Proc 2018;5:3000–7.

[21] Liao K, Schultheisz CR, Hunston DL. Effects of environmental aging on the properties of pultruded GFRP. Compos Part B Eng 1999;30:485–93.

[22] Pothan LA, Thomas S, Neelakantan NR. Short Banana Fiber Reinforced Polyester Composites: Mechanical, Failure and Aging Characteristics. J Reinf Plast Compos 1997;16:744–765.

[23] Boujmal R, Essabir H, Nekhlaoui S, Bensalah MO, Bouhfid R, Qaiss a. Composite from Polypropylene and Henna Fiber: Structural, Mechanical and Thermal Properties. J Biobased Mater Bioenergy 2014;8:246–52.

[24] Arrakhiz FZ, El Achaby M, Kakou AC, Vaudreuil S, Benmoussa K, Bouhfid R, et al. Mechanical properties of high density polyethylene reinforced with chemically modified coir fibers: Impact of chemical treatments. Mater Des 2012;37:379–83.

[25] El Mechtali FZ, Essabir H, Nekhlaoui S, Bensalah MO, Jawaid M, Bouhfid R, et al. Mechanical and Thermal Properties of Polypropylene Reinforced with Almond Shells Particles: Impact of Chemical Treatments. J Bionic Eng 2015;12:483–94.

[26] Gyoung J, Young S, Jin S, Hyun G, Hyeun J. Composites : Part A Effects of chemical treatments of hybrid fillers on the physical and thermal properties of wood plastic composites. Compos Part A 2010;41:1491–7.

[27] Zhi M, Qiu M, Liu Y, Cheng G, Min H. The effect of fiber treatment on the mechanical properties of unidirectional sisal-reinforced epoxy composites. Compos Sci Technol 2001;61:1437–47.

[28] Tang X, Whitcomb JD, Li Y, Sue H. Micromechanics modeling of moisture diffusion in woven composites. Compos Sci Technol 2005;65:817–26.

[29] Amico SC, Angrizani CC, Drummond ML. Influence of the stacking sequence on the mechanical properties of glass/sisal hybrid composites. J Reinf Plast Compos 2010;29:179–89.

[30] Ary Subagia IDG, Kim Y, Tijing LD, Kim CS, Shon HK. Effect of stacking sequence on the flexural properties of hybrid composites reinforced with carbon and basalt

fibers. Compos Part B Eng 2014;58:251–8.

[31] Munikenche Gowda T, Naidu ACB, Chhaya R. Some mechanical properties of untreated jute fabric-reinforced polyester composites. Compos Part A Appl Sci Manuf 1999;30:277–84.

[32] Ray D, Sarkar BK, Das S, Rana AK. Dynamic mechanical and thermal analysis of vinylester-resin-matrix composites reinforced with untreated and alkali-treated jute fibres. Compos Sci Technol 2002;62:911–7.

[33] Laly A, Zachariah O, Thomas S. Dynamic mechanical analysis of banana fiber reinforced polyester composites. Compos Sci Technol 2003;63:283–93.

[34] Arrakhiz FZ, El Achaby M, Benmoussa K, Bouhfid R, Essassi EM, Qaiss A. Evaluation of mechanical and thermal properties of Pine cone fibers reinforced compatibilized polypropylene. Mater Des 2012;40:528–35.

[35] Arrakhiz FZ, Malha M, Bouhfid R, Benmoussa K, Qaiss A. Tensile, flexural and torsional properties of chemically treated alfa, coir and bagasse reinforced polypropylene. Compos Part B Eng 2013;47:35–41.

[36] Abdullah-Al-Kafi, Abedin MZ, Beg MDH, Pickering KL, Khan MA. Study on the Mechanical Properties of Jute/Glass Fiber-reinforced Unsaturated Polyester Hybrid Composites: Effect of Surface Modification by Ultraviolet Radiation. J Reinf Plast Compos 2006;25:575–88.

[37] Malha M, Nekhlaoui S, Essabir H, Benmoussa K, Bensalah MO, Arrakhiz FE, et al. Mechanical and thermal properties of compatibilized polypropylene reinforced by woven doum. J Appl Polym Sci 2013;130:4347–56.

[38] Malha M. Mise en oeuvre, Caractérisation et modélisation de matériaux compoites: Polymère thermoplastique renforcé par des fibres de Doum. Mohammad V - Agdal, Faculté des Sciences Rabat, 2013.

[39] Malha M, Nekhlaoui S, Essabir H, Benmoussa K, Bensalah M-O, Arrakhiz F-E, et al. Mechanical and thermal properties of compatibilized polypropylene reinforced by woven doum. J Appl Polym Sci 2013;130:4347–56.

CHAPTER IV

CHARACTERIZATION AND NUMERICAL SIMULATION OF LAMINATED GLASS FIBER-POLYESTER COMPOSITES FOR A PROSTHETIC RUNNING BLADE*

4.1 Abstract

The objective of this work was to explore different types of deformations (buckling, bending and relaxation) on the properties of laminated composites based on polyester as the matrix and glass fiber (GF) in two forms: woven (WGF) and chopped strand mat (CSM). The specimens were produced with the same thickness but the different number of ply. Also, a thin gelcoat based on clay particles was applied to the CSM samples to get a third series. The results showed that using the same thickness, the mechanical properties, especially in terms of bending and buckling, are influenced by the layers' number. Furthermore, a sports application is presented as an applied investigation for a leg prosthesis. Three different running blades "Flex-foot Cheetah" were manufactured to be experimentally and numerically (ANSYS ACP software) characterized to simulate real conditions. The results showed good agreement between the experimental and numerical values in terms of total deformation.

*

Reprinted in part with permission from Ouarhim W, Rodrigue D, Bensalah M-O, Bouhfid R, Qaiss A. Characterization and numerical simulation of laminated glass fiber-polyester composites for a prosthetic running blade. **Materials Science & Engineering C** (Submitted).

4.2 Résumé

Ce travail a pour objectif d'étudier les différents types de déformations (flambement, flexion et relaxation) des composites stratifiés à base de polyester renforcé de fibres de verre (GF), et ceci suivant deux formes : le tissé (WGF) et le mat à fils coupés (CSM). Les éprouvettes ont été réalisées avec la même épaisseur, tandis que le nombre de plis est différent. De plus, une couche mince de gelcoat à base de particules d'argile a été étalée sur la surface des échantillons de CSM, obtenant ainsi une troisième série. Les résultats ont clairement montré que le nombre de couches joue un rôle important dans l'amélioration des propriétés mécaniques, notamment en flexion et en flambement. En outre, une prothèse de jambe a été présentée comme étant une application dans le domaine sportif des composites stratifiés. Cependant, trois lames de course différentes "Flex-foot Cheetah" ont été fabriquées pour être expérimentalement et numériquement (logiciel ANSYS ACP) caractérisées pour simulation des conditions réelles. Finalement, un bon accord entre les résultats expérimentaux et les résultats numériques fournis par le logiciel ANSYS ACP a été obtenu, en termes de déformation totale.

4.3 Introduction

The polymer composites market is still relatively young, but economically and technologically rapidly growing. Today, polymer composites are commonly used in different fields such as automobile, aeronautics and aerospace industries replacing metal parts due to their higher specific strength, lower density, improved stiffness and lower costs. These composites offer substantial weight savings, increased performance and design flexibility [1-3].

The most used synthetic fibers in composites are glass, carbon and Kevlar (aramid), but glass fibers have been around for a long time and designers/engineers are familiar with their properties, performances and modifications. They have high strength because their processing methods avoid internal or external defects [4]. Moreover, glass fibers are found in different forms including chopped strands, roving, yarns, fabrics and mats [5,6]. Generally, these fibers are not used alone but embedded in an organic matrix such as polyester, vinylester, phenolic and epoxy resins [7]. In this context, roughly 95% of the composite market is based on thermosetting materials [8].

Different structures are used in specific applications, but the most common one consists of bonding several layers one on top of another to form a high strength laminated composite. Using a suitable matrix, the plies are bonded together and this assembly leads to high mechanical properties including planar stiffness, flexural stiffness, strength and coefficient of thermal expansion. Since there is a wide range of fibers and matrices available, polymer composites are becoming increasingly used for structural applications.

One important aspect is the selection of the fiber type and dimensions because they have a direct effect on the final laminate properties; i.e. woven mat or chopped strand mat gives very different mechanical properties. For example, Bhaskar et al. [9] reported that polyester reinforced with chopped strand mat glass fiber has higher strength than that of woven roving glass fibers against flexural, compression and impact. The random arrangement (different orientations) of the glass fibers in the chopped strand mat configuration is the reason why these composites are more resistant for these three mechanical deformation than in woven roving composites in which the fibers are aligned in two directions. The stacking configuration of two or more reinforcement layers is called a laminate and these structures can be obtained by different processes. However, the hand layup process is the simplest

technique to manufacture these composites due to its low tool costs and the use of room temperature cured resins. However, it also presents some drawbacks such as being time consuming and the formation of air bubbles.

This work is decomposed in two parts. The first part presents the processing (formulations and conditions) and the characterization (water absorption and mechanical properties) of the materials selected, while the second part will use these results to develop a prosthetic running blade (processing, characterization and numerical simulation under different deformation).

4.4 Materials and methods

4.4.1 Material properties

The matrix used in this study was a polyester resin crown mixed with its hardener (AKPEROX A50) and its catalyst (Cobalt Octoate 1%) provided by Detail Chimie (Morocco). As reinforcement, two forms of glass fibers were selected: chopped strand mats and woven fabrics with 300 g/m^2 and 400 g/m^2 respectively, also provided by Detail Chimie (Morocco). Figure IV. 1 shows the fumed silica (aerosil) agglomerates (Detail Chimie, Morocco) under optical microscopy (NIKON eclipse LV100ND). Moreover, the Moroccan clay used is denoted as Bayada with a density of 1.52 g/cm^3. The clay was sourced in southern Morocco (Essaouira city) and was purified in our laboratory. It is characterized by a rough surface with an average diameter close to 10 μm [10]. A mold release agent (BARDAHL MAGHREB, Morocco) and transparent plastic sheets were used for easier demolding.

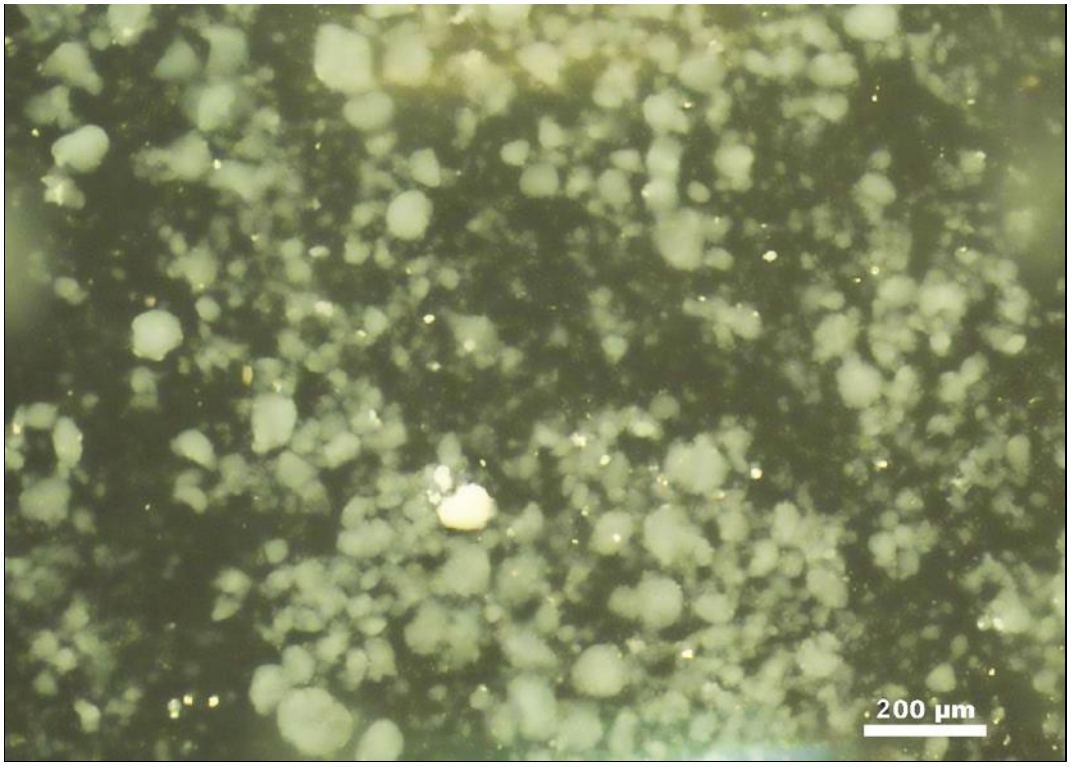

Figure IV. 1: Fumed silica particles under optical microscopy.

4.4.2 Experimental procedure

4.4.2.1 Gelcoat preparation

The gelcoat is a mixture of a polyester resin with its hardener and catalyst (aerosil and clay). After preliminary trials, the best formulation was: 200 g of resin with 7 g of aerosil and 20 g of clay. The procedure was to add the aerosil in the resin with its hardener to be mechanically mixed to obtain a homogeneous viscous mixture. Then the clay was added and mixed again. Finally, the catalyst was added to accelerate the polymerization reaction. This mixture was applied directly on a transparent plastic sheet using a brush on the different sides of the composite.

4.4.2.2 Composite preparation

A mold of 300 mm x 200 mm was used to prepare the composites at room temperature. The first step of the hand layup process was cleaning the mold surface and apply the wax (release agent). Then a transparent plastic sheet was placed to cover the mold and the fibers were prepared. Afterward, the resin mixed with the appropriate hardener and catalyst was applied

on the glass fiber fabrics (chopped strand mats and woven). The thickness was fixed at 6 mm because of the limited load cell of our tensile machine (Tinius Olsen Horizon H10KT). Therefore, this constraint allowed to use 6 layers for chopped strand mats, 7 layers for woven glass fiber and 5 layers of chopped strand mats with two thin layers of gelcoat (one on each side) as presented in Figure IV. 2 and Table IV. 1. Lamination consists of placing the chopped strand mat glass fibers on the gelcoat and impregnating them with the resin using a brush using several successive pressure steps to expel the air bubbles. After the resin crosslinking (about 30 min), the sample was demolded and cut according to the required dimensions for characterization.

Table IV. 1: Composite codes.

Composites	**Designation**	**Woven glass fibers layers**	**Chopped strand mat glass fibers layers**	**Gelcoat layers**
CSMGPC	**C**hopped **s**trand **m**ats **g**lass fibers reinforced with **p**olyester resin **c**omposite	0	6	0
WGPC	**W**oven **g**lass fibers reinforced with **p**olyester resin **c**omposite	7	0	0
CSMGPGC	**C**hopped **s**trand **m**ats **g**lass fibers reinforced with **p**olyester resin coated with **g**elcoat **c**omposite	0	5	2

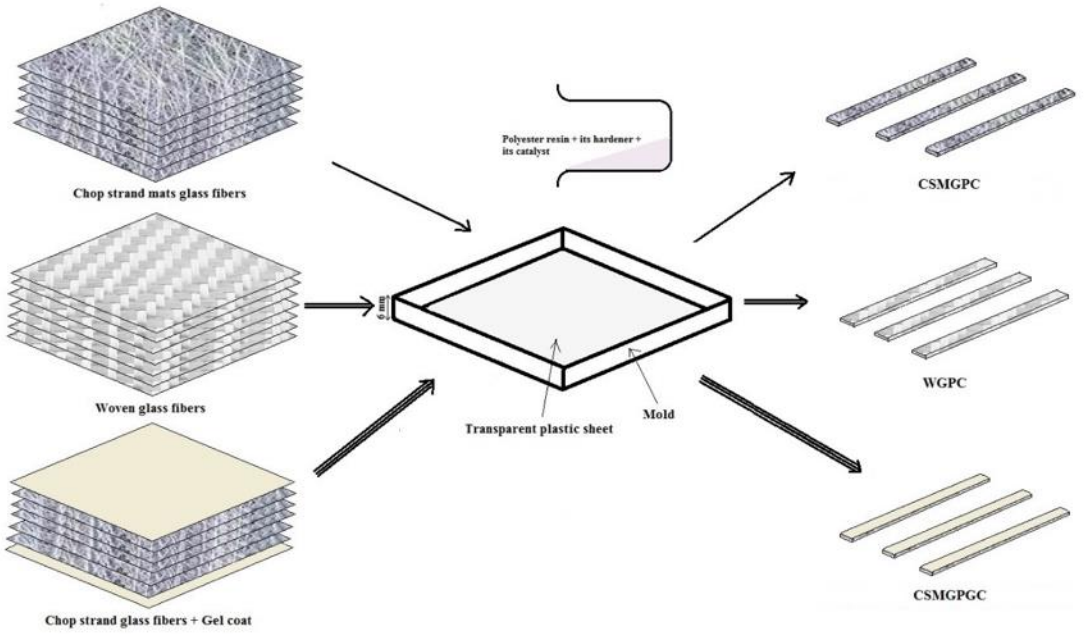

Figure IV. 2: Schematic representation of the composites preparation.

4.4.3 Characterization

4.4.3.1 Scanning electron microscopy (SEM)

Scanning electron microscopy was used to highlight the morphology of the gelcoat. The SEM used in this work was a FEI QUATTRO S (Thermo Fisher Scientific, USA) operated at 15 kV under low vacuum. The hardened gelcoat was cryo-fractured in liquid nitrogen to get clean and clear cross-sections.

4.4.3.2 ATR-FTIR analysis

Fourier transform infrared spectroscopy (FTIR) was used to get the infrared spectrum (absorption or emission) of the gelcoat. The equipment used was a Perkin Elmer Spectrum two spectrometer working under attenuated total reflectance (ATR) Miracle Diamant. The spectra were obtained by the accumulation of 16 scans in the range of 8300 to 350 cm^{-1} at a resolution of 0.5 cm^{-1}.

4.4.3.3 Three-point bending

Flexural testing was carried out using a Tinius Olsen Horizon H10KT under a three-point bending mode according to ASTM D790-03 [11]. One panel is used for each sample (CSMGPC, WGPC and CSMGPGC) to be tested in three different areas as illustrated in

Figure IV. 3. The panel dimensions are 274 x 30 x 6 mm^3. A 5 kN load cell was used for this test. The distance between the supports (span) was fixed at 130 mm and the test was conducted at 5 mm/min.

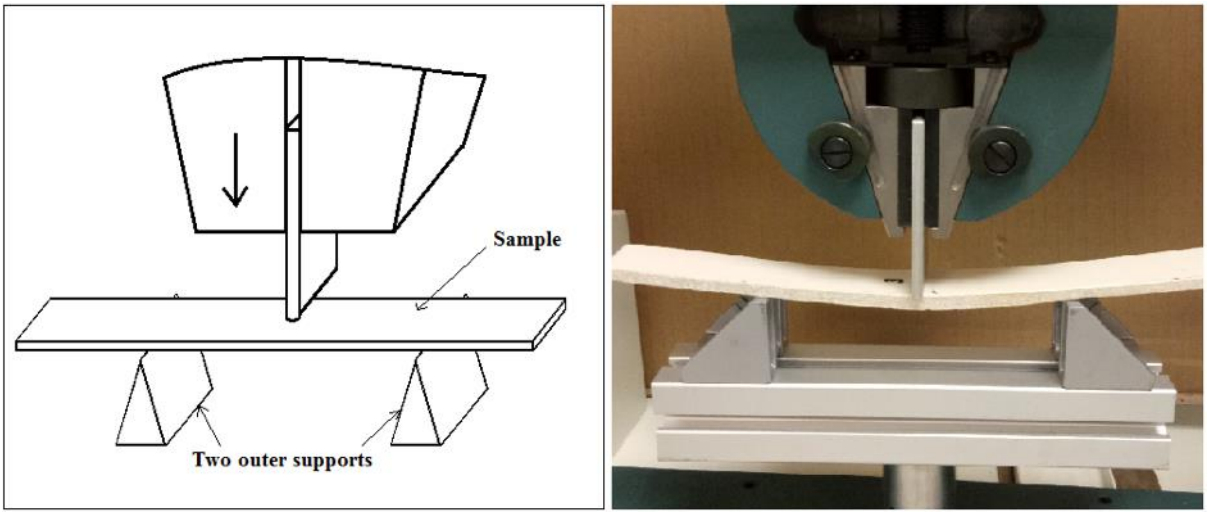

Figure IV. 3: Schematic representation of the three-point bending test.

4.4.3.4 Buckling

This test was performed using a Tinius Olsen Horizon H10KT under a compression mode. The panel dimensions were 30 mm in width, 6 mm in thickness and 274 mm in length. Each panel was tested three times. The load cell used was 5 kN to perform the tests at 5 mm/min.

During the test, the panel is connected to two V-profile beams fixed on the machine jaws and the guidance is provided by the machine. To limit sample-fixture interactions, the panel ends were rounded as shown in Figure IV. 4.

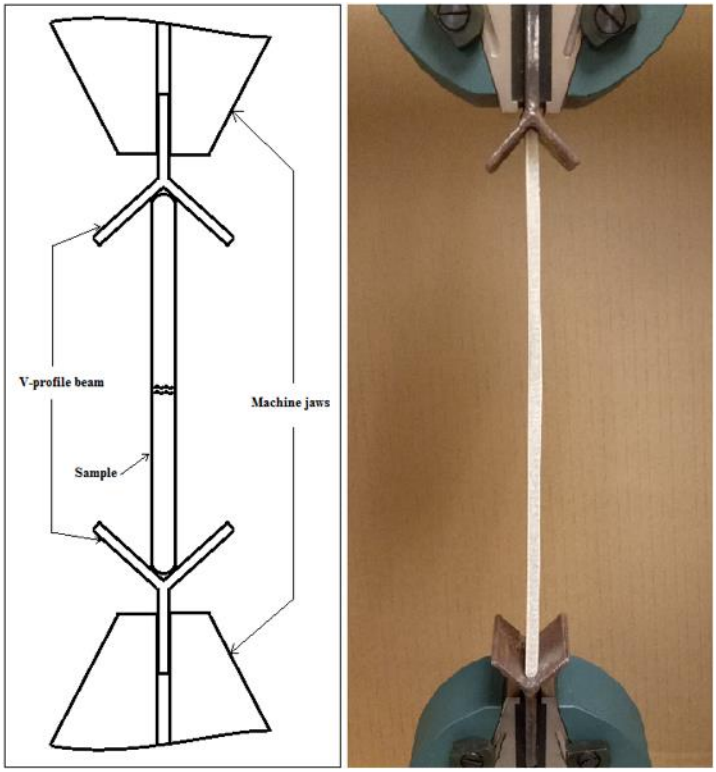

Figure IV. 4: Schematic representation of the buckling test.

4.4.3.5 Relaxation in buckling

The relaxation test in buckling was carried out using a Tinius Olsen Horizon H10KT under a compression mode. This test was conducted at different loading rates (5, 10, 50 and 100 mm/min) up to 2 mm in strain.

4.4.3.6 Moisture absorption

Two samples of 135 mm × 30 mm × 6 mm were used for each composite. All the samples were placed in a beaker filled with saturated salty tap water at room temperature to simulate a marine environment as an extreme condition and the solution was changed every week. All the samples were dried before their immersion in water to remove any moisture. Then, their weight was periodically measured (0, 1, 3, 5, 7, 9, 12, 15, 21 and 30 days). Moisture absorption was assessed as the relative weight gained. It must be noted that for the coated composites, the gelcoat covered all sides.

4.5 Results and discussion

4.5.1 Gelcoat and composite morphological characterization

Figure IV. 5(a) presents the SEM image of the Bayada clay. It can be seen that the particles are ellipsoidal with an average length of 7.75 µm. Figure IV. 5(b) depicts the good distribution and dispersion of the clay particles and fumed silica in the polyester resin (absence of aggregate). This uniform distribution indicates that good conditions were used for mixing [12].

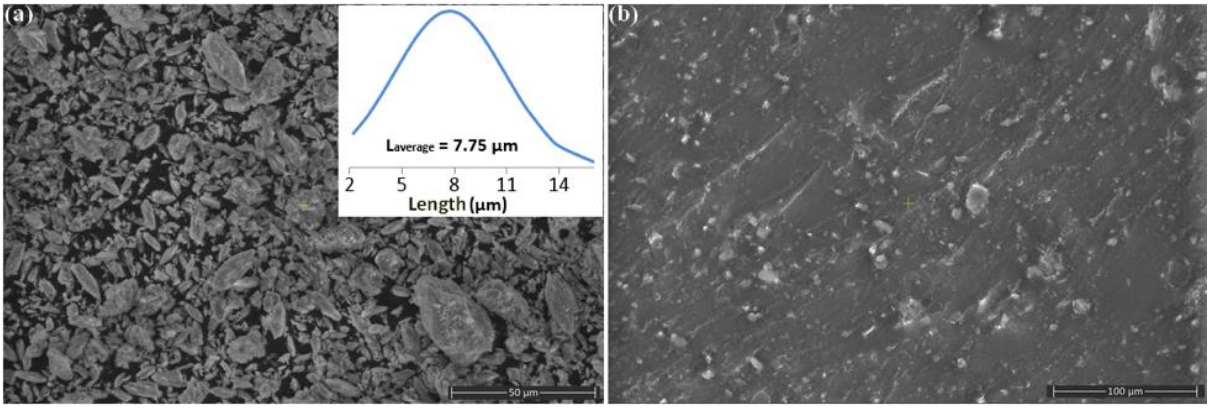

Figure IV. 5: SEM images of: (a) Bayada clay and (b) gelcoat.

4.5.2 Structural characterization of the gelcoat

Figure IV. 6 presents the FTIR spectrum of the Bayada clay, fumed silica, polyester resin and gelcoat. The most intense bands in the gelcoat spectrum are also found in the Bayada clay, aerosil and polyester resin spectra. As expected, this confirms the presence of all three components in the prepared gelcoat. Two intense bands at 2920 and 2850 cm^{-1} are associated to C-H stretching (CH and CH_2) characteristic of the polymer resin. Moreover, the absorption band at 1711 cm^{-1} is due to C=O in the polyester. Bayada clay is composed of several components including calcium carbonate ($CaCO_3$) at 1455 cm^{-1} [13]. In addition, the band at 1260 cm^{-1} is associated to C=O stretching in polyester. Li et al. [14] reported that the absorption bands at 802 and 1079 cm^{-1} are due to Si-O-Si stretching modes in the fumed silica. Also, they stated that the vibration band at 978 cm^{-1} is attributed to Si-OH stretching in Bayada clay. Finally, the 778 cm^{-1} band is associated to Si-O symmetrical stretching in aerosil.

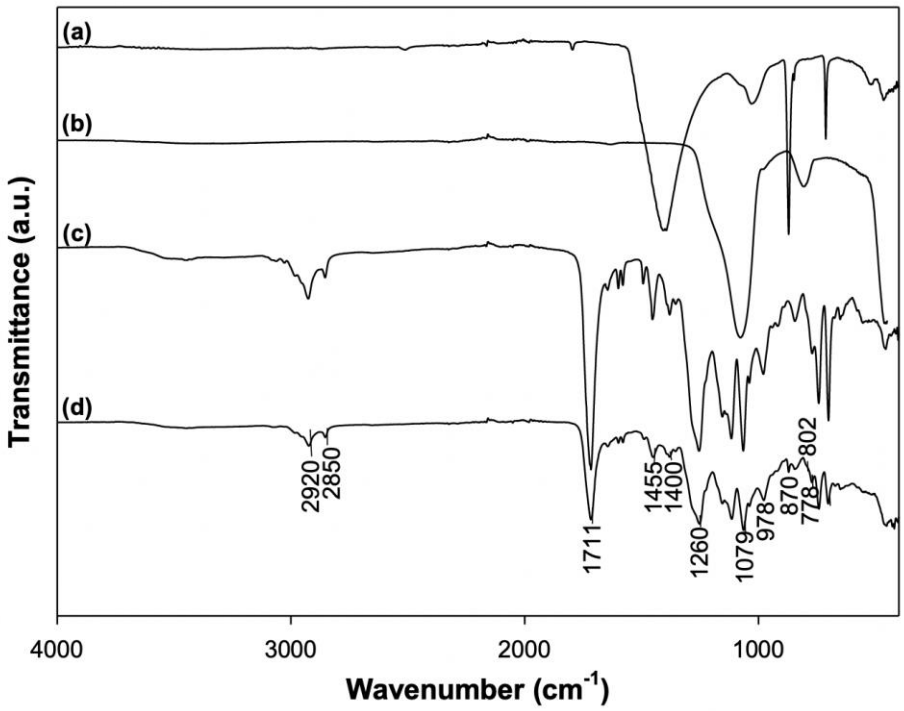

Figure IV. 6: FTIR spectrum of: (a) Bayada clay, (b) fumed silica, (c) polyester resin and (d) elaborated gelcoat.

4.5.3 Three-point bending properties

The bending modulus (modulus of elasticity) in flexion E_B is obtained as:

$$E_B = \frac{L^3 m}{4bd^3} \quad (1)$$

where L stands for the support span and b refers to the beam width, while d and m denote the beam depth and the slope of the initial straight-line portion of the load-deflection curve, respectively. Figure IV. 7 presents the bending modulus of the three laminated panels (CSMGPC, WGPC and CSMGPGC). The results show that the bending modulus of the WGPC panel is higher than of chopped strand mats glass fiber laminated panels. The chopped strand mats, which is based on randomly distributed short length glass fiber, is more likely to yield a composite with almost orthotropic characteristics but lower strength than of a composite produced by a more aligned arrangement of glass fibers of longer length like in woven fabrics [15]. Moreover, the bending modulus of CSMGPGC is lower than CSMGPC

by around 10% because the presence of two gelcoat layers reduced the number of glass fibers layers (Table IV. 1) leading to lower flexural properties [16].

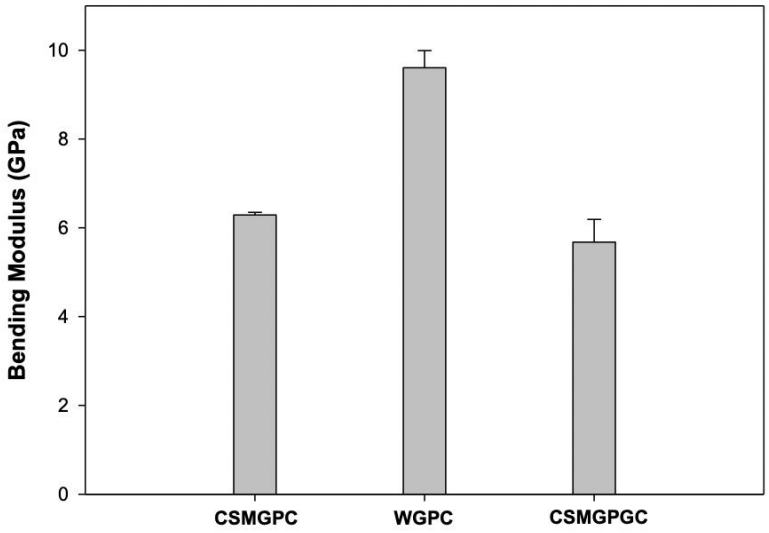

Figure IV. 7: Bending modulus of the sample.

Figure IV. 8 shows the results of the longitudinal elastic stiffness and the maximum stress in buckling. The apparent longitudinal elastic stiffness is the slope of the load vs. displacement plot. When this slope decreases, buckling is initiated.

The longitudinal elastic stiffness and maximum stress in buckling of WGPC are higher than those of CSMGPC and CSMGPGC. In other words, applying the same load to WGPC generate less displacement than in the case of CSMGPC, thereby the slope of the load vs. displacement curve is more important. In the woven fabric, the fibers are characterized by a longitudinal and transverse arrangement giving the fabric a random structure. In this case, the cracks will propagate more easily in the chopped strand mat fabric under a compression load.

After buckling, delamination is another important effect. This phenomenon includes break-up under shear either at the fiber-matrix interface or between adjacent layers [17]. Therefore, delamination decreases the in-plate stiffness, thereby reducing the buckling loads.

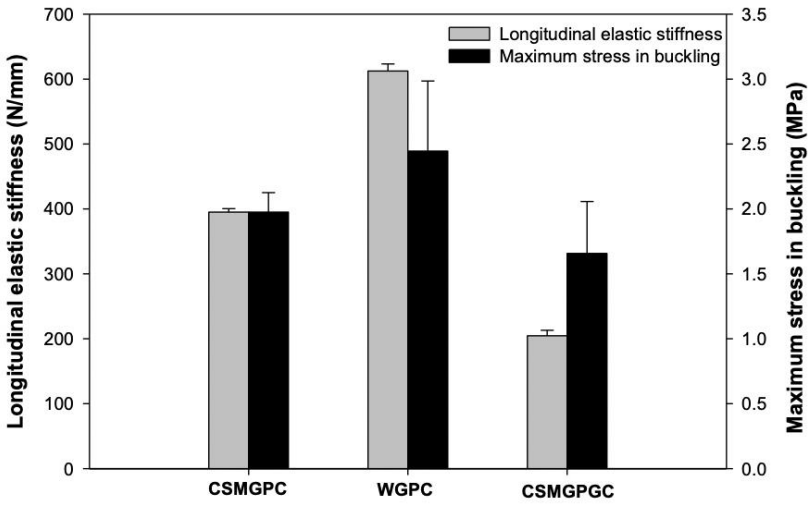

Figure IV. 8: Buckling test results.

.

4.5.4 Relaxation in buckling properties

After applying a compressive force to reach buckling, the laminated panels undergo a relaxation in time. Figure IV. 9(b) depicts the variation of this relaxation time (the time between the start of the relaxation step and the intersection of the initial slope with the equilibrium stress [18]) as shown in Figure IV. 9(a) for the different laminated panels tested under four loading rates. Figure IV. 10 shows that the relaxation time for the same specimen decreases with increasing loading rate from 5 to 100 mm/min. In other words, slower loading rate leads to higher relaxation time. This is expected as higher loading rates generate higher deformation rates and the laminated panels do not have enough time to return to their initial position. The material response is thus affected by incomplete rearrangement of molecular chains [19]. Moreover, it can be seen that WGPC has the lowest relaxation time at slower loading rate, but CSMGPGC has the highest relaxation time at higher loading rate. These results show the effect of the gelcoat on the laminated composites. Due to the added clay particles in the manufactured gelcoat, the relaxation time is high when the loading rate is low. Again this is expected as the presence of clay particles in both gelcoat layers retarded the chain motion leading to slower relaxation [20], which is associated to the geometric confinement of the organoclay network [21]. After releasing the compressive load, the molecular chains of WGPC having higher longitudinal elastic stiffness than CSMGPGC are quickly relaxed back compared to CSMGPGC. Thus, the confined motion of macromolecular

chains by the organoclay network is useful to improve the (dimensional) stability of composites reinforced by clays [22].

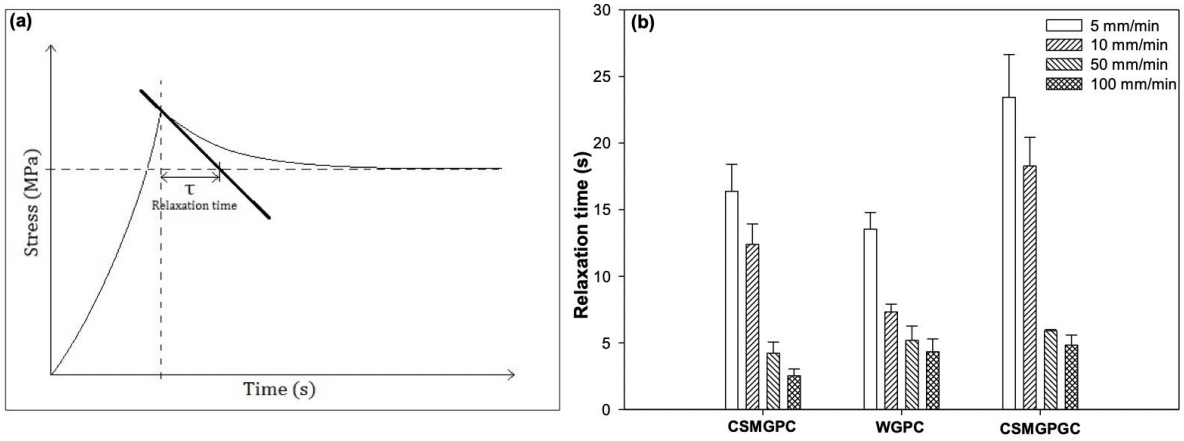

Figure IV. 9: (a) Experimental determination of the relaxation time (τ), and (b) post buckling relaxation time after different loading rates.

Figure IV. 10 shows the variation of the final stress (equilibrium) after buckling. The results indicate that the final stress in relaxation after buckling of CSMGPGC is less important than that of CSMGPC and WGPC for all the loading rates tested. Referring to the results based on relaxation time, the highest final stress is related to the lowest relaxation time. In fact, when the relaxation time is longer, the molecular chains have enough time to return to their initial state. Consequently, the final stress after buckling is lower. This phenomenon is purely related to the viscoelastic behavior of the resin and the composites [23].

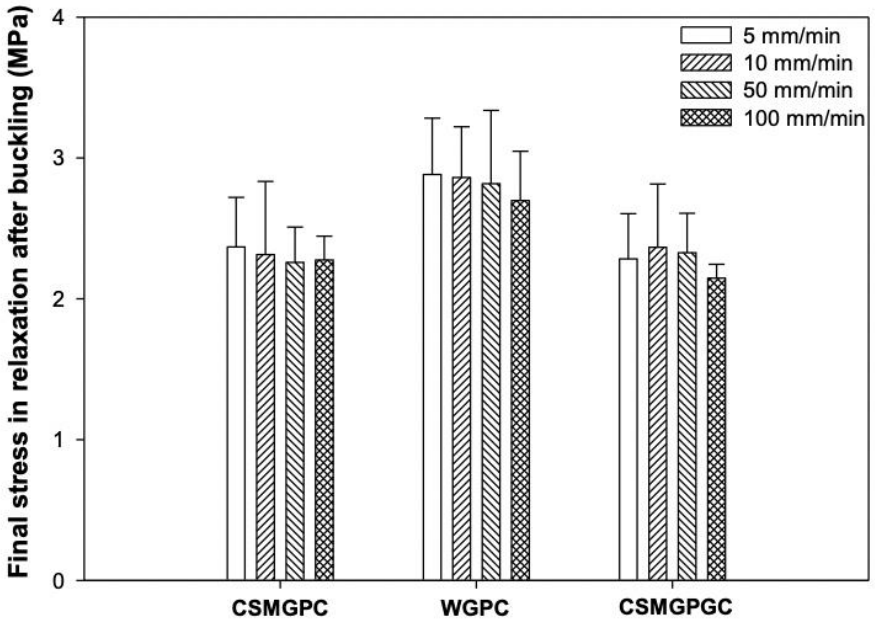

Figure IV. 10: Final stress after relaxation in buckling of chopped strand mats glass fiber (CSMGPC), woven glass fiber (WGPC) and chopped strand mats of glass fiber coated by prepared gelcoat (CSMGPGC).

4.5.5 Gelcoat effect on moisture absorption

The use of composite materials in the marine environment requires an understanding of the phenomenon of moisture absorption. The influence of hygroscopic environment conditions can be represented by moisture absorption; i.e. the net weight gains during a specific moisture uptake time. Table IV. 2 summarizes the density of the reinforcements, polyester and gelcoat, while Figure IV. 11 presents the water absorption (W) results as [24]:

$$W(\%) = \frac{M_w - M_0}{M_0} \times 100 \quad (2)$$

where M_0 denotes the weight of the dried specimen before immersion and M_w stands for the weight of the wet specimen after a determined immersion time.

The results show that the water absorption of CSMGPGC is higher than the other samples without gelcoat. This result is justified by the presence of clays in the gelcoat which is characterized by its hydrophilic character [25]. Moreover, Figure IV. 11 shows that the water absorption rate of CSMGPC is lower than WGPC; i.e. the water uptake of WGPC is more important which is in agreement with the literature [5]. Boukhoulda et al. [26] explained this finding by the fact that the humidity concentration is a function of fiber orientation. It is

worth noting that the plasticization of the polymer network (lower glass transition temperature and the threshold of plasticity) is one of the main consequences of water absorption into polymers [27].

Table IV. 2: Density of different components of the composites.

Component	Density (g/cm^3)	Standard deviation
Woven glass fiber	2.643	0.001
Chopped strand mats glass fiber	2.535	0.001
Hardened polyester	1.234	0.001
Gelcoat	1.311	0.001

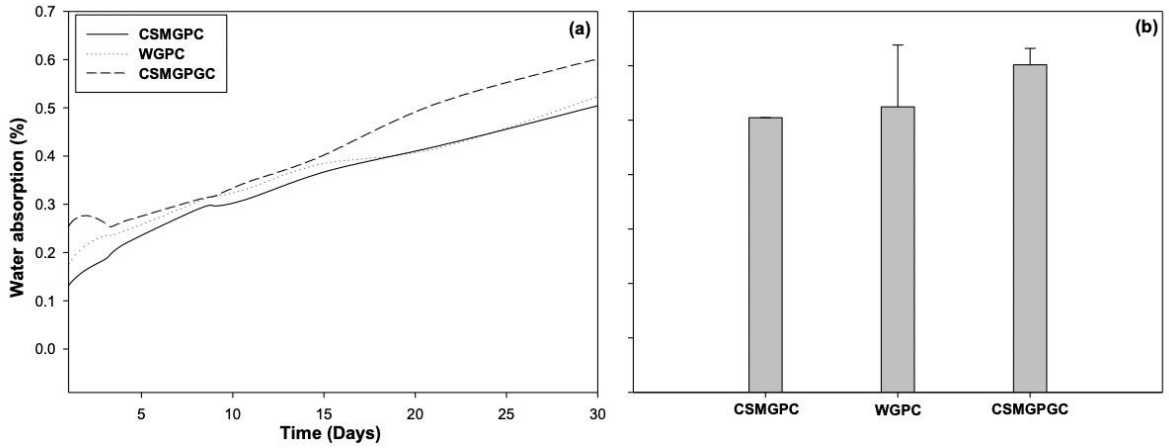

Figure IV. 11: Moisture absorption curves of different composites: (a) as a function of time, and (b) after 30 days (both vertical axes have the same scale).

From the results obtained, the samples produced are now compared for a specific application: a prosthetic leg replacement as described next.

4.6 Application

4.6.1 Background

Nowadays, composite materials are used in different areas especially for sporting goods where their benefits in terms of high stiffness, lightweight, protection and customization are appreciated by elite athletes and enthusiastic amateurs alike. In other words, the

developments made in new composites are used in sport applications including equipment, apparel, safety wear, prosthetics and infrastructure. This is intended for material developers/suppliers, manufacturers, researchers and athletes of all abilities [28]. But a special application is for disabled people to perform their activities. For years, talented athletes, full of determination and energy, had limited possibilities to compete in competitive sports. But important advances in scientific innovation have made it possible, through biomechanics and other technologies, to find innovative solutions to help them. After amputation (leg or arm), a prosthesis remains the only way for people with disabilities to practice their sport. It offers them an opportunity to overcome their handicap. However, the access to sport for disabled people goes through the acquisition of specialized prosthesis (custom made). Recently, prosthetics offered good movement freedom and more comfort, safety, strength and durability owing to the understanding of the biochemical function of the human body as well as the availability of lighter, stronger and more flexible materials combined with the emergence of increasingly advanced engineering technologies. Another important point is the weight. For example, a prosthetic leg would weigh about 4 kg less than a natural leg [29]. This energy-saving is considered by many as a decisive advantage for running. Thus, the amputees run with sportive prosthesis restoring energy. This is why these prostheses must be lightweight with maximum energy restitution. Different types of transtibial prosthesis designs including Cheetah, Flex-Run and Flex-Sprint models are available on the market (see Figure IV. 12). Using these innovative prostheses, disabled runners can store and get back elastic energy during deformation.

Different materials are currently used to produce leg prosthesis such as carbon fiber, titanium and graphite. Not only do these materials reduce the prostheses weight, but they also provide additional strength and energy-storage capabilities [30]. Today, carbon fiber prostheses are the most popular because they allow to actively participate in sporting activities including competitive sports [31]. However, they are expensive limiting their use to professional disabled runners [32].

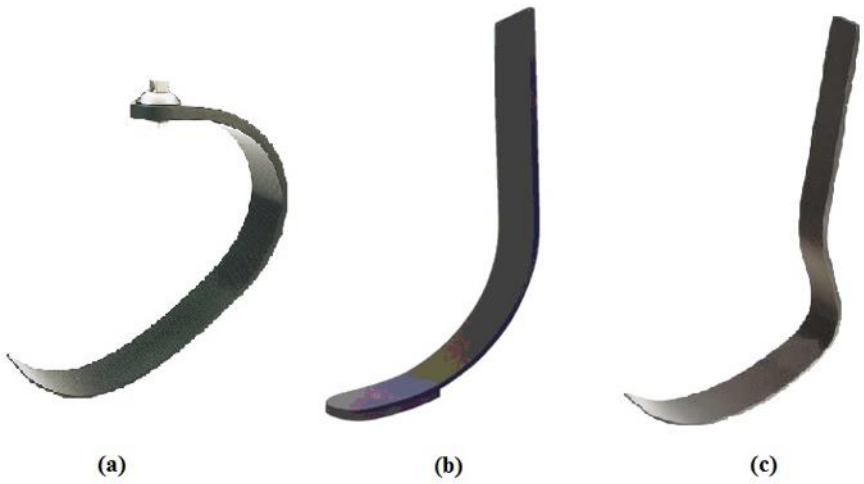

Figure IV. 12: Examples of running blade prosthesis designs: (a) Flex-Run (Össur®), (b) Flex-Sprint (Össur®), and (c) Flex-Foot Cheetah (Össur®).

4.6.2 Motivation

Developing a cheaper and more efficient material is desirable in different industries. Additionally, it is beneficial to use less material and ultimately decreasing the raw materials cost. Today, typical running blades consist of a carbon fiber-based composites giving high performances. The fact that these prostheses are manufactured from particularly expensive materials, they are mainly used by professional athletes. Therefore, accessibility is limited to high level applications while the majority of disabled people, especially the amputee children in third world countries, do not have access to these prostheses. So the objective of our work was to develop a low cost but still high performance prosthesis for children. Thanks to these blades, the leg of amputee children (from birth or after an accident) can be restored. But unlike adults, children need to change these prostheses due to their rapid growth. Therefore, low cost is the main criterion.

4.6.3 Objective of the study

Based on the results of the first part of this study, this section will use the same material to produce the running blade prosthesis. Glass fibers was selected because of their excellent performance/cost ratio. Also, the Flex-foot Cheetah blade design was selected because it provides the highest performance incorporating a pylon and foot in a single unit [32]. So the criteria to take into account are lightweight, low cost and mechanically efficient running

blade to manufacture a layered composite structure using a wood mold. From the samples produced, an experimental (characterization) and numerical investigation is performed. The latter is made using the software ANSYS Composite Prep-post (ACP) because it provides all the necessary functionalities for the analysis of laminated composites. The materials properties are extracted from the first part of the study to run the simulations. Finally, the numerical results are validated with experimental data in terms of deformation under different loading conditions.

4.7 Running blades manufacture

Drawings of the Cheetah prosthetic model were obtained from Ossur.com and used to create solid models. Following the shape design, a wooden mold (220 mm in width) was manufactured. This mold was designed to produce three running blades together as illustrated in Figure IV. 13. So three identical running blades were manufactured using as reinforcements chopped strand mat glass fibers, woven glass fibers and chopped strand mat glass fibers with gelcoat (Table IV. 3).

Figure IV. 13: The wood mold used to produce the “Flex-foot Cheetah” running blade.

A thin layer of demolding wax was applied inside the mold, then transparent plastic sheets were added to provide a better surface finish. After preparation of the fiber fabric layer, the

polyester resin was applied in the mold, then the fiber fabric layers were put on the resin to get good impregnation. This technique was applied for all the different layers. Before resin crosslinking and between each layer, the entrapped air was removed using a spiked roller. For the running blade coated by the gelcoat, the same technique was applied except that the gelcoat formulation was applied with a brush on the transparent plastic sheet and at the end of all steps (see Figure IV. 14). After crosslinking and demolding, the running blade edges were removed (total width of 220 mm) and cut to have three blades of 55 mm in width. The blade edges were polished using 60-grit and 100-grit sandpaper and the residues were removed with tap water. Finally, the blades were oven dried at 60 °C. In the present work, one blade of each type was characterized and the other two were kept for future studies.

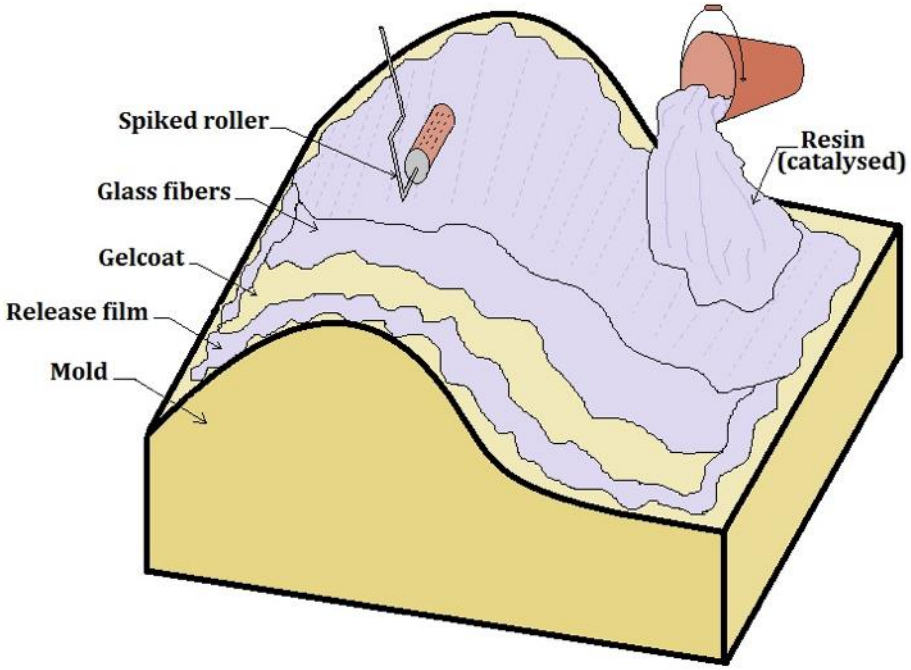

Figure IV. 14: Schematic representation of the hand layup process.

Moreover, the disposition and length of the glass fibers fabric layers (chopped strand mats and woven fabrics) were varied as shown in Figure IV. 15. These different lengths and positions were used to better control the thickness variation following the rules of stacking design [33].

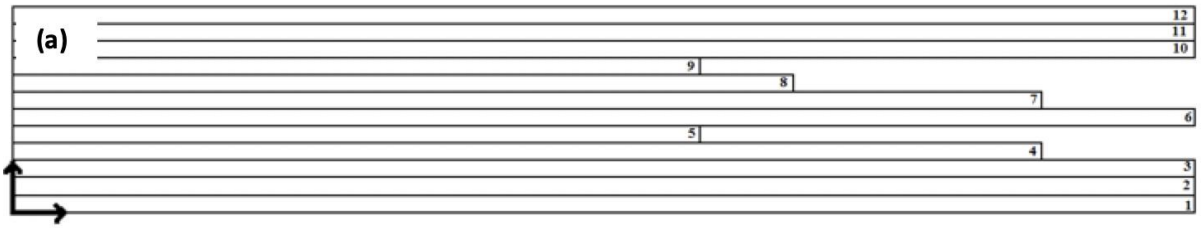

(b)

Layer number	Layer length (mm)
1, 2, 3, 6, 10, 11, 12	50.5
4, 7	45.5
8	33.3
5, 9	29.5

Figure IV. 15: (a) Layer disposition in the plane mold, and (b) the lengths of the different layers.

Table IV. 3: Samples codes for the manufactures running blades.

Blade name	Designation
Running blade reinforced with chopped strand Mat Glass Fibers	RbMGF
Running blade reinforced with Woven Glass Fibers	RbWGF
Running blade reinforced with chopped strand Mat Glass Fibers covered by Gelcoat	RbMGFGC

Figure IV. 16 presents the disposition of the glass fibers layers in the mold. It helps to project the simplest layers in the plane mold as illustrated in Figure IV. 15(a) to the real running blade prosthesis “Flex-foot Cheetah”.

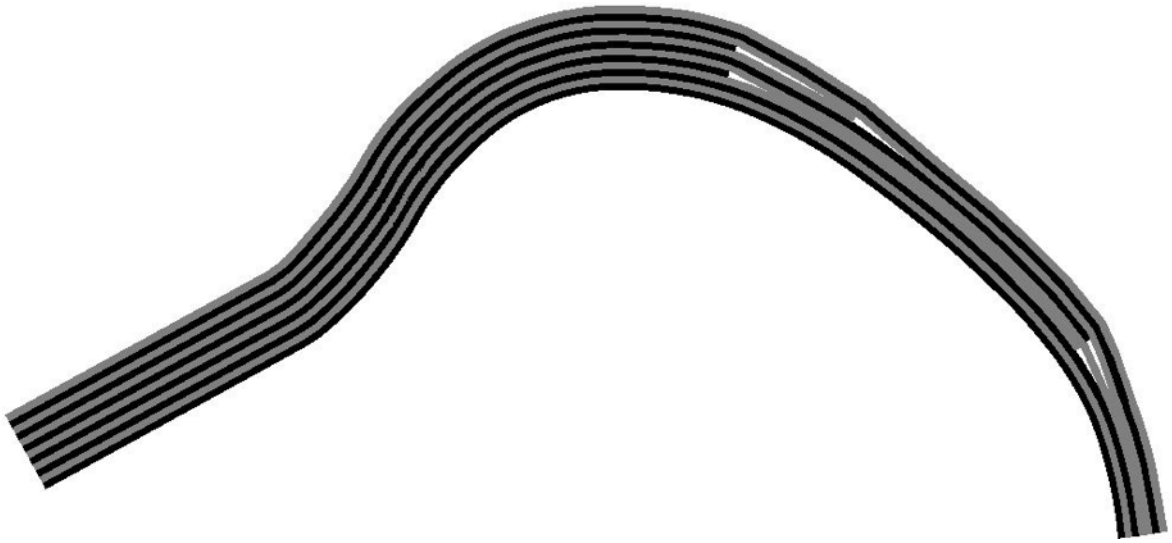

Figure IV. 16: Disposition of the different layers of glass fibers in the blade prosthesis mold.

4.8 Comparison of mass properties

The running blade weight is an essential parameter to obtain an efficient prosthesis. Here, the total area of the glass fibers used is 0.321915 m^2 which is equivalent to 96.5745 g of chopped strand mat glass fibers or 128.766 g of woven glass fibers. The main component is the polyester resin with 76% in the case of the chopped strand mat glass fibers compared to 70 % for woven glass fibers. On the other hand, the estimated gel coat covering the prosthesis on both sides is around 30 g. Thus, the amount of gelcoat used in the prosthesis is 6 % of the running blade total mass. Finally, the weight of the three running blades produced was measured and reported in Table IV. 4. The average weights are in agreement with the literature which is about 500 g [34].

Table IV. 4: Total weight of the three types of running blade produced.

Running blade	Weight (g)
RbMGF	402
RbWGF	439
RbMGFGC	426

4.9 Comparison of material costs

Table IV. 5 presents the costs of the different components used to manufacture the glass fibers running blades. As shown and according to the above calculations, the chopped strand

mat glass fibers cost 0.22 USD compared to 0.45 USD for the woven fabrics. On the other hand, the polyester resin used to manufacture one prosthesis is estimated to cost 0.63 USD, while the resin used to prepare the gelcoat costs around 0.41 USD. In addition, the aerosil and clay costs are 0.08 and 0.02 USD, respectively. Thus, the total raw material cost to elaborate one prosthesis is low allowing to satisfy the low cost criterion.

Table IV. 5: Estimated raw material cost of the different components used to manufacture the prostheses.

Running blade components	**Cost***	**RbMGF Cost (USD)**	**RbWGF Cost (USD)**	**RbMGFGC Cost (USD)**
Glass fiber (Chopped strand mat)	5 kg cost around 11 USD	0.22	-	0.22
Glass fiber (Woven fabric)	20 m^2 cost around 27 USD	-	0.45	-
Fumed silica (Aerosil)	1 kg cost around 11 USD	-	-	0.08
Polyester resin (+ hardener + catalyst)	1 L costs around 2.5 USD	0.63	0.63	0.63 + 0.41
Clay (Bayada)	1 t costs around 100 USD	-	-	0.02
	Total	**0.85**	**1.08**	**1.36**

***These costs are based on the components suppliers.

4.10 Mechanical testing of the prosthesis

4.10.1 Description of the tests

The blades can be used in two cases: standing or running. In the first case, only the weight of the person is applied on the structure (static normal force), while in the second case the maximum load applied can be up to three times the runner's weight in its standing position at an angle of 65° [35]. Therefore, the blades will be tested in both cases. Here, a weight of 80 kg is used for the calculations. In our case, a maximum force of 2400 N corresponds to a maximum displacement of 50 mm.

4.10.2 Mechanical testing

The machine used is a Tinius Olsen Horizon H10KT under compression in static and dynamic mode. It is worth noting that the three blades underwent 40 cycles to determine if they could stand fatigue. Figures IV. 17 and IV. 18 illustrate the configuration of the standing and running position of the prosthesis. In standing, three different loading rates were used (20, 50 and 100 mm/min), while for the running case only 100 mm/min was used and 200 mm/min was applied in the phase of machine relaxation to mimic the speed of release.

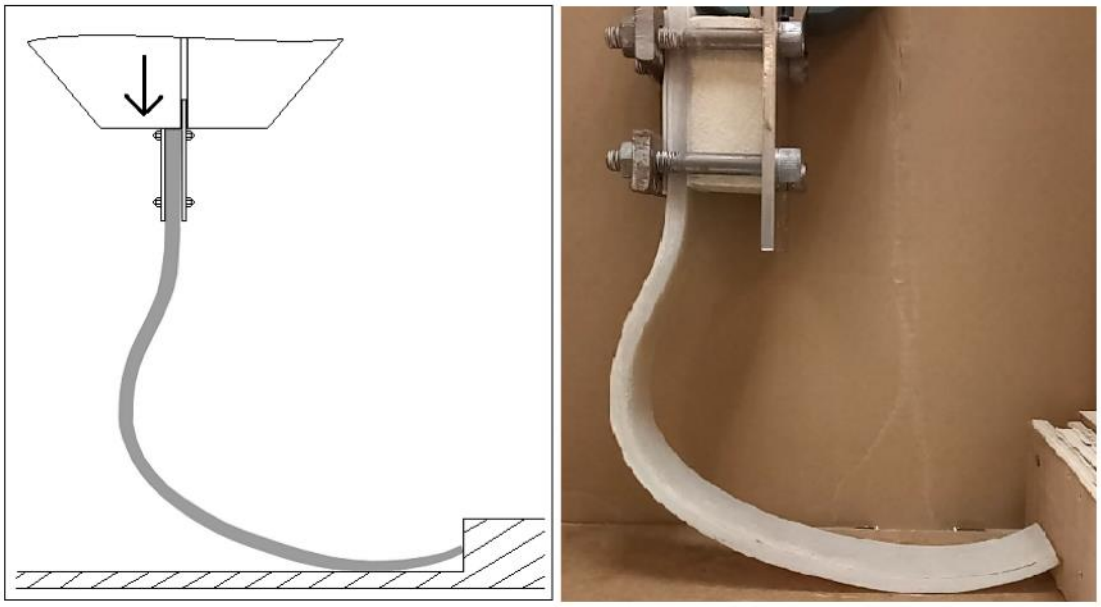

Figure IV. 17: Compression testing of a running blade in the standing case.

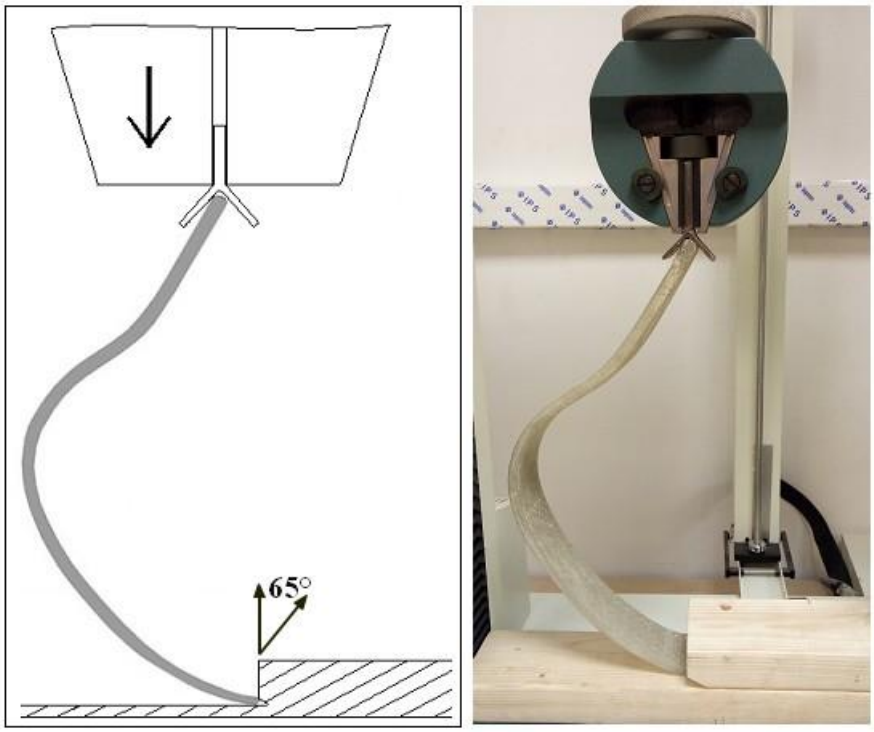

Figure IV. 18: Compression testing of the running blade in the running case.

4.10.3 Prosthesis simulation

As mentioned earlier, the profile design considered in this study is the Cheetah blade. The deformation analysis of this blade was carried out using the ANSYS ACP® software after being modelled as a surface in SolidWorks. To limit the amount of work here, the mechanical simulation is only performed for the standing position and for two materials: RbMGF and RbWGF. The simulations take into account the described layers disposition presented in Figure IV. 14 and mimic the experimental testing conditions. The thickness of each ply is fixed at 0.79 mm to obtain a total thickness of 9.5 mm.

4.11 Results and discussion

The prosthetic running blades produced led to the results presented in Figure IV. 19. The experimental results of maximum displacement for the three running blades under compression in a standing position are reported in Table IV. 6. It is clearly shown that the loading rate has no significant effect on the maximum displacement for the range investigated, but a significant difference is obtained between each type of blade. For example,

a force of 800 N in the standing load gives a maximum displacement of 49.12 mm for RbMGF, while only 36.30 mm for RbWGF and 43.98 mm for RbMGFGC are observed (Table IV. 6).

On the other hand, for the displacement chosen (50 mm) under the running condition, the equivalent forces for each blade after 40 cycles are 318 N for RbMGF, 598 N for RbWGF and 303 N for RbMGFGC. Therefore, the application of the gelcoat allows to decrease the maximum displacement compared with the same running blade without gelcoat. This indicates that the gelcoat significantly increases the energy restitution of the running blade improving the prosthesis properties.

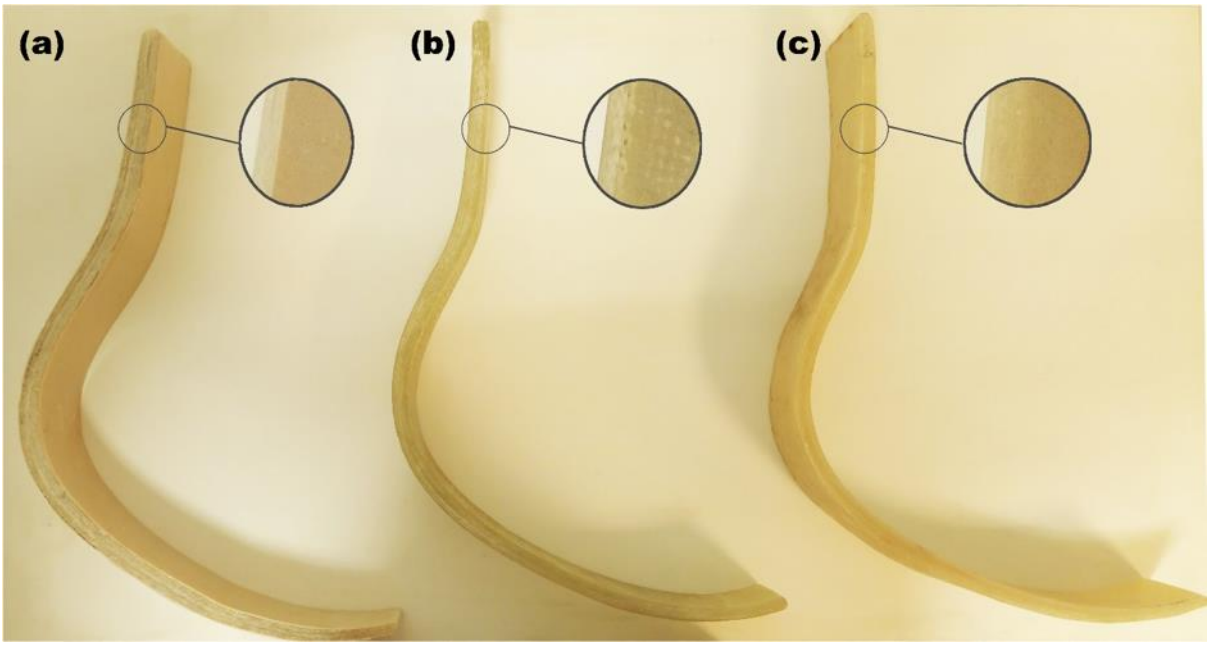

Figure IV. 19: Three tested blades: (a) RbMGFGC, (b) RbWGF, and (c) RbMGF.

Table IV. 6: Experimental maximum displacement (mm) of the three blades in standing (static loading)

Sample	Loading rate (mm/min)		
	20	**50**	**100**
RbMGF	49.065	49.085	49.200
RbWGF	36.343	36.267	36.276
RbMGFGC	45.502	42.260	44.183

Figure IV. 20 shows the variation of the equivalent force corresponding to the displacement of 50 mm under cyclic compression. It can be seen that the force corresponding to 50 mm in displacement significantly decreases with the number of cycle. This behavior corresponds to the oligocyclic area in the Whöler curve [36]. In this zone, the stresses are more important and higher than the macroscopic elastic limit. Moreover, the rupture occurs after a small number of cycle and is preceded by notable plastic deformation. As a result of the maximum stress amplitude, each cycle causes an overall plastic deformation usually coupled with a significant hardening or softening of the material. In this case, the running blades reached a state of plastic accommodation. Therefore, the running blades response (deformation) becomes periodic. Thus, an elastoplastic hysteresis cycle occurs as reported in Figure IV. 21. Generally, fatigue causes extensive damage throughout the specimen volume leading to failure from general degradation of the material instead of a predominant single crack. Fatigue failure can be defined either as a loss of stiffness or strength and can be classified into four basic failure mechanisms in composite materials: matrix cracking, delamination, fiber breakup and interfacial debonding. Due to limited machine capacity, the prostheses damage is not visually observed but microscopic level decohesion at the fiber/matrix interfaces does occur. These decohesions then coalesce to form cracks at a mesoscopic scale. If cracking is not catastrophic for the structure integrity, other types of damage may occur that may be more harmful such as delamination or fiber breakup.

The running blade results in its standing and running position show that RbWGF deforms less than RbMGF and RbMGFGC leading to lower level of mechanical degradation. This is associated to its higher rigidity and energy restitution (elasticity) compared with the other two running blades.

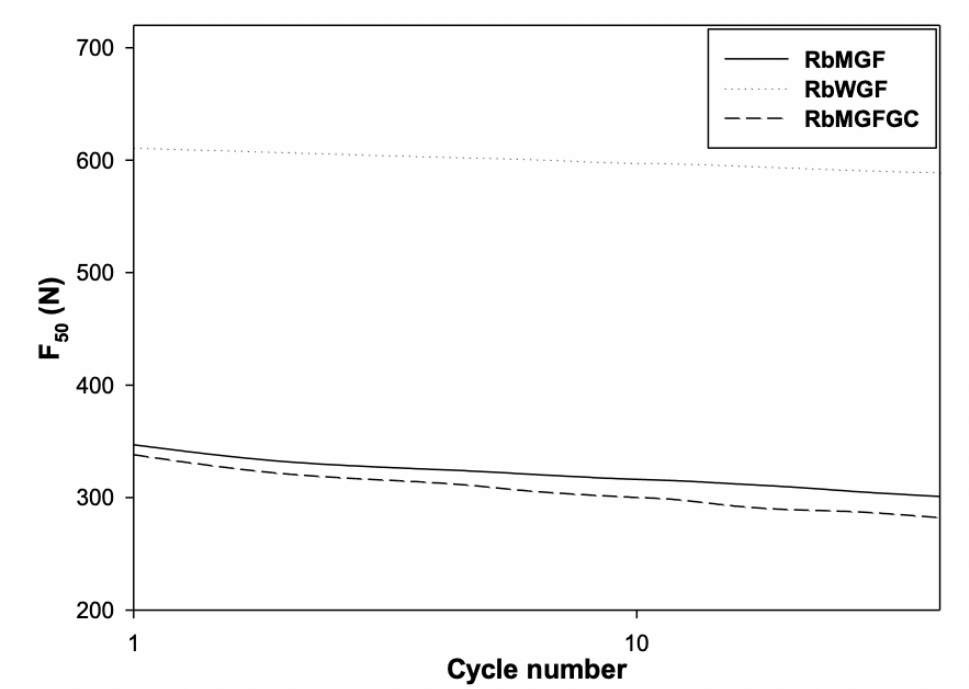

Figure IV. 20: Curves of the equivalent force to obtain 50 mm in displacement (F_{50}) as a function of the cycle number for: RbWGF, RbMGF, and RbMGFGC under running loading.

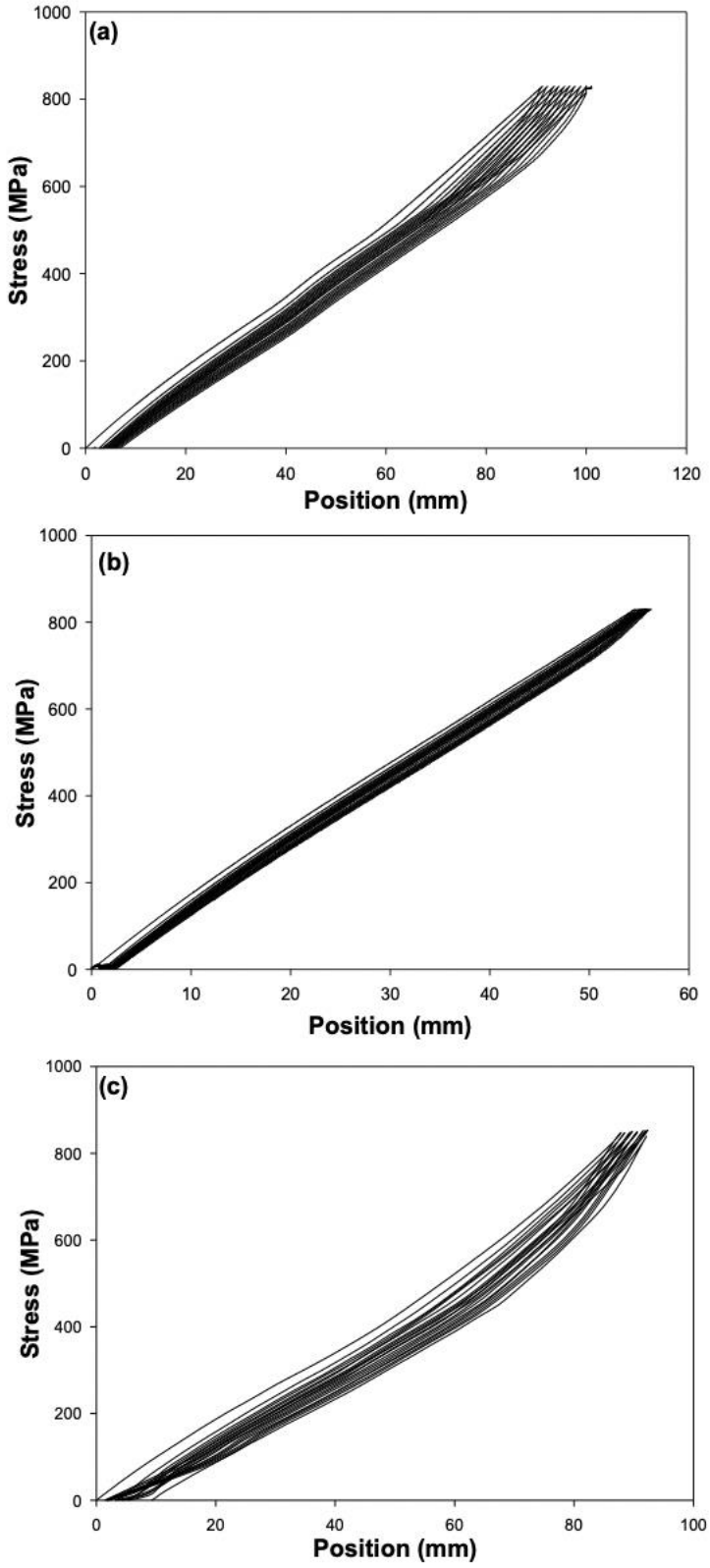

Figure IV. 21: Hysteresis cycle (stress as a function of position) for: (a) RbMGF, (b) RbWGF and (c) RbMGFGC.

Figure IV. 22(a) presents the thickness throughout the running blade. The variation observed is due to the application of different plies on the imported surface (Solidworks model as previously described) as shown in Figure IV. 22(b). This approach provides the same thickness variation as in the real cases.

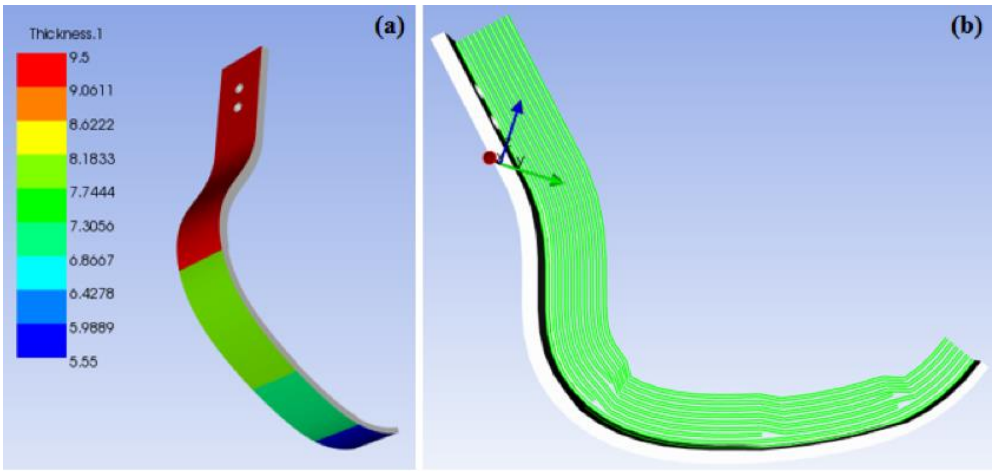

Figure IV. 22: (a) Thickness variation throughout the running blade, and (b) the applied layers on the imported surface of the running blade.

Figure IV. 23(a) and (b) show the total deformation of the running blade in standing position for RbMGF and RbWGF, respectively. Compared with the experimental data, the simulations (blade deformation) are similar and Table IV. 7 compares the results. It can be seen that the simulations for the total deformation are slightly higher (6.5% and 7.9% for RbMGF and RbWGF, respectively) than the experimental ones, but can be considered similar within experimental uncertainty (about 10%).

The results also show that RbWGF undergoes less deformation than RbMGF due to alignment of woven fiber orientation and load application [9]. In the simulation phase, the bonding between the different layers is assumed to be perfect, while in reality (experimentally) there is voids (defects) created during manufacturing even if a spiked roller was used. These voids can act as crack initiation sites in the composites. Nevertheless, the small differences between the experimental and numerical deformation values (Table IV. 7) indicates that the prosthetic running blades manufacture was successful.

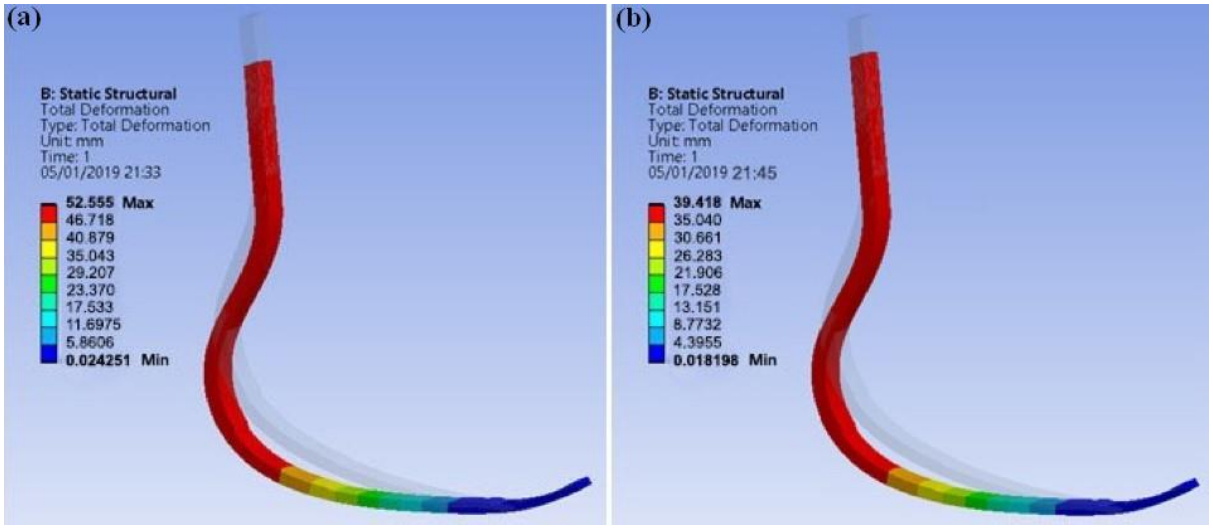

Figure IV. 23: Total deformation of the Cheetah running blades in standing position for: (a) RbMGF, and (b) RbWGF.

Table IV. 7: Summary of the experimental and numerical deformation for RbMGF and RbWGF.

Sample	Experimental deformation (mm)	Numerical deformation (mm)
RbMGF	49.1 ± 1.0	52.6 ± 1.0
RbWGF	36.3 ± 1.6	39.4 ± 0.9

- **Limitations**

This study can be further developed by removing some limitations and assumptions including the spatial displacement capacity of the machine (in compression testing) which prevents further comparison between experimental and numerical conditions applied in running load.

4.12 Conclusion and future works

This work was divided into two steps. The first step was dedicated to study the materials used in this investigation while the second part developed an application in the sports domain (running blade prosthesis). Three different running blades were manufactured and experimentally tested to determine their mechanical behavior under static (standing) and dynamic (running) loadings. The results were also numerically simulated using the ANSYS ACP software. The running blade manufacturing and design took into account the layer stacking of glass fibers with different lengths to control the thickness variation. Excellent

agreement (less than 10 %) between the experimental and numerical deformation indicated that the manual manufacture of the prosthetic running blades was successful and the properties obtained are representative of the total assembly.

Owing to their low cost, children could benefit from several running blades and could change them depending on their growth curve. But this work focused on the standard running blade "flex foot cheetah" and did not took into account that they are specially designed for children. In future work, the form-factor must be taken into account and the effect of weight applied on the prosthesis under a wider range of conditions (static and dynamic conditions) must be investigated. Finally, although the woven glass fibers prosthesis presented better performances than the others, it would be interesting to test the effect of the gelcoat on the prosthesis reinforced with woven glass fibers.

Acknowledgements

This work was supported by MAScIR: Moroccan Foundation for Advanced Science, Innovation and Research, MESRSFC and CNRST, Morocco grant no. 1970/15. The authors would like to highly thank Mr. Mehdi Ait Dahi for his fruitful technical support and assistance.

References

[1] Semlali Aouragh Hassani F-Z, Ouarhim W, Bensalah MO, Essabir H, Rodrigue D, Bouhfid R, et al. Mechanical properties prediction of polypropylene/short coir fibers composites using a self-consistent approach. Polym Compos 2018;1:1–11. doi:10.1002/pc.24967.

[2] Ouarhim W, Essabir H, Bensalah M-O, Zari N, Bouhfid R, Qaiss A el kacem. Structural laminated hybrid composites based on raffia and glass fibers: Effect of alkali treatment, mechanical and thermal properties. Compos Part B Eng 2018;154:128–37. doi:10.1016/j.compositesb.2018.08.004.

[3] Essabir H, Elkhaoulani a., Benmoussa K, Bouhfid R, Arrakhiz FZ, Qaiss a. Dynamic mechanical thermal behavior analysis of doum fibers reinforced polypropylene composites. Mater Des 2013;51:780–8. doi:10.1016/j.matdes.2013.04.092.

[4] Osama ME. Introduction and literature review on buckling of Composite Laminates. vol. 5. Germany: 2015. doi:10.1016/j.jmau.2017.01.001.

[5] Jeffrey KJT, Tarlochan F, Rahman MM. RESIDUAL STRENGTH OF CHOP STRAND MATS GLASS FIBER/EPOXY COMPOSITE STRUCTURES: EFFECT OF TEMPERATURE AND WATER ABSORPTION. Ijame 2011;4:504–19.

[6] Sathishkumar TP, Satheeshkumar S, Naveen J. Glass fiber-reinforced polymer composites - A review. J Reinf Plast Compos 2014;33:1258–75. doi:10.1177/0731684414530790.

[7] Ouarhim W, Zari N, Bouhfid R, Qaiss A el kacem. Mechanical performance of natural fibers–based thermosetting composites. Mech. Phys. Test. Biocomposites, Fibre-Reinforced Compos. Hybrid Compos., 2019, p. 43–60. doi:10.1016/B978-0-08-102292-4.00003-5.

[8] Abramovich H. Introduction to composite materials. Stab. Vib. Thin-Walled Compos. Struct., Elsevier Ltd; 2017, p. 1–47. doi:10.1016/B978-0-08-100410-4.00001-6.

[9] Bhaskar VV, Srinivas K. Mechanical characterization of glass fiber (woven roving/chopped strand mat E-glass fiber) reinforced polyester composites. Int. Conf. Funct. Mater. Charact. Solid State Physics, Power, Therm. Combust. Energy, vol. 20108, 2017, p. 1–5. doi:10.1063/1.4990261.

[10] Essabir H, Boujmal R, Bensalah MO, Rodrigue D, Bouhfid R, Qaiss AEK. Mechanical and thermal properties of hybrid composites: Oil-palm fiber/clay reinforced high density polyethylene. Mech Mater 2016;98:36–43. doi:10.1016/j.mechmat.2016.04.008.

[11] D790 ASTM. Standard Test Method for Flexural Properties of Unreinforced and Reinforced Plastics and Electrical Insulation Materials. ASTM Stand 2015:1–11.

[12] Wang Z, Song M, Sun C, He Y. Effects of particle size and distribution on the mechanical properties of SiC reinforced Al-Cu alloy composites. Mater Sci Eng A 2011;528:1131–7. doi:10.1016/j.msea.2010.11.028.

[13] Robeva-Čukovska L, Šijakova-Ivanova T, Kokolanski Ž. Analytical Study Of The XiV century wall painting and lime mortars in the “St. George” church in Staro Nagoricane, republic of Macedonia. Maced J Chem Chem Eng 2017;36:1–18. doi:10.20450/mjcce.2017.1070.

[14] Li K-M, Jiang J-G, Tian S-C, Chen X-J, Yan F. Influence of silica types on synthesis and performance of amine-silica hybrid materials used for CO2 capture. J Phys Chem C 2014;118:2454–62. doi:10.1021/jp408354r.

[15] Saraf MN, Gupta RK, Balakrishna KJ. Effect of Reinforcement on Strength of Fibreglass Composites with Isophthalic Polyester Resin Matrix 1976;1:132–4.

[16] Fallis A. Mechanical and Physical Properties of Wood-Plastic Composites Made of Polypropylene, Wood Flour and Nanoclay. J Chem Inf Model 2013;53:1689–99. doi:10.1017/CBO9781107415324.004.

[17] Leissa AW. A rewiew of laminated composite plate buckling. Appl Mech Rev 1987;40:575–91.

[18] Ouarhim W, Essabir H, Bensalah M, Rodrigue D, Bouhfid R. A Comparison between

Sabra and Alfa Fibers in Rubber Biocomposites. J Bionic Eng 2019;16:754–67.

[19] Pouriayevali H, Guo YB, Shim VPW. A constitutive description of elastomer behaviour at high strain rates - A strain-dependent relaxation time approach. Int J Impact Eng 2012;47:71–8. doi:10.1016/j.ijimpeng.2012.04.001.

[20] Lee A, Lichtenhan JD. Thermal and Viscoelastic Property of Epoxy – Clay and Hybrid Inorganic – Organic Epoxy Nanocomposites. J Appl Polym Sci 1999;73:1993–2001.

[21] Li J, Zhou C, Wang G, Zhao D. Study on Rheological Behavior of Polypropylene / Clay Nanocomposites. Appl Polym Sci 2003;89:3609–17.

[22] Wang K, Liang S, Deng J, Yang H, Zhang Q, Fu Q, et al. The role of clay network on macromolecular chain mobility and relaxation in isotactic polypropylene / organoclay nanocomposites. Polymer (Guildf) 2006;47:7131–44. doi:10.1016/j.polymer.2006.07.067.

[23] Kachanov LM. Delamination Buckling of Composite Materials. Brookline, Massachusetts, U.S.A: 1988.

[24] Hamada H, Ramakrishna S, Maekawa Z. Environmental effects on the progressive crushing behavior of glass cloth/epoxy composite tubes. Compos Interfaces 1995;3:23–39. doi:10.1163/156855495X00138.

[25] Ladhari A, Ben Daly H, Belhadjsalah H, Cole KC, Denault J. Investigation of water absorption in clay-reinforced polypropylene nanocomposites. Polym Degrad Stab 2010;95:429–39. doi:10.1016/j.polymdegradstab.2009.12.001.

[26] Boukhoulda BF, Adda-Bedia E, Madani K. The effect of fiber orientation angle in composite materials on moisture absorption and material degradation after hygrothermal ageing. Compos Struct 2006;74:406–18. doi:10.1016/j.compstruct.2005.04.032.

[27] NEKHLAOUI S. COMPORTEMENT HYGROTHERMOELASTIQUE DES MATERIAUX COMPOSITES STRATIFIES. 2005.

[28] Ramakrishna S, Mayer J, Wintermantel E, Leong KW. Biomedical applications of

polymer-composite materials: a review. Compos Sci Technol 2001;61:1189–224. doi:10.1016/S0266-3538(00)00241-4.

[29] Herr HM, Grabowski AM. Bionic ankle-foot prosthesis normalizes walking gait for persons with leg amputation. Proc R Soc B Biol Sci 2012;279:457–64. doi:10.1098/rspb.2011.1194.

[30] Webster JB, Levy CE, Bryant PR, Prusakowski PE. Sports and recreation for persons with limb deficiency. Arch Phys Med Rehabil 2001;82:S38–44. doi:10.1016/S0003-9993(01)80036-8.

[31] Scholz MS, Blanchfield JP, Bloom LD, Coburn BH, Elkington M, Fuller JD, et al. The use of composite materials in modern orthopaedic medicine and prosthetic devices: A review. Compos Sci Technol 2011;71:1791–803. doi:10.1016/j.compscitech.2011.08.017.

[32] Wing DC, Hittenberger DA. Energy-storing prosthetic feet. Arch Phys Med Rehabil 1989;70:330–5.

[33] Irisarri F, Lasseigne A, Leroy F, Le R. Optimisation des empilements dans les structures composites stratifiées avec arrêts de plis Stacking sequence optimisation for laminated composite structures with ply-drops 2013:1–10.

[34] McHugh J. Blade Runner 2009:3–8.

[35] Rahman M, Glisson D, Bennett T, Beckley D, Khan J. FINITE ELEMENT ANALYSIS OF PROSTHETIC RUNNING BLADES USING DIFFERENT COMPOSITE MATERIALS TO OPTIMIZE PERFORMANCE. Int. Mech. Eng. Congr. Expo., 2014, p. 1–14.

[36] Belkhiria S, Seddik R, Atig A, Ben Sghaier R, Hamdi A, Fathallah R. Fatigue reliability prediction of rubber parts based on Wöhler diagrams. Int J Adv Manuf Technol 2018;96:439–50. doi:10.1007/s00170-018-1575-z.

Global conclusion

The research work carried out during this PhD thesis, contributed to the development of materials, the environment and to valorise the natural resources.

This work is the fruit of the study of four configurations of the thermoset laminated composites: simple, sandwich, intra-layer and inter-layer laminated composites. Besides, different forms of the fibers are used including random, woven, chopped strand mat.

The following conclusions were based on the results of the experiments carried out throughout this work.

- The results showed that the alkaline treatment used to remove some of the non-cellulosic components of the Raffia fibers, leading to increase the thermal and mechanical properties of the composite.

- Hybridization of Raffia fibers and glass associated with epoxy resin improved the moisture resistance of the Raffia fiber composite by reducing the water absorption.

- Raffia-glass and jute-glass hybridization under different configurations also leads to an increase in the mechanical properties of composite materials, because glass fibers perform better than natural fibers.

- Whatever the laminated architecture, hybridization has a positive effect on the mechanical properties, moisture resistance and morphology of the composites.

- The homogenization technique combined with the mixing rule was successfully used to predict the elastic properties of the samples produced. The deviations between the calculated and measured values can be related to imperfect adhesion between the fibers and matrix as well as other assumptions related to the fibers themselves (orientation, sizes, distribution, etc.).

- The composite manufacturing is judged successful when the void rate is low. Therefore, the low error between the experimental and theoretical results show the success of our manufacturing.

Recommendation for future work

- Use different processing techniques to show the effect of the process on the mechanical properties.

- Investigations could be extended to evaluate other properties of the composites, such as impact test, thermal resistance, and UV resistance.

- Doping of the matrix with nano-fillers, namely clay, carbon nanotube (CNT) in order to improve the properties of the final material.

- Collaboration with orthopaedists for real tests of the running blade.

My Scientific production

Scientific Papers:

1- Ouarhim W, Essabir H, Bensalah M-O, Rodrigue D, Bouhfid R, Qaiss AEK. Production and Characterization of High Density Polyethylene Reinforced by Eucalyptus Capsule Fibers. **Journal of Bionic Engineering**, 2018, **15**(3), 558–66.

2- Ouarhim W, Essabir H, Bensalah M-O, Zari N, Bouhfid R, Qaiss A el kacem. Structural laminated hybrid composites based on raffia and glass fibers: Effect of alkali treatment, mechanical and thermal properties. **Composites Part B: Engineering**, 2018, **154**, 128–37.

3- Ouarhim W, Essabir H, Bensalah M, Rodrigue D, Bouhfid R, Qaiss A. A Comparison between Sabra and Alfa Fibers in Rubber Biocomposites. **Journal of Bionic Engineering**, 2019, **16**, 754–67.

4- Ouarhim W, Essabir H, Bensalah M-O, Zari N, Rodrigue D, Bouhfid R, Qaiss A. Hybrid composites and intra-ply hybrid composites based on jute and glass fibers: a comparative study on moisture absorption and mechanical properties. **Composites Part B: Engineering** (Submitted).

5- Ouarhim W, Rodrigue D, Bensalah M-O, Bouhfid R, Qaiss A. Characterization and numerical simulation of laminated glass fiber-polyester composites for a prosthetic running blade. **Materials Science & Engineering C** (Submitted).

6- Semlali Aouragh Hassani F-Z, Ouarhim W, Bensalah MO, Essabir H, Rodrigue D, Bouhfid R, Qaiss A. Mechanical properties prediction of polypropylene/short coir fibers composites using a self-consistent approach. **Polymer Composites**, 2018, **1**, 1–11.

7- Semlali Aouragh Hassani F, Ouarhim W, Zari N, Bensalah MO, Rodrigue D, Bouhfid R, Qaiss A. Injection Molding of Short Coir Fiber Polypropylene Biocomposites : Prediction of the Mold Filling Phase. **Polymer Composites**, 2019, , 1–14.

8- Hassani FSA, Ouarhim W, Raji M, Mekhzoum EM, Bensalah M, Essabir H, Qaiss A. N-Silylated Benzothiazolium Dye as a Coupling Agent for Polylactic Acid/Date Palm Fiber Bio-composites. **Journal of Polymers and the Environment**, 2020, **21**(3).

9- Semlali Aouragh Hassani F-Z, Ouarhim W, El Achaby M, Tamraoui Y, Bensalah M, Rodrigue D, Bouhfid R, Qaiss A. Recycled tires shreds based polyurethane binder: Production and characterization. **Mechanics of Materials**, 2019 (Under Review).

10- Semlali Aouragh Hassani F-Z, Ouarhim W, Bensalah MO, Rodrigue D, El Achaby M, Bouhfid R, Qaiss A. Injection Molding of Short Fiber Thermoplastic Bio-composites: Prediction of the Fiber Orientation. **Journal of Applied Polymer Science.** 2020 (Submitted).

Book Chapters:

1- Ouarhim W, Zari N, Bouhfid R, Qaiss A el kacem. Mechanical performance of natural fibers–based thermosetting composites. **In: Mechanical and Physical Testing of Biocomposites, Fibre-Reinforced Composites and Hybrid Composites,** Elsevier**,** 2019. p. 43–60.

2- Semlali Aouragh Hassani F, Ouarhim W, Zari N, Bouhfid R, Qaiss A el kacem. Natural fiber-based biocomposites: Effect of orientation on mechanical properties. **In: Biodegradable Composites: Materials, Manufacturing and Engineering,** DE GRUTER, 2019. p. 49–79.

3- OUARHIM W, Semlali Aouragh Hassani F-Z, Qaiss A el kacem, Bouhfid R. Rheology of polymer nanocomposites. **In: Rheology of polymer blends and nanocomposites: Theory, Medelling and Applications,** Elsevier, 2019. p. 73–96.

4- Ouarhim W, Bouhfid R, Qaiss A el kacem. Natural fibers based composites: Hygrothermoelastic behavior.

5- Semlali Aouragh Hassani F, Ouarhim W, Zari N, Bouhfid R, Qaiss A el kacem. Effect of mold design on the fiber orientation in the case of injection molding: Experimental and simulation. **In: Polymers and Composites Manufacturing.**

6- Ouarhim W, Semlali Aouragh hassani F, Bouhfid R, Qaiss A el kacem. Numerical, Experimental, and Simulation study of natural fibers based composites on injection Molding. **In: Polymers and Composites Manufacturing.**

7- Ouarhim W, Bouhfid R, Qaiss A el kacem. Mechanical Characterization of Cellulose Nanoparticle Based Advanced Materials.

Patents:

1- Matériau bio-composite à base de fibre d'eucalyptus.

2- Recyclage des lambeaux des pneus pour des applications de sols en caoutchouc.

Conferences:

Oral Communication:

1- Structural laminated hybrid composites based on raffia and glass fibers: Effect of alkali treatment, mechanical and thermal properties. **1st workshop between MSN and CNC centers**. UM6P, Benguerir.

2- Production and Characterization of High Density Polyethylene Reinforced by Eucalyptus Capsule Fibers. **1st international Symposium on composite and nanocomposite materials (1st ISymposite)**. Mascir Foundation, Rabat. (**Organizing committee**).

3- Hybrid composites and intra-ply hybrid composites based on jute and glass fibers: a comparative study on moisture absorption and mechanical properties. **2nd Wood & Biofibre International Conference (WOBIC 2019)**, UPM, Malaysia.

Poster Communication:

- Structural laminated hybrid composites based on raffia and glass fibers: Effect of alkali treatment, mechanical and thermal properties. **1st international Symposium on composite and nanocomposite materials (1st ISymposite)**. Mascir Foundation, Rabat. (**Organizing committee**).

Résumé

Cette thèse a pour objectif la conception et le développement de nouveaux matériaux composites à matrices thermodurcissables. En effet, des composites renforcés par des fibres naturelles, des fibres synthétiques, et l'hybridation des deux sont objet d'étude dans cette thèse. Pour ce faire, les composites stratifiés simples et hybrides sont deux configurations utilisés dans ce travail. La configuration hybride, à son tour, se compose de trois architectures : sandwich, inter-couche et intra-couche.

Les fibres naturelles (le raphia et le jute) et les fibres synthétiques (le verre) ont été choisis comme des renforts de deux matrices thermodurcissables (époxy et polyester). Différentes formes de fibres sont adoptées, notamment mat et tissé. La fabrication des composites stratifiés est assuré par la technique de stratification manuelle.

Les propriétés des composites fibres/résine ont été définies à l'aide d'essais de traction, de flexion, de torsion, de cisaillement, de test de gouttelettes, d'absorption d'humidité et de conductivité thermique. La microscopie électronique à balayage et la spectroscopie infrarouge à transformée de Fourier ont été utilisées pour étudier, respectivement, les propriétés morphologiques et structurelles des composites.

Les résultats expérimentaux de différentes configurations sont comparés aux modèles théoriques (loi de mélange, technique d'homogénéisation) et à la simulation numérique (ANSYS ACP). Par conséquent, un bon accord entre les résultats est trouvé en tenant compte des hypothèses retenues.

Mots-clefs (5) : Composites stratifiés, Matrices thermodurcissables, Hybridation, Design, propriétés mécaniques.

Abstract

This thesis focuses on the design and development of new thermoset composite materials. Indeed, composites reinforced with natural fibers, synthetic fibers, and both of them (hybrid composite) were selected for study in this thesis. For this purpose, two laminated configurations are used, including simple and hybrid laminated composites. This later, in turn, consist of three configurations: sandwich structure, inter-layer, and intra-layer configurations.

The fibers used in this study were Raffia and jute as natural fibers and glass as synthetic fiber reinforcing two thermoset matrices (epoxy and polyester) through hand lay-up technique. Different fiber forms are adopted including mat and woven.

The properties of the fibers/resin composites were defined by using tensile, flexural, torsion, shearing, droplet test, moisture absorption, thermal conductivity tests. Scanning electron microscopy (SEM) and Fourier transform infrared spectroscopy (FTIR) has been used to study the morphological and structural properties of the composites, respectively.

The experimental results for all laminated configurations are compared with theoretical models (mixing law, homogenization technique) and numerical simulation (ANSYS ACP). Therefore, a good agreement between results is found taking into account the considered assumptions.

Key Words (5): Laminated Composites, Thermoset Matrices, Hybridization, Design, Mechanical properties.